

ACONITINE-INDUCED NEUROGENIC PULMONARY EDEMA
IN THE RAT: AN ELECTRON MICROSCOPIC STUDY

by

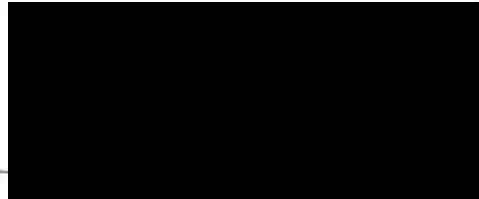
Fred Luers, Minnear,

A THESIS

Presented to the Department of Anatomy
and the Graduate Division
of the University of Oregon Health Sciences Center
in partial fulfillment of
the requirements for the degree of

DOCTOR OF PHILOSOPHY
October 1979

APPROVED:

A large black rectangular redaction box covering the signature of the Professor in Charge of Thesis.

(Professor in Charge of Thesis)

A large black rectangular redaction box covering the signature of the Chairman, Graduate Council.

(Chairman, Graduate Council)

ACKNOWLEDGEMENTS

I wish to thank Dr. Reid S. Connell for his guidance in this work and for his help in analyzing the electron micrographs. Many thanks to Dr. Harry Weitlauf for his scientific advice and to Dr. Vaughn Critchlow for his assistance in reviewing the manuscript. Gratitude is also expressed to Mike Webb for passing on his knowledge of electron microscopy, to Valerie Baughman for her able assistance in the laboratory and to Elaine Jendritza and Diane Hogan for typing the thesis. Thanks also to Roger Hoversland for his advice on statistical matters.

Special thanks to Dr. F.L. Minnear and Elinor Luers Minnear for their continual support and encouragement and to Denise for being the rock of our foundation.

TABLE OF CONTENTS

| | <u>PAGE</u> |
|---|-------------|
| ACKNOWLEDGEMENTS | i |
| TABLE OF CONTENTS. | ii |
| LIST OF TABLES | iv |
| LIST OF FIGURES | v |
| | |
| I. STATEMENT OF THE PROBLEM | 1 |
| II. REVIEW OF LITERATURE | 3 |
| A. Introduction | 3 |
| B. The Role of the Autonomic Nervous System in NPE. | 4 |
| C. Hemodynamic Alterations Associated with NPE. | 7 |
| D. Ultrastructural Alterations Associated with NPE. | 11 |
| E. Respiratory Disorders Associated with NPE. | 13 |
| F. Treatment of NPE | 14 |
| G. References. | 17 |
| | |
| III. PAPER 1. A Comparison of Changes in Pulmonary Ultra- structure in Mild and Severe Forms of Aconi- tine-Induced Neurogenic Pulmonary Edema. | 23 |
| A. Abstract | 24 |
| B. Introduction | 25 |
| C. Materials and Methods. | 26 |
| D. Results. | 28 |
| E. Discussion | 32 |
| F. References | 38 |
| G. Figures and Tables | 41 |

TABLE OF CONTENTS (Cont'd)

| | <u>PAGE</u> |
|--|-------------|
| IV. PAPER 2. Alterations in the Capillary-Alveolar | 62 |
| Barrier Associated with Increased Permeability in Aconitine-Induced Neurogenic Pulmonary Edema. | |
| A. Abstract. | 63 |
| B. Introduction. | 64 |
| C. Materials and Methods | 65 |
| D. Results | 66 |
| E. Discussion. | 68 |
| F. References. | 73 |
| G. Figures and Table | 75 |
| V. PAPER 3. Prevention of Aconitine-Induced Neurogenic | 90 |
| Pulmonary Edema by Phlebotomy or Pretreatment with Methylprednisolone Sodium Succinate | |
| A. Abstract | 91 |
| B. Introduction. | 92 |
| C. Materials and Methods | 92 |
| D. Results | 95 |
| E. Discussion. | 97 |
| F. References. | 102 |
| G. Figures and Table | 105 |
| VI. SUMMARY | 116 |

LIST OF TABLES

| | | <u>PAGE</u> |
|--------------------|---|-------------|
| <u>PAPER 1</u> | | |
| TABLE | | |
| 1 | Criteria for grading pathologic changes in gross appearance of the lungs. | 42 |
| 2 | Criteria for grading pathologic changes in the ultrastructure of the lungs. | 43 |
| 3 | Relationship between the dose of aconitine and changes in gross appearance and ultrastructure of the lungs. | 45 |
| 4 | Relationship between the ratio of lung weight and changes in gross appearance and ultrastructure of the lungs. | 46 |
| 5 | The effect of aconitine injected into the preoptic area on systolic blood pressure. | 60 |
| 6 | The effect of aconitine injected into the preoptic area on diastolic blood pressure. | 61 |
| <u>PAPER 2</u> | | |
| TABLE | | |
| i | The effect of aconitine injected into the preoptic region on the ratio of lung weight to body weight in rats. | 76 |
| <u>PAPER 3</u> | | |
| TABLE | | |
| 1 | The effects of phlebotomy or methylprednisolone sodium succinate (MPSS) on the ratio of lung weight to body weight (LW/BW) in aconitine-induced neurogenic pulmonary edema. | 105 |

LIST OF FIGURES

| | | <u>PAGE</u> |
|----------------|--|-------------|
| <u>PAPER 1</u> | | |
| <u>FIGURE</u> | | |
| 1 | The effect of increasing the dose of aconitine, | 41 |
| | injected into the preoptic area, on LW/BW. | |
| 2 | A coronal section of a rat brain showing the | 44 |
| | injection sites. | |
| 3 | Lungs from a rat injected with 197 pmoles/kg. | 47 |
| | of aconitine. | |
| 4 | Electron micrograph of a lung biopsy from a | 48 |
| | sham-operated rat. | |
| 5 | Lungs from a rat injected with 387 pmoles/kg. | 49 |
| | of aconitine. | |
| 6 | Electron micrograph of a lung biopsy from a | 50 |
| | rat injected with 774 pmoles/kg of aconitine and showing alveolar exudates and a swollen Type I cell. | |
| 7 | Electron micrograph of a lung biopsy from a | 51 |
| | rat injected with 774 pmoles/kg of aconitine and showing rarefied, swollen and discontinuous Type I cells. | |
| 8 | Electron micrograph of a lung biopsy from a | 52 |
| | rat injected with 1550 pmoles/kg of aconitine and showing a discontinuous Type I cell and alveolar exudates. | |
| 9 | Electron micrograph of a lung biopsy from a rat | 53 |
| | injected with 1550 pmoles/kg of aconitine and showing four features that characterized the degeneration of Type I cells. | |
| 10 | Electron micrograph of a lung biopsy from a rat | 54 |
| | injected with 387 pmoles/kg of aconitine and showing a capillary endothelial cell protruding into the capillary lumen. | |
| 11 | Lungs from a rat injected with 774 pmoles/kg | 55 |
| | of aconitine. | |

LIST OF FIGURES (Cont'd)

| | | <u>PAGE</u> |
|----------------|--|-------------|
| <u>PAPER 1</u> | | |
| FIGURE | | |
| 12 | Electron micrograph of a lung biopsy from a rat injected with 1550 pmoles/kg of aconitine and showing three features that characterized the degeneration of Type I cells. | 56 |
| 13 | Electron micrograph of a lung biopsy from a rat injected with 1550 pmoles/kg of aconitine and showing discontinuous Type I epithelial and capillary endothelial cells and dense alveolar exudates. | 57 |
| 14 | Electron micrograph of a lung biopsy from a rat injected with 774 pmoles/kg of aconitine and showing exudates and fibrin in the alveolar air spaces. | 58 |
| 15 | The effects of different doses of aconitine, injected into the preoptic region, on systolic (a) and diastolic (b) blood pressures. | 59 |
| <u>PAPER 2</u> | | |
| FIGURE | | |
| 1 | Representative tracing of SAP from a rat in- jected with aconitine (1550 pmoles/kg) and killed at the time of peak SAP (8 min.). | 75 |
| 2 | Representative tracing of SAP from a rat in- jected with aconitine (1150 pmoles/kg) and killed at the initiation of frothing from the nose (15 min.). | 75 |
| 3 | Lungs from a rat injected with aconitine. (1550 pmoles/kg) and killed at the time of peak SAP. | 77 |
| 4 | Lungs from a rat injected with aconitine. (1550 pmoles/kg) and killed at the time of frothing. | 78 |
| 5 | Electron micrograph of a lung biopsy from a rat injected with aconitine and killed at the time of peak SAP and showing ferritin confined to the capillary lumen. | 79 |

LIST OF FIGURES (Cont'd)

| | | <u>PAGE</u> |
|----------------|--|-------------|
| <u>PAPER 2</u> | | |
| FIGURE | | |
| 6 | Electron micrograph of a lung biopsy from a rat injected with aconitine and killed at the time of frothing and showing an intact capillary endothelial junction. | 80 |
| 7 | Electron micrograph of a lung biopsy from a rat injected with aconitine and killed at the time of frothing and showing a protruded capillary endothelial cell adjacent to a rarefied Type I epithelial cell. | 81 |
| 8 | Electron micrograph of a lung biopsy from a rat injected with aconitine and killed at the time of frothing and showing a rarefied and swollen Type I epithelial cell and an intact epithelial junction. | 82 |
| 9 | Electron micrograph of a lung biopsy from a rat injected with aconitine and killed at the time of frothing and showing structural damage to the capillary endothelium. | 83 |
| 10 | Electron micrograph of a lung biopsy from a rat injected with aconitine and killed at the time of frothing and showing ferritin in an intercellular cleft between two endothelial cells. | 84 |
| 11 | Electron micrograph of a lung biopsy from a rat injected with aconitine and killed at the time of frothing and showing an endothelial junction that appears open. | 85 |
| 12 | Electron micrograph of a lung biopsy from a rat injected with aconitine and killed at the time of peak SAP and showing an endothelial junction that appears open and ferritin and fibrin that are present in the alveolar air space. | 86 |
| 13 | Electron micrograph of a lung biopsy from a rat injected with aconitine and killed at the time of peak SAP and showing two endothelial cells separated at what appears to be a junctional complex. | 87 |

LIST OF FIGURES (Cont'd)

| | <u>PAGE</u> |
|----------------|---|
| <u>PAPER 2</u> | |
| FIGURE | |
| 14 | Electron micrograph of a lung biopsy from a 88 rat injected with aconitine and killed at the time of peak SAP and showing a discontinuous capillary endothelial cell. |
| 15 | Electron micrograph of a lung biopsy from a 89 rat injected with aconitine and killed at the time of frothing and showing a discontinuous Type I epithelial cell. |
| <u>PAPER 3</u> | |
| FIGURE | |
| 1 | The effect of MPSS on systolic blood pressure 106 after the injection of aconitine (774 pmoles/kg) in the preoptic area. |
| 2 | Lungs from a rat injected with 774 pmoles/kg of 107 aconitine. |
| 3 | Electron micrograph of a lung biopsy from a rat 108 injected with 1550 pmoles/kg of aconitine and showing discontinuous Type I epithelium and capillary endothelium. |
| 4 | Lungs from a rat injected with 1550 pmoles/kg 109 of aconitine and phlebotomized when SAP reached a peak level. |
| 5 | Electron micrograph of a lung biopsy from a rat 110 injected with 1550 pmoles/kg of aconitine and phlebotomized when SAP reached a peak level and showing a rarefied Type I epithelial cell. |
| 6 | Electron micrograph of a lung biopsy from a rat 111 injected with 1550 pmoles/kg of aconitine and phlebotomized when SAP reached a peak level and showing exudates in an alveolar air space. |

LIST OF FIGURES (Cont'd)

PAGE

PAPER 3

FIGURE

| | | |
|----|---|-----|
| 7 | Electron micrograph of a lung biopsy from a | 112 |
| | rat injected with 1550 pmoles/kg of aconitine and phlebotomized when SAP reached a peak level and showing alveolar exudates and dis- continuous Type I epithelium. | |
| 8 | The effect of phlebotomy on SAP following in- | 113 |
| | jection of 1550 pmoles/kg of aconitine. | |
| 9 | Lungs from a rat treated with MPSS and injected | 114 |
| | with 774 pmoles/kg of aconitine. | |
| 10 | Electron micrograph of a lung biopsy from a rat | 115 |
| | treated with methylprednisolone sodium succinate and injected with 774 pmoles/kg of aconitine and showing a normal appearing interalveolar septum. | |

I. STATEMENT OF THE PROBLEM

Neurogenic pulmonary edema (NPE) is a well-documented clinical and experimental entity that is associated with various injuries of the brain or spinal cord (10,14,25,29,41,65,70,72). The severity of this syndrome is variable (65,69). In a mild form, it is transient and there may be little or no impairment of pulmonary function. However, in more severe forms, the amount of edema is significant, pulmonary function is rapidly compromised, and the patients often die. Under these conditions, it has been difficult to determine the pathogenesis of NPE in humans. Several experimental models of NPE have been developed in animals using large increases in intracranial pressure (18,37), cerebral compression (19), blunt cerebral trauma (5,46) or hypothalamic injections of a lethal dose of aconitine (63,73). Such procedures lead to transient increases in systemic and pulmonary blood pressures (26,50,58,69,73) and pulmonary blood volume (12,26,42,44,58,59), persistent increases in microvascular permeability (11,13,16,51) and lung water content (50) and severe alterations of the pulmonary ultrastructure (36,37). Unfortunately, these models of producing NPE cause the syndrome to develop rapidly, and the experimental animals usually die within minutes. Therefore, these methods have limited value in studies designed to determine the sequence of events leading to the development of NPE. New experimental models that would permit control of the severity of the syndrome between sublethal and lethal forms would facilitate research in this area.

A better understanding of the hemodynamic and morphologic changes associated with NPE may be of value in improving therapy. Presently,

treatment for NPE is aimed at improving oxygenation and reducing the pulmonary edema (31,66). Adjunctive therapy for NPE aimed at reducing the hemodynamic changes and reversing the changes in pulmonary vascular permeability has not been used (66). Since corticosteroids have been attributed with having these effects, they might be beneficial in the treatment of NPE (21,43,54,62).

NPE has been produced by injecting aconitine into the preoptic area of the brain (63,73). Preliminary data from this laboratory suggested that sublethal as well as lethal forms of NPE can be produced by varying the dose of aconitine used. Therefore, the present study was designed to:

- 1) Determine if a dose-response relationship exists between aconitine and the changes in systemic arterial blood pressure and the ratio of lung weight to body weight.
- 2) Characterize the pulmonary ultrastructural changes at approximately 8, 15, and 60 min after injection of aconitine into the preoptic area.
- 3) Determine the route taken by plasma across the capillary-alveolar barrier in the lung with cadmium-free ferritin, an electron-dense tracer.
- 4) Examine the efficacy of a corticosteroid and phlebotomy in preventing the development of NPE.

II. REVIEW OF LITERATURE

Introduction

It is well documented that various clinical disorders of the central nervous system (CNS) such as non-traumatic cerebral hemorrhage (72), cerebral trauma (41,65,70), intracranial tumors (29), convulsive disorders (10), increased cerebrospinal fluid pressure (25) and lesions of the cervical spinal cord (14) may produce pulmonary edema and, if uncontrolled, pulmonary insufficiency. This variety of pulmonary edema is called neurogenic pulmonary edema (NPE) due to the apparent role of the CNS in the pathogenesis of the disease. NPE has been produced experimentally in rats, rabbits, cats, dogs, and sheep by intracisternal injection of fibrin (16,60) or veratrine (45), blunt cerebral trauma (5,46), increased intracranial pressure (18,26,35,37,50), placement of electrolytic lesions in the hypothalamus (32,47,57) or nucleus tractus solitarius (23,24), hypothalamic injection of aconitine (63,73) and intracerebroventricular injection of scorpion toxin (tityustoxin) (2).

Despite the extensive amount of clinical and experimental literature on the subject, the pathogenesis of NPE is not well defined. Experimental studies show that NPE is characterized by rapid onset and development, marked but transient increases in systemic and pulmonary vascular pressures (26,50,58,60) and pulmonary blood volume (12,26,42,44,58,59), a marked and persistent increase in pulmonary microvascular permeability (11,13,16,51) and protein-rich edema fluid (16,72). These hemodynamic events are thought to be initiated by the hypothalamus (69) and can be prevented by alpha adrenergic blockade (5,12,23,46,49) and CNS depressants (2,5,46,63). In a review article, Theordore and Robin (69) stated that any theory of the pathogenesis of this disease must account for the

above characteristics.

The Role of the Autonomic Nervous System in NPE

The rapidity of onset and the depressant effects of phenobarbital, ether, urethane and chloral hydrate (2,5,46,63) suggest that the genesis of NPE is related to a rapid outpouring of neural impulses from the CNS (69). This is the only plausible explanation for the high incidence of pulmonary edema found in soldiers in Vietnam who were killed instantly from clean head wounds (65). How these neural impulses are generated is unknown. It is known, however, that brain damage can initiate a cascade of events leading to ischemia of neural tissue (31). Cerebral edema can interrupt blood flow and oxygen supply to the damaged neural tissues and increase intracranial pressure which can further impair pulmonary respiration and the flow of blood to the brain (31). Cushing (20) showed that the CNS responds to either an ischemic crisis or an elevation in intracranial pressure by rapidly and markedly increasing systemic arterial blood pressure. When mean arterial pressure exceeds intracranial pressure, perfusion of the brain is reestablished. Whether vasomotor areas of the hypothalamus, medulla or spinal cord initiate the CNS response to ischemia is unknown.

The intensity and duration of the neural insult and the site of injury can affect the severity of the pulmonary lesion. Blunt cerebral trauma (5,46), cerebral compression (19) and intracranial hypertension (18,37) cause fulminating pulmonary edema and death within a few minutes. On the other hand, electrolytic lesions placed in the nucleus tractus

solitarius (23) or the preoptic-anterior hypothalamic area (47,55) produce the same responses that develop slowly over a period of hours. Small increases in intracranial pressure produce a milder form of NPE (13,50).

A variety of intracranial and spinal disorders are associated with pulmonary edema. Bilateral damage to the dorsal nuclei of the vagus and the medial reticular nuclei has been shown to be a common finding in association with pulmonary edema of neural origin (3). Attention has also been focused on the hypothalamus and adjacent structures because electrolytic lesions placed stereotaxically in the preoptic - anterior hypothalamic area consistently produce pulmonary edema (32, 47,55). Maire and Patton (47) hypothesized that destruction of tissue in the preoptic region causes pulmonary edema by removing an inhibitory influence on a postchiasmatic "edemagenic center". Reynolds (57) suggested that electrolytic lesions irritate the surrounding tissue and thus stimulate adjacent sympathetic pathways. Interruption of the neural pathways projecting caudally from the hypothalamus prevented the alpha adrenergic mediated hypertension, associated with NPE, following placement of electrolytic lesions in the nucleus tractus solitarius (23), whereas it had no protective effect after rapid cerebral compression (19). In the latter study, it was suggested that the vasomotor areas of the medulla and spinal cord are responsible for activating NPE. Therefore, the existing evidence suggests that the activation or destruction of localized areas in the hypothalamus, brain stem or spinal cord is responsible for initiating NPE. It remains to be determined if these structures are essential for the development of

the disease following massive cerebral injury.

Evidence suggests that the neural impulses which originate in the CNS and cause NPE are mediated by sympathetic nerves and involve peripheral alpha adrenergic receptors. NPE closely resembles norepinephrine- (7,19) and epinephrine-induced pulmonary edema (45,74). Measurement of plasma catecholamines after intracranial hypertension shows marked but transient increases in norepinephrine, epinephrine and dopamine (34). Transection of the cervical spinal cord (19,26,47,65) and pre-treatment with alpha adrenergic blocking agents such as phenoxybenzamine, dibenzylamine and phentolamine, prevent NPE (5,12,23,46,49). The effects of catecholamines released from the adrenal medulla, however, are not clear. Adrenalectomy prevented pulmonary changes in some studies (48,55) and had no effect in others (19,46). Almeida et al. (2) found that adrenalectomy or guanethidine, an alpha and beta adrenergic post-ganglionic blocking agent, slightly reduced the amount of pulmonary edema, and the combination of these treatments prevented it completely. Similarly, systemic injections of 6-hydroxydopamine, which destroys sympathetic nerve terminals, in combination with adrenalectomy prevented the alpha adrenergic mediated hypertension produced by placement of electrolytic lesions in the nucleus tractus solitarius (24).

The parasympathetic nervous system appears to enhance but not initiate NPE. Bilateral cervical vagotomy (18) and atropine (17) provided protection against pulmonary edema produced by cerebral compression or intracisternal injection of fibrin (16). It was suggested that pulmonary vascular overload resulting from increased vagal tone on the heart (17) causes pulmonary edema. Vagal-mediated arrhythmias

which were prevented by vagotomy and propantheline have also been demonstrated following subarachnoid hemorrhage (27) and stimulation of the posterior hypothalamus (28). Other studies, however, found that vagotomy or atropine had no effect on the hemodynamic and morphologic changes associated with NPE (8,19,47,60,63). Chen et al.(19) showed that after cerebral compression vagotomy prevented bradycardia but had no effect on systemic hypertension or the changes in pulmonary morphology. These investigators also found that bradycardia developed in animals with transected spinal cords, but systemic hypertension and pulmonary edema were absent. Because pulmonary edema was not significantly affected by vagotomy, it was suggested that vagal-mediated bradycardia is not essential to the development of NPE but may enhance it (19).

Hemodynamic Alterations Associated with NPE

It has been hypothesized that an injury to the CNS initiates a rapid and massive outflow from the autonomic nervous system that directly increases pulmonary microvascular permeability (11,13,16,51), constricts systemic and pulmonary blood vessels (50,58,60,69) and causes a shift in blood from the systemic to the pulmonary circulation (12,26,42,44,58,59). Increased blood volume and/or pulmonary vasoconstriction is thought to cause the rise in pulmonary capillary pressure (26,44,50,58,60). Although not confirmed by microscopic techniques, it was assumed that pulmonary edema resulted from an increase in pulmonary capillary pressure and subsequent loosening of tight junctions of the lining cells of the capillary-alveolar barrier or rupture of these cells (69). Recent physiologic and ultrastructural evidence, however, suggests that cerebral trauma may affect pulmonary capillary permeability by direct neural effects (11,13,16,51).

Intracisternal injection of fibrin (58,59), intracranial hypertension (26) and transfusion with norepinephrine (42) have been shown to cause a significant shift in blood volume of up to 30% from the splanchnic to the pulmonary vascular bed (42). Under resting conditions, the splanchnic vascular bed contains about 20% of the total blood volume (64). Maire and Patton (48) found that bilateral sectioning of the splanchnic nerves prevented pulmonary edema in rats following placement of hypothalamic lesions. On the other hand, adrenal demedullation had no detectable protective effect. Therefore, they suggested that sympathetic constriction of the splanchnic venous reservoir and the increase in venous return causes pulmonary vascular overload and pulmonary edema. In support of this hypothesis, arterio-venous shunting has been demonstrated in somatic and splanchnic vascular beds after induction of intracranial hypertension (8).

Whether an increase in pulmonary blood volume or pulmonary vasoconstriction causes the increase in pulmonary hydrostatic pressure associated with NPE is not known. Removal of the sympathetic innervation to the lungs in dogs, by performing an upper thoracic sympathectomy, before injecting fibrin intracisternally did not prevent the increase in pulmonary artery and venous pressures (60). Also, no significant changes in pulmonary hypertension were observed in association with increased intracranial pressure when pulmonary blood flow was kept constant in an isolated perfused lung. In the latter study, it was concluded that pulmonary hypertension resulted from an increase in pulmonary blood volume and not from a direct sympathetic-mediated vasomotor effect on the pulmonary vasculature (44). Another study, however, demonstrated that the pulmonary vasoconstriction occurring when intracranial pressure is

maintained below the mean arterial pressure is mediated by alpha adrenergic mechanisms (50).

NPE is described as permeability edema because the protein concentrations of the edema fluid and lung lymph approach that in plasma (11, 13, 16, 51, 66, 69, 72). The mechanism of permeability edema, however, is unknown. In 1949, Cameron and De (16) suggested that the initial cause of NPE is an increase in pulmonary capillary permeability that is mediated by neural impulses and occurs independently of hemodynamic changes. This concept was put to rest for a period of 25 years in favor of more "explosive" causes. High pulmonary pressures were demonstrated in association with increased pulmonary blood volume and left ventricular end-diastolic volume and decreased left ventricular compliance (26, 45). Pulmonary edema was shown to develop only when left ventricular end-diastolic pressure exceeded 40 mm Hg (33, 45). It was assumed that left ventricular failure resulted in pulmonary vascular overload and an increase in pulmonary capillary pressure (26, 33, 45). Increased pulmonary capillary permeability may result from such a transient elevation in pulmonary capillary pressure. However, pulmonary hypertension maintained for 2 to 3 hours in sheep did not increase the protein concentration of lung lymph (67). Therefore, it is unlikely that transient increases in pulmonary capillary pressure can fully account for the marked pulmonary edema unless the lining cells are physically altered. In a review article, Theodore and Robin (69) emphasized the involvement of left ventricular abnormalities and stressed the importance of rapid but transient increases in pulmonary blood volume and pulmonary vascular pressures in causing structural damage to the capillary vessels. A

recent case report of a patient with a clinical diagnosis of intracranial hemorrhage supports this hypothesis (75). The patient presented with pulmonary edema and a high systemic blood pressure, but his pulmonary arterial and capillary wedge pressures were normal. During the next 6 h the patient experienced 3 episodes of increased vascular pressures. Systemic blood pressure doubled and pulmonary vascular pressures increased more than 4-fold above initial values. Each episode lasted approximately 5 min. The patient remained in pulmonary edema for the next 72 h with normal blood pressures. It was assumed that the patient experienced an earlier episode of high vascular pressures before entering the hospital. On the basis of these findings, it was suggested that the etiology and persistence of the NPE were due to an increase in pulmonary capillary permeability brought about by increased pulmonary hydrostatic pressure.

Recently, it was reported that experimentally induced subarachnoid hemorrhages in dogs (27) and electrical stimulation of the posterior hypothalamus in cats (28) caused sinus bradycardia and ventricular arrhythmias within minutes and seconds, respectively. The arrhythmias were thought to be mediated by reflex activity of the vagus that was evoked by the rise in arterial blood pressure. The response was transient, lasting for only seconds to a few minutes (27,28). Therefore, it is possible that a sudden development of sinus bradycardia and ventricular arrhythmia occurs during NPE and when coupled with a rapid increase in pulmonary blood volume causes pulmonary vascular overload and a marked, transient increase in pulmonary capillary hydrostatic pressure that ruptures the capillary-alveolar barrier.

Recent data from sheep, however, support the earlier hypothesis of

Cameron and De (16) that the initial cause of NPE is an increase in pulmonary capillary permeability produced independently of pulmonary hemodynamic alterations (11,13,51). Increasing intracranial pressure to 50 to 60 mm Hg by subdural infusion of saline caused a significant increase in both pulmonary lymph flow and the ratio of lymph to plasma protein concentration with only a small decrease or increase in left atrial pressure. Pretreatment with phentolamine prevented the increase in permeability (49). There is also evidence from studies on adipose tissue to support the hypothesis that the sympathetic nervous system controls capillary permeability (4,38). Stimulation of the nerve supply to adipose tissue in vivo caused increased microvascular permeability, in association with a decrease in mean capillary pressure, that was prevented by alpha adrenergic blockade (4).

Ultrastructural Alterations Associated with NPE

Many investigators of NPE have used light microscopy to study the associated morphologic changes. These changes, however, cannot be observed in sufficient detail with the light microscope due to its limited resolution. Therefore, electron microscopic studies are needed. Hücker et al. (37) characterized the changes in pulmonary fine structure associated with NPE following a large increase in intracranial pressure. It was found that the initial pulmonary pathology occurred at the alveolar level. The capillary endothelium and alveolar epithelium lining the thin portion of the interalveolar septum were structurally damaged. The endothelium was separated from its underlying basal lamina and showed evidence of increased pinocytotic activity. Aggregates of platelets were occasionally found adhering to

altered endothelium. The lining cells of the thick portion of the septum were intact, but the interstitial space exhibited evidence of fluid accumulation and disorganized bundles of collagen. The alveolar air space contained exudates and fibrin. Although total rupture of the capillary-alveolar barrier was occasionally observed, the tight junctions between capillary endothelial and type I epithelial cells appeared intact.

Hücker and associates (36) also attempted to trace the pathways of edema and the sites of fluid accumulation, in lungs fixed by vascular perfusion, using horseradish peroxidase (HRP, 300 mg/kg). At 1 minute after increased intracranial pressure, the reaction product was found in intercellular clefts and tight junctions of the capillary endothelium and in intercellular clefts of the type I alveolar epithelium. Reaction product accumulated evenly in the interstitium of the thick portion of the alveolar septum. At 3 minutes, the alveolar air space contained tracer particles. Although the intercellular clefts between type I epithelial cells contained reaction product, the zonulae occludens appeared intact and free of tracer particles. Nevertheless, it was suggested that the main pathway of edema was through altered tight junctions of capillary endothelium and alveolar epithelium.

Experimental models such as large increases in intracranial pressure used by Hücker and associates (36,37), unfortunately, cause fulminating pulmonary edema, and the animals usually die within minutes. Under such conditions, it is difficult to determine the morphologic changes in the lung as the syndrome develops. In addition, the use of HRP, especially in conjunction with perfusion fixation, as a vascular marker to demonstrate changes in vascular permeability has been questioned. Ultra-

structural evidence suggests that intravascular and extravascular spaces bordering the pulmonary capillary endothelium communicate through 4 nm slits in the junctions between endothelial cells (30,68). Large molecules (MW > 90,000) usually do not traverse these pores under normal capillary hydrostatic pressures, but smaller molecules such as HRP (MW of 40,000 and a diameter of 5 nm) can pass through (68). It has been demonstrated with electron microscopy and measurements of lung lymph that HRP readily crosses intact capillary endothelium under normal capillary pressures (40,52). Another study showed that HRP was confined to the capillary lumen for up to 6 min when injected in a small volume of saline, but an injection of HRP in a large volume resulted in leakage through endothelial junctions (66). Therefore, a less severe form of NPE and a larger ultrastructural tracer would facilitate the study of the morphologic changes in the lung as NPE develops.

Respiratory Disorders Associated with NPE

Intracranial hypertension, an experimental method of producing NPE, has been shown to cause arterial hypoxemia and hypercapnia. The mechanism, however, is not clear (8,39,50). A mismatch of ventilation-perfusion, atelectasis, decreased minute ventilation and alveolar and terminal bronchiolar edema have been suggested as possible causes. It has been suggested that a decrease in alveolar surface activity, which may result in atelectasis, caused the pulmonary edema that developed following placement of electrolytic lesions in the preoptic area and after cerebral compression (6,56). However, atelectasis was discounted as a cause of arterial hypoxemia through experiments in which animals were often hyper-ventilated to prevent alveolar collapse (8). Similar findings were observed

in studies on humans (53,61). Mechanical ventilation or hyperinflation of the lungs did not reverse the arterial hypoxemia. In those studies, arterial hypoxemia was attributed to a mismatch of ventilation and perfusion. However, in another study, increased minute ventilation reversed the arterial hypoxemia and hypercapnia associated with NPE produced by elevating intracranial pressure (39). It was argued that this reversal could not have occurred if an inequality of ventilation and perfusion was the cause. Alveolar and terminal bronchiolar edema might also cause or contribute to the presence of abnormal blood gases by interfering with gas exchange (39,50), although animals have become hypoxemic following an increase in intracranial pressure in the absence of pulmonary edema (39). Therefore, as evidenced by the inconsistencies in the literature, the causes of arterial hypoxemia and hypercapnia associated with NPE have not been clearly delineated.

Treatment of NPE

Therapy for NPE, as in other types of shock, is aimed at improving oxygenation with positive end expiratory pressure (PEEP) and eliminating pulmonary edema with osmotically active agents such as crystalloids and macromolecules (31,66). PEEP is also thought to increase perimicrovascular pressure that can mechanically inhibit fluid filtration caused by increased hydrostatic pressure. Whereas it is common to assume that lung water content is decreased by PEEP, some investigators claim that it is increased (66). Bo and associates (9) attempted to explain these divergent theories. They emphasized that the key factor is whether lung volume increases or remains constant during PEEP. If lung volume increases, pressures in the extra-alveolar compartment (pleural and

interstitial connective tissue) decrease relative to the pressures in the alveolar compartment (microvascular and perimicrovascular). The result is an increase in the pressure gradient across the capillary-connective tissue wall and an increase in lung water content. If lung volume remains constant, fluid filtration is always decreased as pleural pressure is increased in parallel with alveolar pressure. Staub et al. (66) showed that 10 cm of PEEP increases lung volume and pleural and pulmonary vascular pressures and does not significantly affect steady state lung lymph flows. Lung water content increased, but the change was not significantly different. Therefore, it was suggested that PEEP increases perimicrovascular pressure but at the expense of increasing microvascular pressure which enhances the filtration of fluid into the extravascular connective tissue space.

Extracting edema fluid with the use of osmotically active agents (crystalloids and macromolecules) also appears to be controversial (66). The primary goal is to increase microvascular osmotic pressure and draw the fluid from the interstitium back into the vasculature. Unfortunately, the endothelial junctions are freely permeable to crystalloids. It appears, however, that crystalloids also extract intracellular water (66). Since endothelial cells constitute approximately 30% of the interalveolar septal tissue mass (71), a substantial fraction of the extracted water probably comes from within the endothelial cells (66). Extraction of intracellular water could be important as endothelial cells are known to swell during shock, which may affect blood flow and junctional integrity (66). Macromolecules can be effective in extracting interstitial water over a period of a few hours until equilibration occurs (66). However, if the integrity of the pulmonary vasculature is compromised, administra-

tion of macromolecules may be severely detrimental.

Alternative methods for treating NPE that would reduce the hemodynamic changes and reverse the changes in permeability of the capillary-alveolar barrier are not available (66). However, corticosteroids which have been attributed with having these effects may be beneficial in the treatment of NPE (21,43,54,62). Adjunctive therapy with corticosteroids has been effective in treating hemorrhagic (43) and endotoxic (54) shock and as prophylactic therapy during cardiopulmonary bypass (22). In one report, dexamethasone appeared to maintain satisfactory pulmonary function in patients with massive cerebral trauma (1). Therefore, further study is needed to determine the efficacy of corticosteroids in preventing the development of NPE.

REFERENCES

1. Abrams, J.S., Deane, R.S. and Davis, J.H. Pulmonary function in patients with multiple trauma and associated severe head injury. *J. Trauma*, 16:543-549, 1976.
2. Almeida, H.O., Lima, E.G. and Maia, L.F. Mechanism of the acute pulmonary edema induced by intracerebroventricular injection of scorpion toxin (tityustoxin) in the unanesthetized rat. *Toxicon*, 14:435-440, 1976.
3. Baker, A.B. Poliomyelitis. 16. A study of pulmonary edema. *Neurology*, 7:743-751, 1957.
4. Ballard, K.W. Functional characteristics of the microcirculation in white adipose tissue. *Microvasc. Res.*, 16:1-18, 1978.
5. Bean, J.W. and Beckman, D.L. Centrogenic pulmonary pathology in mechanical head injury. *J. Appl. Physiol.*, 27:807-812, 1969.
6. Beckman, D.L. and Bean, J.W. Pulmonary pressure-volume changes attending head injury. *J. Appl. Physiol.*, 29:631-636, 1970.
7. Berk, J.L., Hagen, J.F., Tong, R. and Maly, G. Pulmonary insufficiency produced by norepinephrine: A comparison with epinephrine. *Circ. Shock*, 4:247-251, 1977.
8. Berman, I.R. and Ducker, T.B. Pulmonary, somatic and splanchnic circulatory responses to increased intracranial pressure. *Ann. Surg.*, 169:210-216, 1969.
9. Bo, G., Hauge, A., Nicolaysen, D. Alveolar pressure and lung volume as determinants of new transvascular fluid filtration. *J. Appl. Physiol.*, 42:476-482, 1977.
10. Bonbrest, H.C. Pulmonary edema following an epileptic seizure. *Am. Rev. Respir. Dis.*, 91:97-100, 1965.
11. Bowers, R.E., McKeen, C.R., Park, B.E. and Brigham, K.L. Increased pulmonary vascular permeability follows intracranial hypertension in sheep. *Am. Rev. Respir. Dis.*, 119:637-641, 1979.
12. Brashear, R.E. and Ross, J.C. Hemodynamic effects of elevated cerebrospinal fluid pressure: Alterations with adrenergic blockade. *J. Clin. Invest.*, 49:1324-1333, 1970.
13. Brigham, K.L. Factors affecting lung vascular permeability. *Am. Rev. Respir. Dis.*, 115:165-172, 1977.
14. Brisman, R., Kovach, R.M., Johnson, D.O., Roberts, C.R. and Ward, G.S. Pulmonary edema in acute transection of the cervical spinal cord. *Surg., Gynecol. and Obstet.*, 139:363-366, 1974.

15. Brueggemann, M.W., Loudon, R.G. and McLaurin, R.L. Pulmonary compliance changes after experimental head injury. *J. Trauma*, 16:16-20, 1976.
16. Cameron, G.R. and De, S.N. Experimental pulmonary edema of nervous origin. *J. Pathol. Bact.*, 61:375-387, 1949.
17. Campbell, G.S., Haddy, F.J., Adams, W.L. and Visscher, M.B. Circulatory changes and pulmonary lesions in dogs following increased intracranial pressure, and the effect of atropine upon such changes. *Am. J. Physiol.*, 158:96-102, 1949.
18. Campbell, G.S. and Visscher, M.B. Pulmonary lesions in guinea pigs with increased intracranial pressure and the effect of bilateral cervical vagotomy. *Am. J. Physiol.*, 157:130-134, 1949.
19. Chen, H.I., Sun, S.C. and Chai, C.Y. Pulmonary edema and hemorrhage resulting from cerebral compression. *Am. J. Physiol.*, 224:223-229, 1973.
20. Cushing, H. Concerning a definite regulatory mechanism of the vasomotor center which controls blood pressure during cerebral compression. *Bull. Johns Hopkins Hosp.*, 12:290-292, 1901.
21. Dietzman, R.H., Castaneda, A.R., Lillehei, C.W., Ersek, R.A., Motsay, G.J. and Lillehei, R.C. Corticoids as effective vasodilators in the treatment of low output syndrome. *Chest*, 57:440-453, 1970.
22. Dietzman, R.H., Lunseth, J.B., Goott, B. and Berger, E.C. The use of methylprednisolone during cardiopulmonary bypass. A review of 427 cases. *J. Thorac. Cardiovasc. Surg.*, 69:870-873, 1975.
23. Doba, N. and Reis, D.J. Acute fulminating neurogenic hypertension produced by brainstem lesions in the rat. *Circ. Res.*, 22:584-593, 1973.
24. Doba, N. and Reis, D.J. Role of central and peripheral adrenergic mechanisms in neurogenic hypertension produced by brainstem lesions in rat. *Circ. Res.*, 34:293-301, 1974.
25. Ducker, T.B. Central nervous system pressure and pulmonary edema. *Trans. Am. Neurol. Assoc.*, 92:225-227, 1967.
26. Ducker, T.B. and Simmons, R.L. Increased intracranial pressure and pulmonary edema. II. The hemodynamic response of dogs and monkeys to increased intracranial pressure. *J. Neurosurg.*, 28:118-123, 1968.
27. Estanol, B.V., Loyo, M.V., Mateos, J.H., Foyo, E., Cornejo, A. and Guevara, J. Cardiac arrhythmias in experimental subarachnoid hemorrhage. *Stroke*, 8:440-447, 1977.

28. Evans, D.E. and Gillis, R.A. Reflex mechanisms involved in cardiac arrhythmias induced by hypothalamic stimulation. *Am. J. Physiol.*, 234:H199-H209, 1978.
29. Felman, A.H. Neurogenic pulmonary edema. Observations in 6 patients. *Am. J. Roentgenol. Radium Ther. Nucl. Med.*, 112:393-396, 1971.
30. Fishman, A.P. Pulmonary edema: The water-exchanging function of the lung. *Circ.*, 46:390-408, 1972.
31. Frost, E.A.M. Respiratory problems associated with head trauma. *Neurosurg.*, 1:300-306, 1977.
32. Gamble, J.E. and Patton, H.D. Pulmonary edema and hemorrhage from preoptic lesions in rats. *Am. J. Physiol.*, 172:623-631, 1953.
33. Goodman, W.B., Leonard, J.R., Seaber, A.V., Sealy, W.C. and Nashold, B.S. Hemorrhagic pulmonary edema following stereotactic hypothalamic lesions in dogs. *Surg. Forum*, 27:472-473, 1976.
34. Graf, C.J. and Rossi, N.P. Catecholamine response to intracranial hypertension. *J. Neurosurg.*, 49:862-868, 1978.
35. Hoff, J.T. and Nishimura, M. Experimental neurogenic pulmonary edema in cats. *J. Neurosurg.*, 48:383-389, 1978.
36. Hücker, H., Frenzel, H., Kremer, B. and Richter, I.E. Time sequence and site of fluid accumulation in experimental neurogenic pulmonary edema. *Res. Exp. Med.*, 168:219-227, 1976.
37. Hücker, H., Schäfer, U. and Meinen, K. Early morphological alterations of the rat lung with increased intracranial pressure. I. A light and electron microscopic study. *Virchows Arch. A. Path. Anat. Histol.*, 362:331-342, 1974.
38. Intaglietta, M. and Rosell, S. Capillary permeability and sympathetic activity in canine subcutaneous adipose tissue. *Nature*, 249:481-482, 1974.
39. Jennett, S. and Hoff, J.T. Arterial blood gases during raised intracranial pressure in anesthetized cats under controlled ventilation. *J. Neurosurg.*, 48:390-401, 1978.
40. Karnovsky, M.J. The ultrastructural basis of capillary permeability studied with peroxidase as a tracer. *J. Cell. Biol.*, 35:213-236, 1967.
41. Katsurada, K., Yamada, R. and Sugimoto, T. Respiratory insufficiency in patients with severe head injury. *Surg.*, 73:191-199, 1973.

42. Korner, P. The effect of noradrenaline-induced systemic vasoconstriction on the formation of pulmonary edema. *Aust. J. Exp. Biol. Med. Sci.*, 31:405-423, 1953.
43. Kusajima, K., Wax, S.D. and Webb, W.R. Effects of methylprednisolone on pulmonary microcirculation. *Surg., Gynecol. and Obstet.*, 139:1-5, 1974.
44. Lloyd, T.C., Jr. Effect of increased intracranial pressure on pulmonary vascular resistance. *J. Appl. Physiol.*, 35:332-335, 1973.
45. Luisada, A.A. Mechanism of neurogenic pulmonary edema. *Am. J. Cardiol.*, 20:66-68, 1967.
46. MacKay, E.M. Experimental pulmonary edema. IV. Pulmonary edema accompanying trauma to the brain. *Proc. Soc. Exp. Biol. Med.*, 74:695-697, 1950.
47. Maire, F.W. and Patton, H.D. Neural structures involved in the genesis of 'preoptic pulmonary edema', gastric erosions and behavior changes. *Am. J. Physiol.*, 184:345-350, 1956.
48. Maire, F.W. and Patton, H.D. Role of the splanchnic nerve and the adrenal medulla in the genesis of 'preoptic pulmonary edema'. *Am. J. Physiol.*, 184:351-355, 1956.
49. Malik, A.B. Personal communication.
50. Malik, A.B. Pulmonary vascular response to increase in intracranial pressure: role of sympathetic mechanisms. *J. Appl. Physiol.: Respir. Environ. Exercise Physiol.*, 42:335-343, 1977.
51. Malik, A.B., Lee, B.C., van der Zee, H. and Johnson, A. Mechanism of neurogenic pulmonary edema. *Am. Rev. Respir. Dis.*, 117:367, 1978.
52. Michel, R.P., Inque, S. and Hogg, J.C. Pulmonary capillary permeability to HRP in dogs: A physiological and morphological study. *J. Appl. Physiol.: Respir. Environ. Exercise Physiol.*, 42:13-21, 1977.
53. Moss, I.R., Wald, A. and Ransohoff, J. Respiratory functions and chemical regulation of ventilation in head injury. *Am. Rev. Respir. Dis.*, 109:205-215, 1974.
54. Motsay, G.J., Alho, A., Jaeger, T., Schultz, L.S., Dietzman, R.H. and Lillehei, R.C. Effects of methylprednisolone, phenoxybenzamine, and epinephrine tolerance in canine endotoxin shock: Study of isogravimetric capillary pressures in forelimb and intestine. *Surg.*, 70:271-279, 1971.

55. Nathan, M.A. and Reis, D.J. Fulminating arterial hypertension with pulmonary edema from release of adrenomedullary catecholamines after lesions of the anterior hypothalamus in the rat. *Circ. Res.*, 37:226-235, 1975.
56. Park, C.D. and Sutnick, A.I. Pulmonary surface activity alterations associated with pulmonary edema following preoptic hypothalamic lesions in rats. *Proc. Soc. Exp. Biol. Med.*, 142:1025-1030, 1973.
57. Reynolds, R.W. Pulmonary edema as a consequence of hypothalamic lesions in rats. *Science*, 141:930-932, 1963.
58. Sarnoff, S.J. and Berglund, E. Neurohemodynamics of pulmonary edema. IV. Effect of systemic vasoconstriction and subsequent vasodilation on flow and pressures in systemic and pulmonary vascular beds. *Am. J. Physiol.*, 170:588-600, 1952.
59. Sarnoff, S.J., Berglund, E. and Sarnoff, C. Neurohemodynamics of pulmonary edema. III. Estimated changes in pulmonary blood volume accompanying systemic vasoconstriction and vasodilation. *J. Appl. Physiol.*, 5:367-374, 1953.
60. Sarnoff, S.J. and Sarnoff, L.C. Neurohemodynamics of pulmonary edema. II. The role of sympathetic pathways in the elevation of pulmonary and systemic vascular pressures following the intracisternal injection of fibrin. *Circ.*, 6:51-62, 1952.
61. Schumacker, P.T., Rhodes, G.R., Newell, J.C., Dutton, R.E., Shah, D.M., Scovill, W.A. and Powers, S.R. Ventilation-perfusion imbalance after head trauma. *Am. Rev. Respir. Dis.*, 119:33-43, 1979.
62. Schumer, W. and Nyhus, L.M. The role of corticoids in the management of shock. *Surg. Clin. N. Amer.*, 49:147-161, 1969.
63. Seager, L.D. and Wood, C.D. Aconitine induced pulmonary edema. *Proc. Soc. Exp. Biol. Med.*, 111:120-121, 1962.
64. Shepherd, J.T. and Vanhoutte, P.M. Role of the venous system in circulatory control. *Mayo Clin. Proc.*, 53:247-255, 1978.
65. Simmons, R.L., Martin, A.M., Jr., Heisterkamp, C.A., III, and Ducker, T.B. Respiratory insufficiency in combat casualties: II. Pulmonary edema following head injury. *Ann. Surg.*, 170:39-44, 1969.
66. Staub, N.C. Pulmonary edema due to increased microvascular permeability to fluid and protein. *Circ. Res.*, 43:143-151, 1978.
67. Staub, N.C. "State of the Art" review. Pathogenesis of pulmonary edema. *Am. Rev. Respir. Dis.*, 109:358-372, 1974.
68. Szidon, J.P., Pietra, G.G. and Fishman, A.P. The alveolar-capillary membrane and pulmonary edema. *New Eng. J. Med.*, 286:1200-1204, 1972.

69. Theodore, J. and Robin, E.D. Speculations on neurogenic pulmonary edema (NPE). *Am. Rev. Respir. Dis.*, 113:405-411, 1976.
70. Urabe, M., Segawa, Y., Tsubokawa, T., Yamamoto, K., Araki, K. and Izumi, K. Pathogenesis of the acute pulmonary edema occurring after brain operation and brain trauma. *Jap. Heart J.*, 2:147-169, 1961.
71. Weibel, E.R. and Knight, B.W. A morphometric study on the thickness of the pulmonary air-blood barrier. *J. Cell Biol.*, 21:367-384, 1964.
72. Weisman, S.J. Edema and congestion of the lungs resulting from intracranial hemorrhage. *Surg.*, 6:722-729, 1939.
73. Wood, C.D., Seager, L.D. and Ferrell, G. Influence of autonomic blockade on aconitine induced pulmonary edema. *Proc. Soc. Exp. Biol. Med.*, 116:809-811, 1964.
74. Worthen, M., Argano, B., Siwaslowski, W., Bruce, D.W., MacCanon, D.M. and Luisada, A.A. Epinephrine-induced pulmonary edema in cross circulated animals. *Jap. Heart. J.*, 10:142-148, 1969.
75. Wray, N.P. and Nicotra, M.B. Pathogenesis of neurogenic pulmonary edema. *Am. Rev. Respir. Dis.*, 118:783-788, 1978.

PAPER 1

A Comparison of Changes in Pulmonary Ultrastructure
in Mild and Severe Forms of Aconitine-Induced
Neurogenic Pulmonary Edema

ABSTRACT

Neurogenic pulmonary edema (NPE) of varying severity was induced in rats by injecting different doses of aconitine into the preoptic area of the brain. Those animals injected with 1058 pmoles/kg or more developed severe pulmonary edema and were dead or dyspneic at 1 h. The lungs of these animals were completely covered with hemorrhages, and the ratios of lung weight to body weight (LW/BW) were between 1.00 and 1.86. A mild form of NPE followed the administration of 423 pmoles/kg or less. In these animals, the LW/BWs were less than 1.00, and the rats were conscious and ambulatory at 1 h and were not dyspneic. The animals receiving the intermediate dose of 774 pmoles/kg exhibited more variation in response. LW/BWs in half of these rats were high and half were low. Therefore, 774 pmoles/kg was considered the approximate median effective dose for aconitine-induced NPE in rats.

Lung biopsies were examined with the electron microscope. Fibrin and exudates were observed in the alveoli of all rats injected with doses of 194 pmoles/kg of aconitine or greater. In the most severe form of the syndrome, both the capillary endothelium and the type I alveolar epithelium were severely damaged, whereas in the mild form intact capillary endothelium was found in association with damaged type I epithelium. The reason for the differential sensitivity of type I epithelium and capillary endothelium in NPE cannot be determined from the present study.

INTRODUCTION

Pulmonary edema is associated with various injuries to the brain or spinal cord (32,35,40). The severity of this syndrome, known as neurogenic pulmonary edema (NPE), is variable (12,32,35,40). In a mild form, it is transient and there may be little or no impairment of pulmonary function. However, in more severe forms, the amount of edema is significant, pulmonary function is rapidly compromised, and the patients often die. Under these conditions, it has been difficult to determine its pathogenesis in humans. Several experimental models of NPE have been developed in animals using large increases in intracranial pressure (6,15), cerebral compression (7), blunt cerebral trauma (2,21) or hypothalamic injections of a lethal dose of aconitine (31,39). Such procedures lead to transient increases in systemic and pulmonary blood pressures (10,22,30,39) and pulmonary blood volume (4,10,18,30), persistent increases in microvascular permeability (3,5,23,40) and lung water content (22,35) and severe alterations of the pulmonary ultrastructure (14,15). Unfortunately, these methods of producing NPE cause the syndrome to develop rapidly, and the experimental animals usually die within minutes. Therefore, these models have had limited value in studies designed to determine the sequence of events leading to the development of NPE.

Recently, it has been shown that moderate increases in intracranial pressure in sheep produce mild forms of NPE that do not cause immediate death (3,5,22). In the present study, NPE of varying severity was also induced in rats by injecting different doses of aconitine into the preoptic area of the brain. In this way, it was possible to compare changes in the ultrastructure of the lungs in animals with mild and severe forms of NPE.

MATERIALS AND METHODS

Aconitine (Sigma), aconitine nitrate or saline was injected into the preoptic area in 42 adult female Charles River (CD) and King rats (220-276 g) under light ether anesthesia. With the aid of a stereotaxic instrument, a 22 gauge stainless steel guide tube was positioned 1.3 mm anterior to bregma, 0.7 mm lateral from midline and 2.85 mm below the cortical surface. A 50 μ l Hamilton syringe connected by 10 mm of polyethylene tubing to a 28 gauge stainless steel cannula was lowered through and extended 5 mm past the guide tube into the preoptic area. Varying doses of aconitine or aconitine nitrate, as shown in Fig. 1, were prepared fresh in saline and injected manually in a volume of 100 μ l/kg within 15 sec. The same procedure was repeated contralaterally within 2 min. Six rats received only the saline vehicle in the preoptic area and served as sham-operated controls. In addition, 3 rats were injected iv with aconitine (1550, 3100 or 6200 pmoles/kg) to determine whether the drug had a direct effect on the lungs. Body weights were recorded pre- and postoperatively to determine the amount of blood loss due to surgical procedures. Those animals with a loss of 12% or more of their calculated blood volume were rejected from the study since hypovolemia prevents the development of NPE (26).

Animals that survived 1 h after administration of aconitine were anesthetized with ether and killed by severing the abdominal aorta. Those animals that stopped breathing before 1 h were autopsied immediately. The thoracic cavity was opened, and the lungs were excised and weighed to the nearest 0.1 g. A lung weight to body weight ratio (LW/BW) was calculated (lung weight/body weight \times 100) for each rat and used as an index of pulmonary edema. The extent of grossly visible hemorrhages

on the lungs was graded on a 0 to 5 scale using the criteria described in Table 1. The upper and lower lobes of the right and left lungs were biopsied. The tissues were cut into 1 mm cubes and fixed for 1 h in 3% glutaraldehyde buffered to pH 7.38 with 0.1 M sodium cacodylate. Following a 10 min rinse in 0.1 M sodium cacodylate, the tissues were postfixed for 1 h in 1% osmium tetroxide buffered to pH 7.38 with 0.1 M sodium cacodylate, dehydrated in a graded series of acetone and embedded in Epon 812. Thin sections were cut with a diamond knife on a LKB ultratome, mounted on 300 mesh grids, stained with uranyl acetate and lead citrate to enhance contrast and examined with a Philips 301 electron microscope. The pulmonary ultrastructure was examined separately by the authors, and pathologic changes were graded subjectively on a 0 to 5 scale using the criteria described in Table 2.

Brains were removed at autopsy and fixed in formalin. The placements of injections in the preoptic area were verified histologically on alternate frozen sections (50 μ m) stained with thionin (Fig. 2). Animals with injection sites located outside the preoptic-anterior hypothalamic area were rejected from the study.

Systemic arterial blood pressure (SAP) was measured in a second group of 33 rats, weighing 276-343 g, that were injected with 387 (7 rats), 774 (11 rats) and 1550 pmoles/kg (10 rats) of aconitine or saline (3 rats) as described above. In addition, 2 rats were injected iv with 1550 pmoles/kg of aconitine. The tail artery was cannulated with PE-50 tubing, and the SAP was measured by a Statham P23Db strain gauge and recorded with a Grass Model 79D polygraph. The patency of the cannula was maintained by continuous infusion (0.5 ml/h) of 1% heparinized saline through a Sorenson valve. After injection of aconitine or saline, the

rats were transferred to a cage that restricted movement, and the SAP was continuously monitored. At 1 h, the animals were autopsied as described above except that lung tissues were not processed for electron microscopy.

Statistical Analysis

The LW/BWs of rats injected with aconitine or aconitine nitrate were shown to be similar by analysis of covariance and a Bartlett's test and were combined. One-way analysis of variance and the Newman-Keuls' multiple-range test were used to compare the effects of treatments on LW/BWs.

The systolic and diastolic blood pressures were averaged at each minute for the first 20 min after injection. The effects of varying the dose of aconitine on these blood pressures were analyzed with a two-way analysis of variance for repeated measures (38) and the Newman-Keuls' multiple range test. The rate of increase in SAP was determined using regression analysis. Correlation analysis was used to study the relationships between LW/BW and rate of change in SAP. Differences were considered significant at $P < 0.05$.

RESULTS

The effect of increases in dose of aconitine or aconitine nitrate on LW/BW is shown in Fig. 1. LW/BWs were comparable in sham-operated controls (0.53 ± 0.03 , mean \pm SEM) and in animals that received the lowest dose of aconitine (0.54 ± 0.03) and increased to 1.41 ± 0.13 with the highest dose. The data fitted a sigmoidal log dose-effect curve as shown by regression analysis ($y = ax^3 + bx^2 + cx + d$, $r = 0.85$, $P < 0.01$). Animals injected with aconitine iv had LW/BWs (0.53 ± 0.04) comparable to those of sham-operated controls. Thus, the effect of aconitine on LW/BW appears to

be mediated by actions exerted on the central nervous system and not directly on the lungs.

Of the 13 rats injected with doses of 1058 pmoles/kg or greater, 10 frothed profusely from the nose and died before 1 h. Animals that received 423 pmoles/kg or less were conscious, upright and ambulatory at 1 h. Therefore, doses of 1058 pmoles/kg or greater are designated as lethal and those of 423 pmoles/kg or less as sublethal. Animals injected with doses of 774 and 846 pmoles/kg showed more variation in response; 2 had high LW/BWs similar to animals given a lethal dose, and 5 had low LW/BWs similar to animals injected with a sublethal dose. In subsequent experiments on 24 rats injected with 774 pmoles/kg, half had high (1.40 ± 0.08) and half low (0.67 ± 0.05) LW/BWs. Therefore, this dose was considered the approximate median effective dose (ED50).

Changes in Gross Appearance and Ultrastructure of the Lungs

The extent of grossly visible hemorrhages and the ultrastructural changes of the lungs generally increased in severity with an increase in dose (Table 3). However, since some variation in response was seen at all doses, these alterations were more closely related to the amount of change in LW/BW (Table 4). The lungs appeared normal, both grossly and ultrastructurally, in rats with LW/BWs under 0.77 (Figs. 3 and 4). Focal changes in gross appearance and ultrastructure were noted in rats injected with sublethal doses or the ED50 of aconitine and had LW/BWs which ranged between 0.77 and 1.14. In these animals, the surfaces of the lungs were covered with a few punctate hemorrhages (Fig. 5). At the cellular level, type I alveolar epithelial cells were rarefied, swollen and often discontinuous, exposing the underlying basal lamina, and were usually found adjacent to intact capillary endothelium (Figs.

6,7,8 and 9). Occasionally, the capillary endothelium was separated from its underlying basal lamina and protruded into the capillary lumen (Fig. 10). Small amounts of exudates, composed of plasma and cellular debris, and fibrillar protein were frequently observed in the alveolar air spaces. It seems likely that the clotting mechanism was activated because of the observed cellular damage, and, therefore, it is assumed that the fibrillar protein was fibrin rather than aggregated or precipitated fibrinogen (34,36).

Similar, but more severe and widespread pathology was observed in rats injected with lethal doses of aconitine or with LW/BWs greater than 1.35. In these animals, the lungs were completely covered with punctate hemorrhages (Fig. 11), and the lung parenchyma showed marked hepatization indicative of severe consolidation. Examination of the fine structure revealed that capillary endothelial changes were as severe but not as widespread as those involving type I epithelium. The capillary endothelial and type I epithelial cells were frequently absent or appeared as spherical blebs adjacent to the denuded basal lamina (Figs. 9,12 and 13). Fibrin and exudates were observed in the alveolar air spaces adjacent to damaged type I epithelial cells, and fibrin was also observed interwoven with degranulated platelets in the capillary lumen (Fig. 14).

Granular precipitates, indicative of interstitial edema, and aggregates of platelets and leukocytes were rarely observed. Type II epithelium appeared unaltered, and frank ruptures of the capillary-alveolar barrier were not observed.

Systemic Arterial Blood Pressure

Systolic (Fig. 15a) and diastolic (Fig. 15b) blood pressures decreased

by 30 mm Hg immediately after injection of aconitine and began to rise rapidly after 2 min. The magnitude of the SAP response did not differ between doses; however, the rate of increase was greater as the dose of aconitine was increased. Mean systolic blood pressures of rats injected with a lethal dose were significantly greater ($P < 0.05$) from 5 to 10 min than those of animals given a sublethal dose (Table 5); the time to reach peak systolic blood pressure was almost twice as long in animals injected with a sublethal dose. Diastolic blood pressures also differed ($P < 0.05$) from 5 to 13 min between the lethal and sublethal doses (Table 6). Since the mean LW/BWs for rats that received the sublethal dose were significantly lower than for those receiving the lethal dose, it appeared that the rate of increase in SAP was correlated with LW/BW. When group data were analyzed, the correlation coefficient approached significance ($r=0.985$, $df=1$). However, when data from individual animals were compared, the correlation coefficient was low ($r=0.10$). Furthermore, the rates of increase in SAP for animals with low and high LW/BWs in the intermediate dose or ED50 were comparable. Thus, it appears that the rate of increase in SAP does not predict the change in LW/BW in a given animal.

SAP decreased from 5 to 15 mmHg after injection of saline in sham-operated controls and returned to pre-anesthetic levels within 10 to 50 min. This finding suggests that the initial decrease in SAP after injection of aconitine is an effect of the injection procedure and is probably not a specific effect of aconitine. When aconitine (1550 pmoles/kg) was injected iv, the blood pressure dropped from 145/114 to 120/100 in 1 rat, whereas the SAP in the other rat did not change. Thus, the effects of aconitine on SAP and LW/BW appear to be mediated

by actions exerted on the central nervous system and not directly on the lungs.

DISCUSSION

In the present study, NPE of varying severity was produced by injecting different doses of aconitine into the preoptic area of the brain. The syndrome in its most severe form was characterized by rapid increases in SAP, high LW/BWs, respiratory distress and death. These findings are in agreement with those of Seager and Wood (31,39). In addition, it was found that a dose-response relationship existed between the dose of aconitine used and the change in LW/BW and the rate of increase in SAP. The extent of grossly visible hemorrhages and ultrastructural changes of the lungs also generally increased in severity with an increase in dose of aconitine but were more closely related with the amount of change in LW/BW.

Increases in LW/BW indicate fluid accumulation in the lungs and have been used to provide a measure of the severity of pulmonary edema (2,7,31). The maximum LW/BWs observed and reported in this study (> 1.00 and up to 1.86), in animals that were dead or dyspneic at 1 h, were comparable to those reported by Seager and Wood (31,39) and occurred with doses of aconitine of 1058 pmoles/kg or greater. A mild form of NPE followed the injection of 423 pmoles/kg of aconitine; the LW/BWs were lower (< 1.00), and the rats were conscious and ambulatory at 1 h and were not dyspneic. Animals injected with 774 pmoles/kg of aconitine exhibited more variation in responses. That the variation was due to differences in the strength of the drug on a day-to-day basis was discounted because animals injected from the same freshly-prepared stock solution responded at the opposite extremes. There was no reason

to believe that the strength of the drug deteriorated during the 6 h of experimentation because rats responded similarly at the beginning or at the end of the experimental period. Therefore, 774 pmoles/kg was considered the approximate ED50 for aconitine-induced NPE in rats.

The present finding that both the capillary endothelium and the type I epithelium were severely damaged in a severe form of NPE is in agreement with that reported by Hücker et al. (15). However, the consistent finding that type I cells were damaged in the presence of intact capillary endothelial cells in the mild form of NPE was unexpected. In other types of shock (11,13,17,24,27), the capillary endothelium has been shown to be more susceptible to injury than the alveolar epithelium. Once the endothelium is damaged, the alveolar epithelium becomes the limiting barrier between the capillary lumen and the air space. If the pulmonary insult is severe enough, the alveolar epithelium may also be altered, possibly due to a metabolic defect, resulting in alveolar edema.

The reason for the differential sensitivity of the type I epithelium and capillary endothelium in a mild form of NPE cannot be determined from the present study. However, possible explanations include: 1) a direct toxic effect of aconitine on type I cells; 2) a colloid osmotic effect of alveolar exudates; 3) an impairment of metabolic processes caused by a reduction in required nutrients; or 4) a difference in the level of metabolic activity.

The possibility that a direct toxic effect of aconitine was responsible for selectively damaging type I cells was ruled out because the injection of lethal doses of aconitine into the systemic circulation did not damage either type of cell. The accumulation of fibrin, exudates

and transudates in the alveoli may also have a direct toxic effect on type I cells, or as suggested by Hücker et al. (15), may damage the cells by means of a colloid osmotic effect. However, Kistler (17) has shown that type I cells were unaffected when exposed to exudates and fibrin in the air spaces for 6 h. Thus, it seems unlikely that either a direct toxic effect of exudates and fibrin or a colloid osmotic effect is responsible for damaging type I epithelium.

Chiu (8) has suggested that the reduction in availability of oxygen and metabolic substrates is responsible for the early degeneration of epithelial cells that occurs in various organs during "low flow states". Degeneration of type I cells may also occur early in the "shock lung syndrome" due to the presence of alveolar exudates that cause collapse of the air spaces and the subsequent shunting of blood away from the affected area (1,19,28). Consequently, the type I cells may be deprived of nutrients from both capillary and alveolar sides. The presence of alveolar exudates in association with damaged type I cells in the present study is compatible with such a mechanism in NPE as well. That the capillary endothelium generally appeared intact in mild NPE suggests that it survives because of its proximity to a source of nutrients or because it has a lower requirement for oxygen and metabolites than the type I epithelium. It was of interest that, in the present study and in the study by Hücker et al. (15), the type II alveolar epithelium was for the most part intact. That this cell is rich in organelles and appears to be metabolically self-sufficient (37) lends support to the idea that the rapid development of NPE adversely affects the metabolic activity of type I cells.

The observation in the present study that fibrin and exudates

were present in the alveolar air space in the absence of frank ruptures of the capillary-alveolar barrier demonstrates that this barrier became permeable to plasma proteins. Although it has been suggested that the pathway of edema in NPE is through loosened junctions of microvascular endothelium and alveolar epithelium (14,33), the mechanism by which permeability is increased is not known. It has been proposed that the release of substances such as histamine, a direct neural effect via adrenergic pathways or secondary metabolic changes in the cells are responsible (3,5,23). Since the alveolar air space was the main site of fibrin deposition, it seems likely that the increase in permeability of the capillary-alveolar barrier allowed fibrinogen to enter the air space, where it was exposed to damaged type I cells and/or denuded basal lamina and thus converted to fibrin. It is also possible that fibrin was formed in the blood vessels and was deposited in the alveoli through available openings in the capillary-alveolar barrier. However, fibrin has been shown to increase the permeability of endothelial junctions, as measured by the protein concentrations in lung lymph and pulmonary interstitial fluid, after iv infusion of thrombin (9) and has been observed within some of these junctions. These investigators have also identified a "permeability increasing factor" that may be a degradation product of fibrin and that is released slowly from fibrin microemboli (20,29). It has been postulated that fibrin increases the permeability of vascular endothelial cells by causing these cells to migrate and thus disrupting the structure of the junction (16). In that study, it was shown that separation between endothelial cells occurs within 1 h after contact with a fibrin clot and within 3 to 6 h, the monolayer appearance of normal endothelium changes to a random

distribution of individual cells. However, since fibrin was found in the alveolar air spaces as early as 3 min after injection of aconitine (25) and because the effect of fibrin on permeability appears delayed (29), it seems unlikely that fibrin is responsible for the leakage of plasma proteins observed in this study.

The present findings that the magnitude of the SAP response in rats injected with a lethal, ED50 or sublethal dose reached comparable maximum values and that the average rate of increase in SAP was different between animals given lethal and sublethal doses are in agreement with those reported by Chen et al. (7). In that study, it was shown that the severity of the pulmonary changes, in response to rapid or slow compression of the brain or rapid or slow infusion of norepinephrine, is not related to the magnitude of the increase in SAP. However, the rate of increase in SAP was found to be greater after rapid compression of the brain or rapid infusion of norepinephrine, and the pulmonary changes in these animals were more severe than those occurring after slow application of either stimulus. It was suggested that a slower activation of sympathetic mechanisms may allow time for the cardiovascular system to adjust to the altered systemic and pulmonary blood pressures and the increase in pulmonary blood volume.

In contrast to the results of Chen and associates (7), in the present study no correlation was found between the rate of increase in SAP and the change in LW/BW in individual animals. The basis for the discrepancy is not known, but it appears to be related to the use of group data by Chen et al. (7) and data from individual animals in the present study. Thus, it is suggested that changes in SAP do not predict the severity of NPE in an individual animal. Other indices

such as pulmonary blood pressures, blood volume and vascular permeability may be more useful in predicting the severity of the pulmonary response to various injuries of the central nervous system.

The present findings demonstrate that NPE produced by injecting aconitine into the preoptic area of the brain can be varied between a mild and severe form of the syndrome. The most interesting observations were made in the mild form of NPE; fibrin was present in the alveolar air spaces and damaged type I cells were consistently found in association with intact endothelium. Although the presence of fibrin and exudates in the alveoli in the absence of frank ruptures of the capillary-alveolar barrier indicates that it became permeable to plasma proteins, further study is needed to determine the route taken by plasma from the vascular to the alveolar air space.

REFERENCES

1. Albert, R. K., Lakshminarayan, S., Hildebrandt, J., Kirk, W. and Butler, J. Increased surface tension favors pulmonary edema formation in anesthetized dogs' lungs. *J. Clin. Invest.*, 63: 1015-1018, 1979.
2. Bean, J. W. and Beckman, D. L. Centrogenic pulmonary pathology in mechanical head injury. *J. Appl. Physiol.*, 27: 807-812, 1969.
3. Bowers, R. E., McKeen, C. R., Park, B. E. and Brigham, K. L. Increased pulmonary vascular permeability follows intracranial hypertension in sheep. *Am. Rev. Respir. Dis.*, 119: 637-641, 1979.
4. Brashear, R. E. and Ross, J. C. Hemodynamic effects of elevated cerebrospinal fluid pressure: Alterations with adrenergic blockade. *J. Clin. Invest.*, 49: 1324-1333, 1970.
5. Brigham, K. L. Factors affecting lung vascular permeability. *Am. Rev. Respir. Dis.*, 115: 165-172, 1977.
6. Campbell, G. S. and Visscher, M. B. Pulmonary lesions in guinea pigs with increased intracranial pressure and the effect of bilateral cervical vagotomy. *Am. J. Physiol.*, 157: 130-134, 1949.
7. Chen, H. I., Sun, S. C. and Chai, C. Y. Pulmonary edema and hemorrhage resulting from cerebral compression. *Am. J. Physiol.*, 224: 223-229, 1973.
8. Chiu, C. J. Epithelial lesions in low flow states: A unifying concept. *Med. Hypotheses*, 3: 159-161, 1977.
9. Costabella, P. M., Lindquist, O., Kapanci, Y. and Saldeen, T. Increased vascular permeability in the delayed microembolism syndrome: Experimental and human findings. *Microvasc. Res.*, 15: 275-286, 1978.
10. Ducker, T. B. and Simmons, R. L. Increased intracranial pressure and pulmonary edema. II. The hemodynamic response of dogs and monkeys to increased intracranial pressure. *J. Neurosurg.*, 28: 118-123, 1968.
11. Freudenberg, N. Endothelium and shock. *Path. Res. Pract.*, 162: 105-114, 1978.
12. Frost, E. A. M. Respiratory problems associated with head trauma. *Neurosurg.*, 1: 300-306, 1977.
13. Harrison, M. W., Connell, R. S., Campbell, J. R. and Webb, M. C. Microcirculatory changes in the lung of the hypoxic and hypovolemic puppy: An electron microscope study. *Ann. Surg.*, 185: 311-317, 1977.

14. Hücker, H., Frenzel, H., Kremer, B. and Richter, I. E. Time sequence and site of fluid accumulation in experimental neurogenic pulmonary edema. *Res. Exp. Med.*, 168: 219-227, 1976.
15. Hücker, H., Schäfer, U. and Meinen, K. Early morphological alterations of the rat lung with increased intracranial pressure. I. A light and electron microscopic study. *Virchows Arch. A. Path. Anat. Histol.*, 362: 331-342, 1974.
16. Kadish, J. L., Butterfield, C. E. and Folkman, J. The effect of fibrin on cultured vascular endothelial cells. *Tissue and Cell*, 11: 99-108, 1979.
17. Kistler, G. S., Caldwell, P. R. B. and Weibel, E. R. Development of fine structural damage to alveolar and capillary lining cells in oxygen-poisoned rat lungs. *J. Cell Biol.*, 32: 605-628, 1967.
18. Korner, P. The effect of noradrenaline-induced systemic vasoconstriction on the formation of pulmonary edema. *Aust. J. Exp. Biol. Med. Sci.*, 31: 405-423, 1953.
19. Levitsky, S., Annable, C. A., Park, B. S., Davis, A. L. and Thomas, P. A. Depletion of alveolar surface active material by transbronchial plasma irrigation of the lung. *Ann. Surg.*, 173: 107-115, 1971.
20. Lindquist, O., Saldeen, T., Svensjo, E. and Wallin, R. On the cause of increased vascular permeability in the delayed microembolism syndrome. 9th Europ. Conf. Microcirc., Antwerp 1976. *Bibl. Anat.*, No. 16, pp. 409-411 (Karger, Basel 1977).
21. MacKay, E. M. Experimental pulmonary edema. IV. Pulmonary edema accompanying trauma to the brain. *Proc. Soc. Exp. Biol. Med.*, 74: 695-697, 1950.
22. Malik, A. B. Pulmonary vascular response to increase in intracranial pressure: role of sympathetic mechanisms. *J. Appl. Physiol.: Respirat. Environ. Exercise Physiol.*, 42: 335-343, 1977.
23. Malik, A. B., Lee, B. C., van der Zee, H. and Johnson, A. Mechanism of neurogenic pulmonary edema. *Am. Rev. Respir. Dis.*, 117: 367, 1978.
24. Meyrick, B., Miller, J. and Reid, L. Pulmonary edema induced by ANTU, or by high or low oxygen concentrations in rat - an electron microscopic study. *Br. J. Exp. Pathol.*, 53: 347-358, 1972.
25. Minnear, F. L. and Connell, R. S. Alterations in the capillary-alveolar barrier associated with increased permeability in aconitine-induced neurogenic pulmonary edema. Manuscript in preparation.
26. Minnear, F. L. and Connell, R. S. Prevention of aconitine-induced neurogenic pulmonary edema by phlebotomy or pretreatment with methylprednisolone sodium succinate. Manuscript in preparation.

27. Riede, U. N., Joachim, H., Hassenstein, J., Costabel, U., Sandritter, W., Augustin, P. and Mittermayer, C. H. The pulmonary air-blood barrier of human shock lungs (a clinical, ultrastructural and morphometric study). *Path. Res. Pract.*, 162: 41-72, 1978.
28. Said, S. I., Avery, M. E., Davis, R. K., Banerjee, C. M. and El-Gohary, M. Pulmonary surface activity in induced pulmonary edema. *J. Clin. Invest.*, 44: 458-464, 1965.
29. Saldeen, T. The microembolism syndrome. *Microvasc. Res.*, 11: 227-259, 1976.
30. Sarnoff, S. J. and Berglund, E. Neurohemodynamics of pulmonary edema. IV. Effect of systemic vasoconstriction and subsequent vasodilation on flow and pressures in systemic and pulmonary vascular beds. *Am. J. Physiol.*, 170: 588-600, 1952.
31. Seager, L. D. and Wood, C. D. Aconitine induced pulmonary edema. *Proc. Soc. Exp. Biol. Med.*, 111: 120-121, 1962.
32. Simmons, R. L., Martin, A. M., Jr., Heisterkamp, C. A., III and Ducker, T. B. Respiratory insufficiency in combat casualties: II. Pulmonary edema following head injury. *Ann. Surg.*, 170: 39-44, 1969.
33. Staub, N. C. Pulmonary edema due to increased microvascular permeability to fluid and protein. *Circ. Res.*, 43: 143-151, 1978.
34. Stryer, L., Cohen, C. and Langridge, R. Axial period of fibrinogen and fibrin. *Nature*, 197: 793-794, 1963.
35. Theordore, J. and Robin, E. D. Speculations on neurogenic pulmonary edema (NPE). *Am. Rev. Respir. Dis.*, 113: 405-411, 1976.
36. Tooney, N. M. and Cohen, C. Crystalline states of a modified fibrinogen. *J. Mol. Biol.*, 110: 363-385, 1967.
37. Weibel, E. R. The ultrastructure of the alveolar-capillary membrane or barrier. In: *The Pulmonary Circulation and Interstitial Space*. Ed. by Fishman, A. P. and Hecht, H. H. Univ. Chicago Press: Chicago, London, pp. 9-27, 1969.
38. Winer, B. J. *Statistical Principles in Experimental Design*. McGraw Hill: New York, 1962.
39. Wood, C. D., Seager, L. D. and Ferrell, G. Influence of autonomic blockade on aconitine induced pulmonary edema. *Proc. Soc. Exp. Biol. Med.*, 116: 809-811, 1964.
40. Wray, N. P. and Nicotra, M. B. Pathogenesis of neurogenic pulmonary edema. *Am. Rev. Respir. Dis.*, 118: 783-786, 1978.

Fig. 1. The effect of increasing the dose of aconitine, injected into the preoptic area, on LW/BW. Values are mean \pm SEM (3-6 rats/group).

Pulmonary Response at One Hour to Preoptic Injections of Aconitine and Aconitine Nitrate

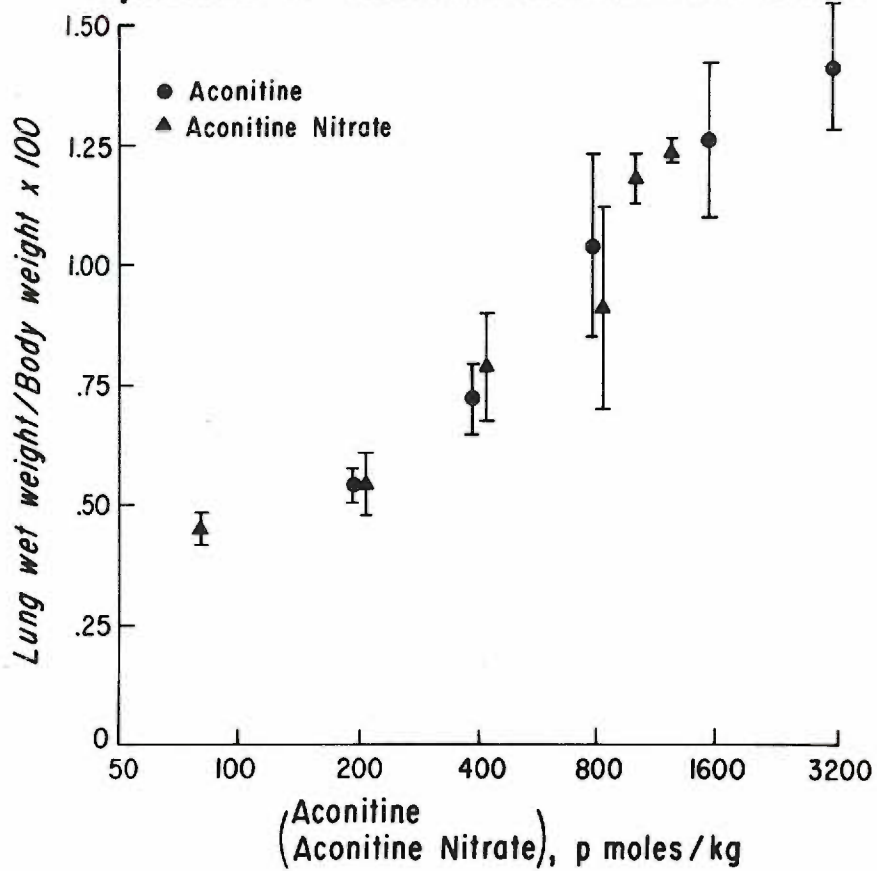


Table 1. Criteria for grading pathologic changes in gross appearance of the lungs

| <u>Grade*</u> | <u>Criterion</u> |
|---------------|--|
| 1 | Punctate hemorrhages restricted to 1 lobe |
| 2 | Punctate hemorrhages restricted to 2 lobes (Fig. 5**) |
| 3 | Punctate hemorrhages partially covering all lobes |
| 4 | Punctate hemorrhages covering all lobes except at the angles |
| 5 | Punctate hemorrhages completely covering all lobes (Fig. 11) |

*A grade of 0 designates normal appearing lungs. Changes in the gross appearance of the right and left lungs were usually comparable but when a difference was observed, the more severe change was recorded.

**Figures in the text that show characteristics of a specific grade.

Table 2. Criteria for grading pathologic changes in the ultrastructure of the lungs

| | <u>Grade*</u> | <u>Criterion</u> |
|----------------------------------|---------------|---|
| Capillary Endothelial Cell | 1 | Separated from the basal lamina (Fig. 10**) |
| | 2 | Discontinuous, exposing the basal lamina (occasional) |
| | 3 | Absent or appeared as spherical blebs (occasional, Fig. 13) |
| | 4 | Discontinuous, exposing the basal lamina (widespread) |
| | 5 | Absent or appeared as spherical blebs (widespread) |
| Type I Epithelial Cell | 1 | Rarefied (less electron-dense than normal) and swollen (Fig. 6) |
| | 2 | Discontinuous, exposing the basal lamina (occasional, Figs. 7,8) |
| | 3 | Absent or appeared as spherical blebs (occasional, Figs. 9,12,13) |
| | 4 | Discontinuous, exposing the basal lamina (widespread) |
| | 5 | Absent or appeared as spherical blebs (widespread) |
| Alveolar Exudates | 1 | Present in only 1 air space in a grid opening (Figs. 6,8) |
| | 2 | Occupied 2 or more air spaces in a grid opening (occasional) |
| | 3 | Dense accumulation (occasional, Fig. 13) |
| | 4 | Occupied 2 or more air spaces in a grid opening (widespread) |
| | 5 | Dense accumulation (widespread) |
| Fibrin | 1 | Present in only 1 air space in a grid opening |
| | 2 | Occupied 2 or more air spaces in a grid opening (occasional) |
| | 3 | Same as grade 2 and interwoven with degranulating platelets (occasional, Fig. 14) |
| | 4 | Occupied 2 or more air spaces in a grid opening (widespread) |
| | 5 | Same as grade 4 and interwoven with degranulating platelets (widespread) |
| Interstitial Edema | 1 | Interstitial space (IS) appeared widened |
| | 2 | IS appeared widened and contained disorganized bundles of collagen (occasional) |
| | 3 | Same as grade 2 and contained granular precipitates (occasional, Fig. 10) |
| | 4 | IS appeared widened and contained disorganized bundles of collagen (widespread) |
| | 5 | Same as grade 4 and contained granular precipitates (widespread) |

*A grade of 0 designates normal ultrastructure. A grade of 3 represents a severe change that was occasionally observed, whereas a grade of 5 depicts a severe change that was widespread.

**Figures in the text that show characteristics of a specific grade.

Fig. 2. A coronal section of a rat brain showing the bilateral placement (arrows) of the 28 gauge cannula used to inject aconitine into the pre-optic region. ac, anterior commissure; oc, optic chiasm

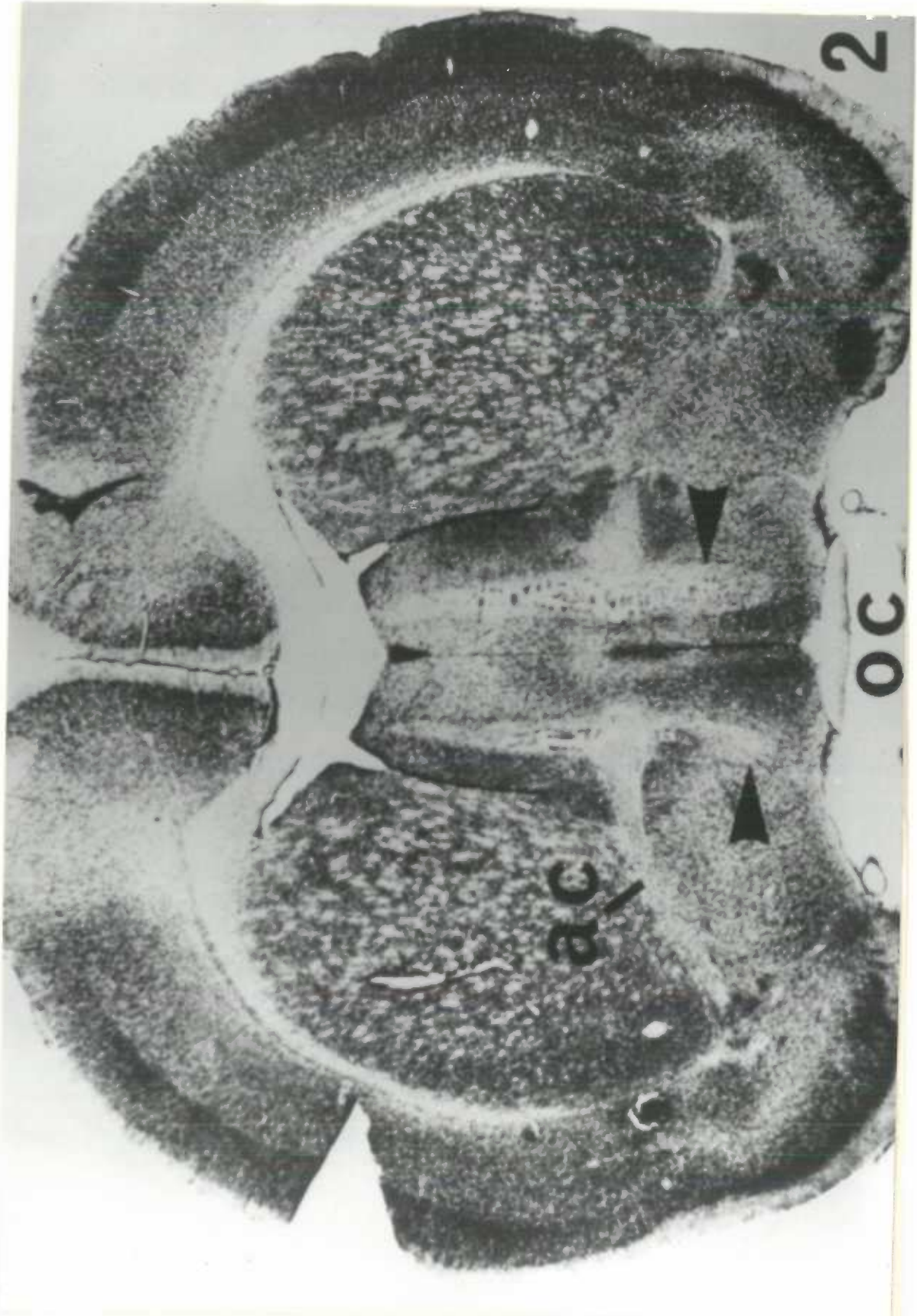


Table 3. Relationship between the dose of aconitine and changes in gross appearance and ultrastructure of the lungs

| Dose of Aconitine (pmoles/kg) | n | Gross appearance* | Ultrastructure* | | | | |
|-------------------------------|---|-------------------|-----------------------|-------------------|-------------------|--------|--------------------|
| | | | Capillary endothelium | Type I epithelium | Alveolar exudates | Fibrin | Interstitial edema |
| 0** | 3 | 0.0 | 0.0 | 0.2 | 0.6 | 0.0 | 0.2 |
| 194 | 4 | 0.0 | 0.0 | 0.2 | 0.4 | 0.0 | 0.2 |
| 387 | 5 | 1.2 | 0.4 | 0.5 | 1.4 | 0.4 | 0.6 |
| 774 | 9 | 2.9 | 1.0 | 2.4 | 1.8 | 2.0 | 1.1 |
| 1550 | 3 | 4.7 | 2.0 | 3.5 | 3.2 | 4.0 | 1.8 |
| 3100 | 3 | 4.7 | 2.3 | 3.3 | 3.0 | 3.0 | 0.7 |

*pathologic changes in gross appearance and ultrastructure of the lungs were graded on a

0 to 5 scale according to the criteria presented in table 1 and are shown as mean values.

**Saline vehicle only.

Table 4. Relationship between the ratio of lung weight to body weight and changes in gross appearance and ultrastructure of the lungs

| Lung weight Body weight (range) | n | Gross appearance* | Ultrastructure* | | | | |
|---------------------------------------|----|----------------------|--------------------------|----------------------|----------------------|---------------------------------|-----|
| | | | Capillary endothelium | Type I epithelium | Alveolar exudates | Fibrin Interstitial edema | |
| 0.49 - 0.72 | 12 | 0.0 | 0.1 | 0.2 | 0.5 | 0.0 | 0.3 |
| 0.77 - 1.14 | 9 | 2.8 | 1.0 | 1.7 | 2.1 | 1.1 | 1.0 |
| 1.35 - 1.86 | 8 | 4.2 | 1.8 | 3.3 | 2.8 | 4.0 | 1.3 |

*Pathologic changes in gross appearance and ultrastructure of the lungs were graded on a 0 to 5 scale according to the criteria presented in table 1 and are shown as mean values.

Fig. 3. Lungs from a rat injected with 197 pmoles/kg of aconitine. No abnormalities are noted (grade 0). The LW/BW was 0.67.



Fig. 4. Lung biopsy from a sham-operated rat. A type I epithelial cell (Ep I) lining an alveolar air space (AAS) is separated from an endothelial (En)-lined capillary (Cap) by an interstitial space (IS). Note the intact junctions between contiguous endothelial cells (small arrows). The LW/BW was 0.67. RBC, red blood cell.

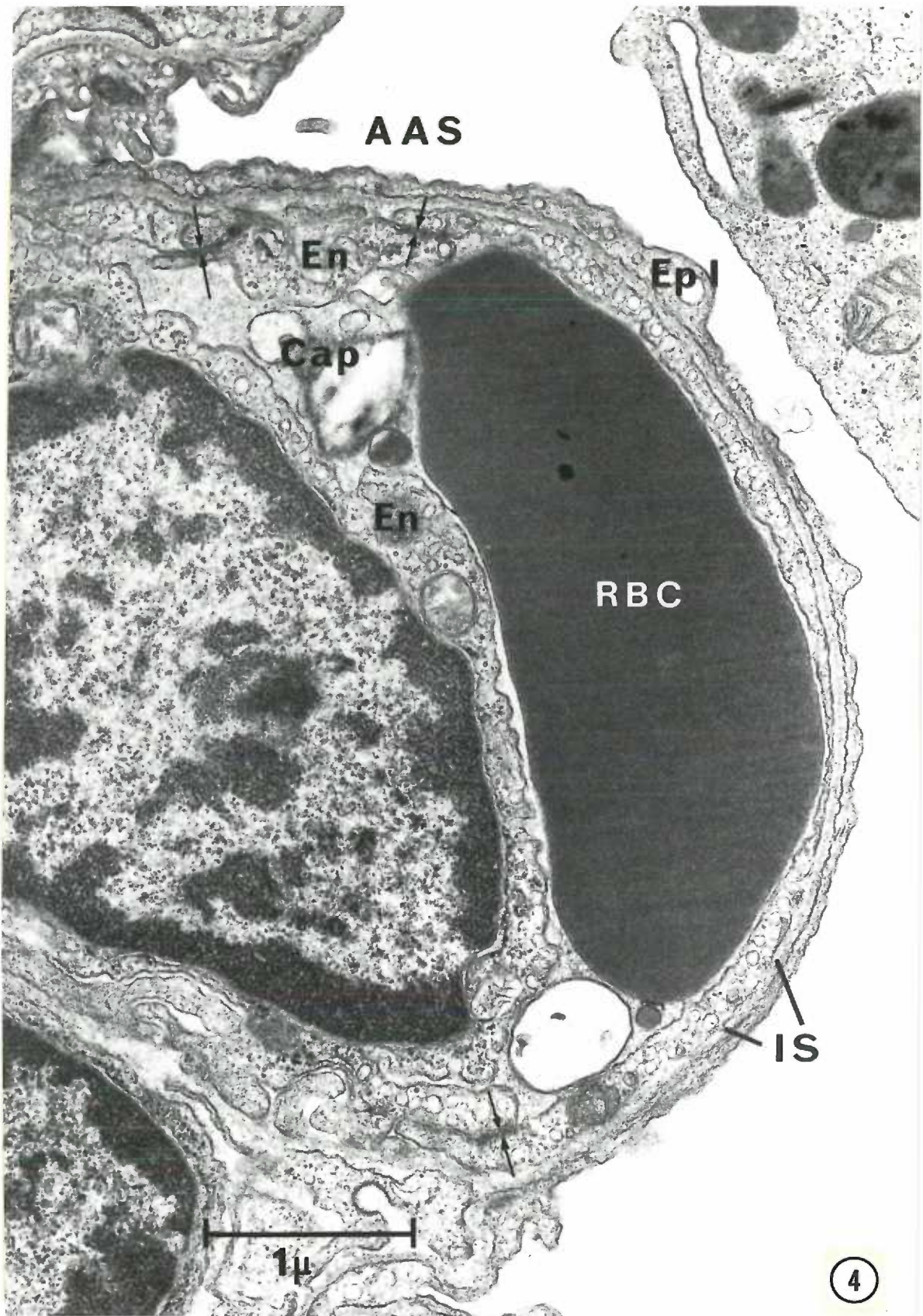


Fig. 5. Lungs from a rat injected with 387 pmoles/kg of aconitine. The right lung is covered with a few punctate hemorrhages (grade 2). The LW/BW was 0.88.



Fig. 6. Lung biopsy from a rat injected with 774 pmoles/kg of aconitine. Exudates fill the alveolar air space (AAS) that is lined by rarefied and slightly swollen type I epithelium (Ep I). In contrast, the adjacent capillary endothelium (En) appears intact. The LW/BW was 0.97. Cap, capillary.

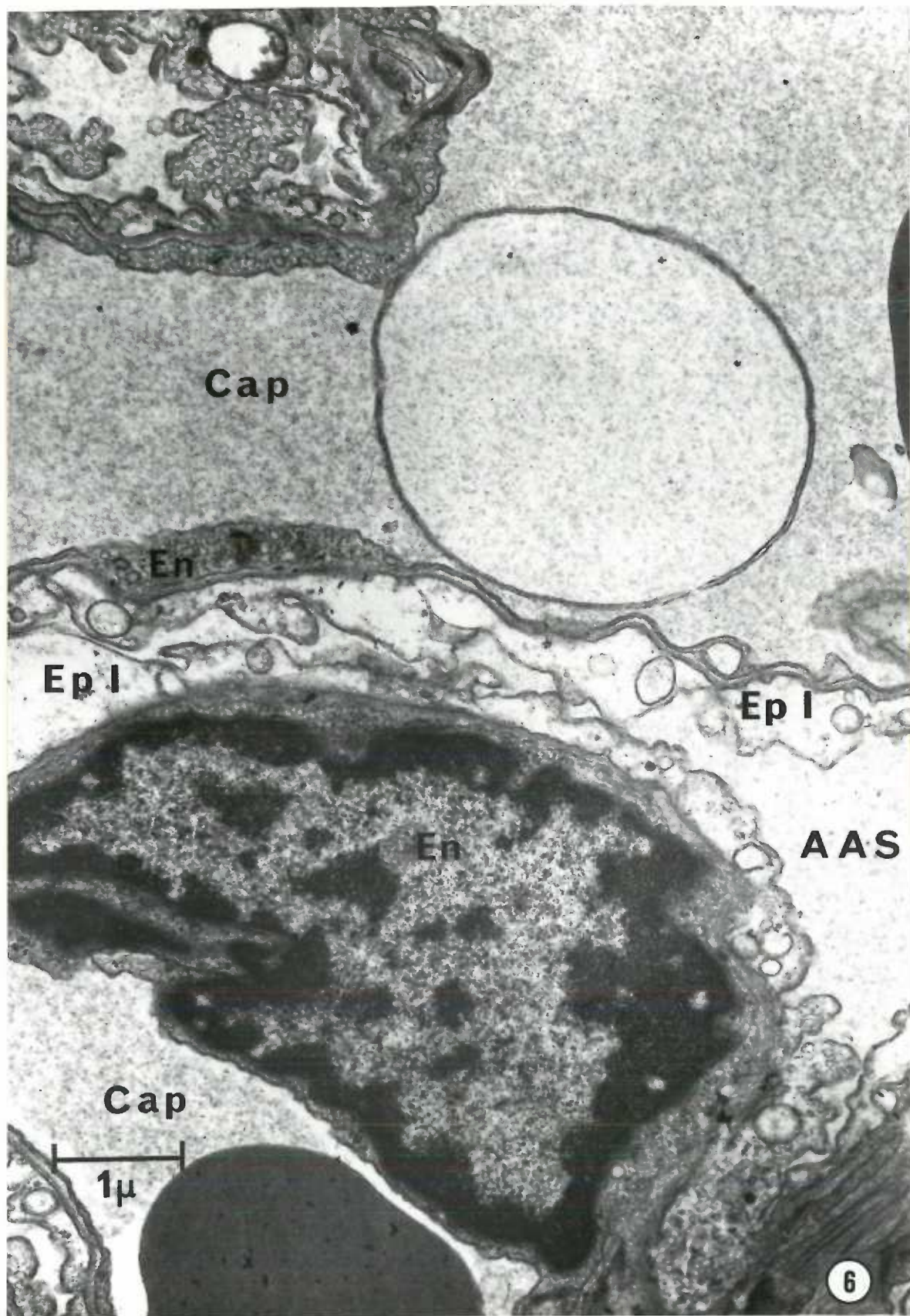


Fig. 7. Lung biopsy from a rat injected with 774 pmoles/kg of aconitine. A rarefied and swollen type I epithelial cell (Ep I) is adjacent to an intact endothelial cell (En). Note that a type I cell is also discontinuous (large arrows). The LW/BW was 1.14. AAS, alveolar air space; Cap, capillary; RBC, red blood cell; WBC, white blood cell.

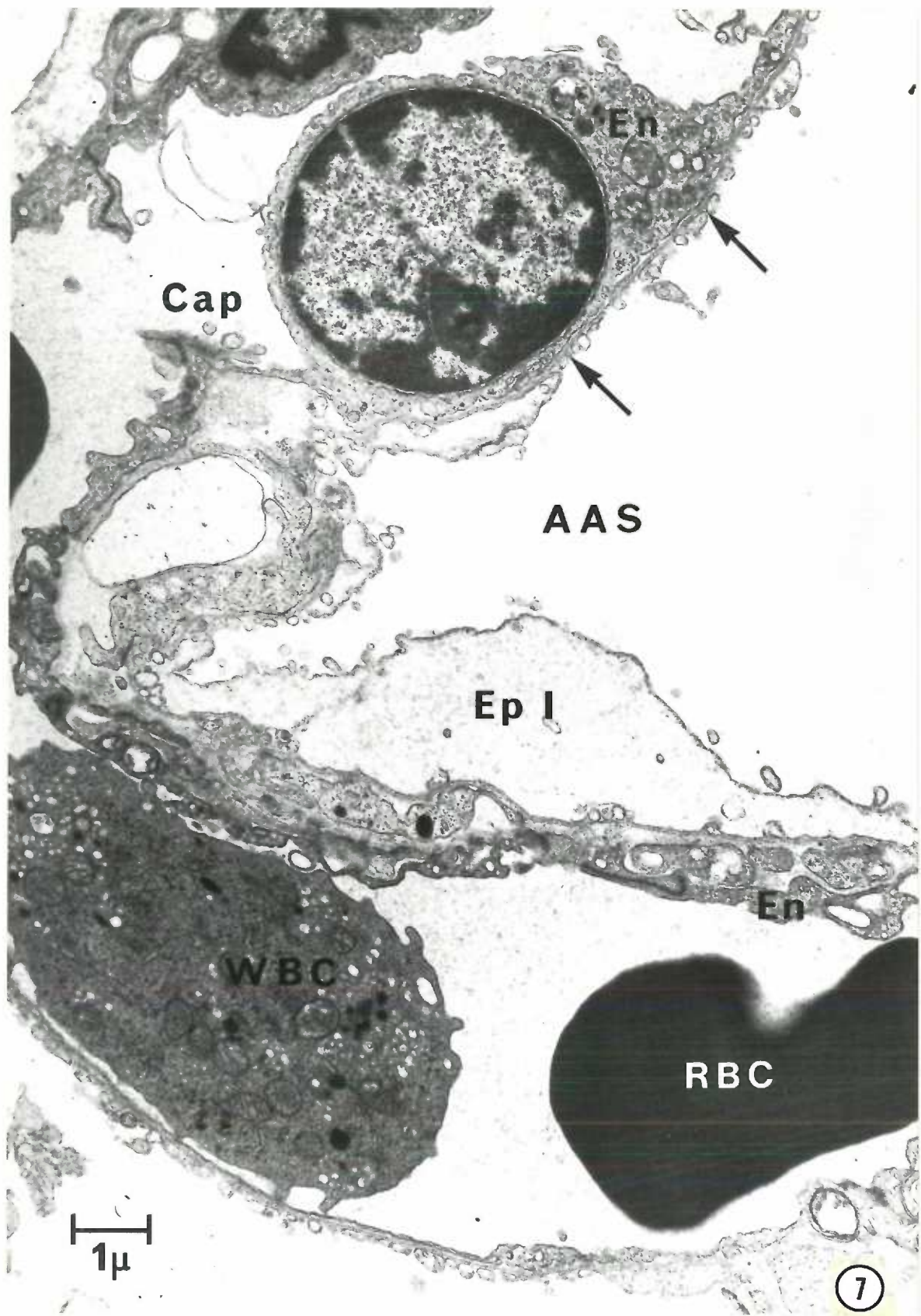


Fig. 8. Lung biopsy from a rat injected with 1550 μ moles/kg of aconitine. Gaps in the type I epithelium (Ep I) expose the underlying basal lamina (BL and large arrows). The endothelium (En) appears intact, and exudates fill the alveolar air space (AAS). The LW/BW was 0.99. RBC, red blood cell; Cap, capillary; IS, interstitial space; Ep II, type II alveolar epithelium.

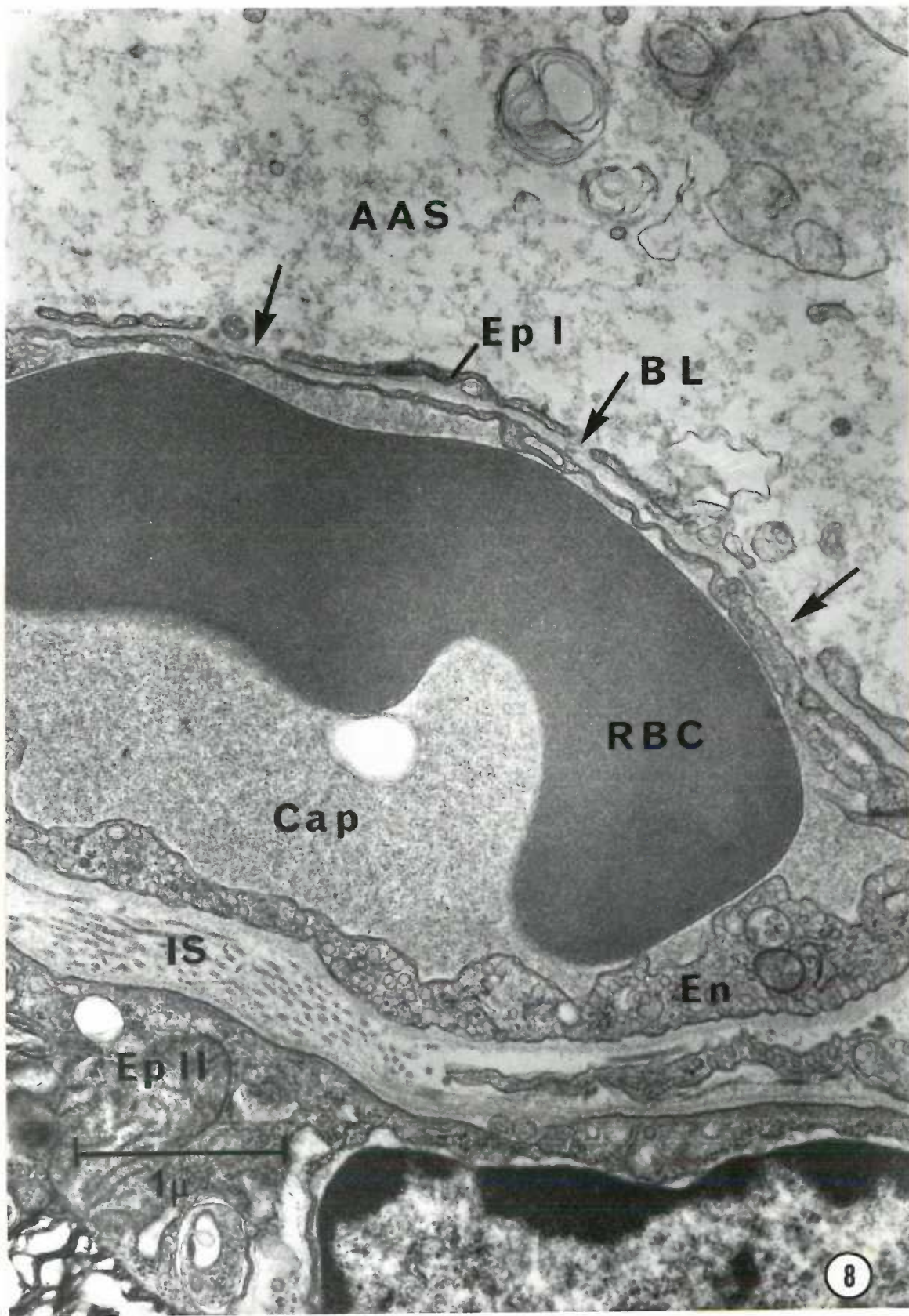


Fig. 9. Lung biopsy from a rat injected with 1550 $\mu\text{moles/kg}$ of aconitine. Four features that characterized the degeneration of type I epithelium can be observed: The type I cell is rarefied and swollen (1), separated from its basal lamina (2), discontinuous and appears as spherical blebs (3) or absent, exposing the basal lamina (4). The capillary endothelium (En) appears intact. Note the intact junction between contiguous endothelial cells (small arrows). The LW/BW was 0.99. AAS, alveolar air space; Cap, capillary; RBC, red blood cell.

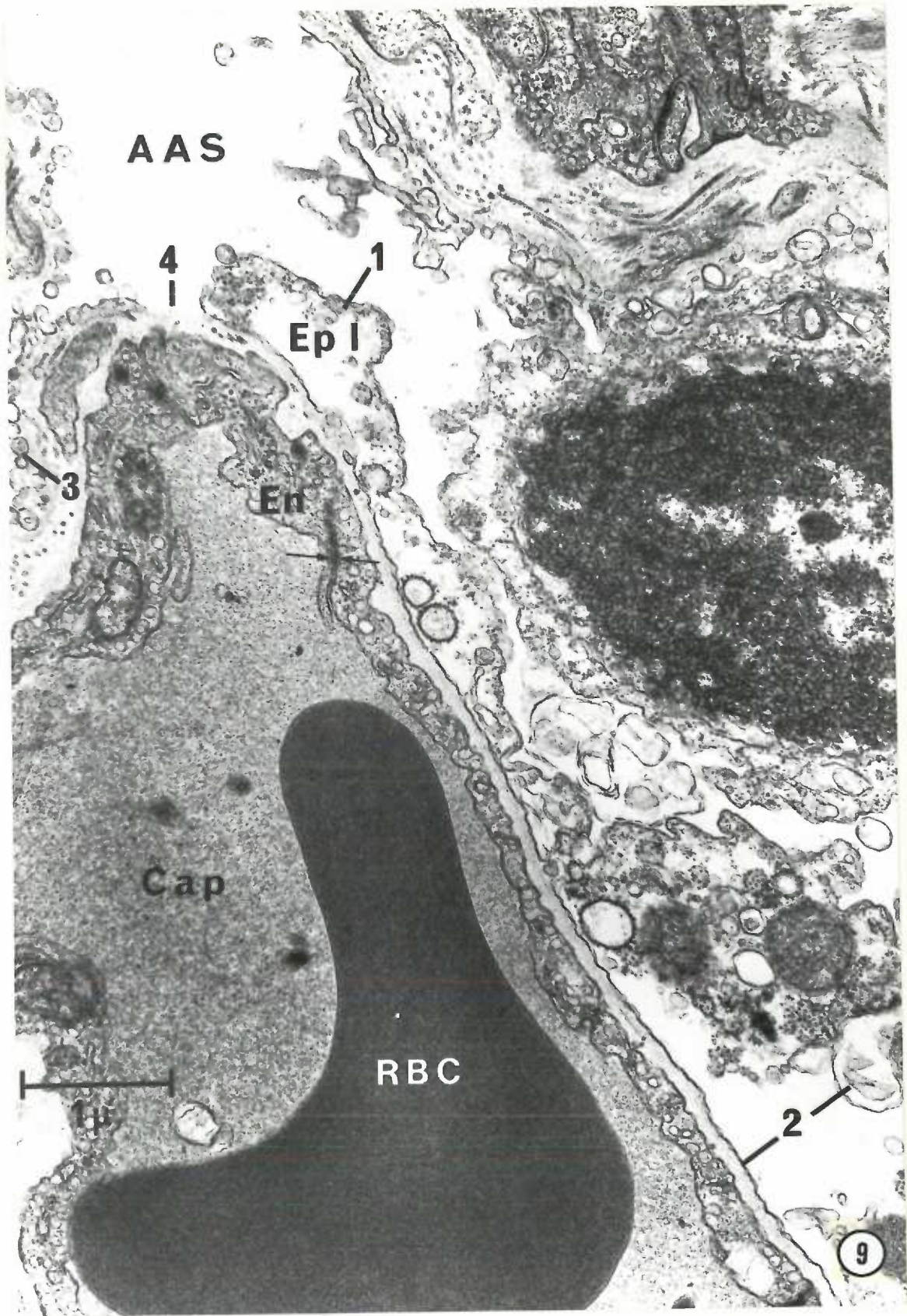


Fig. 10. Lung biopsy from a rat injected with 387 $\mu\text{moles/kg}$ of aconitine. The capillary endothelium (En) is separated (small arrows) from its basal lamina (BL) and protrudes into the capillary lumen (Cap). A small break (large arrow) can be seen in the protruded endothelium. The LW/BW was 0.88. RBC, red blood cell; IS, interstitial space; Ep I, type I alveolar epithelium; AAS, alveolar air space.

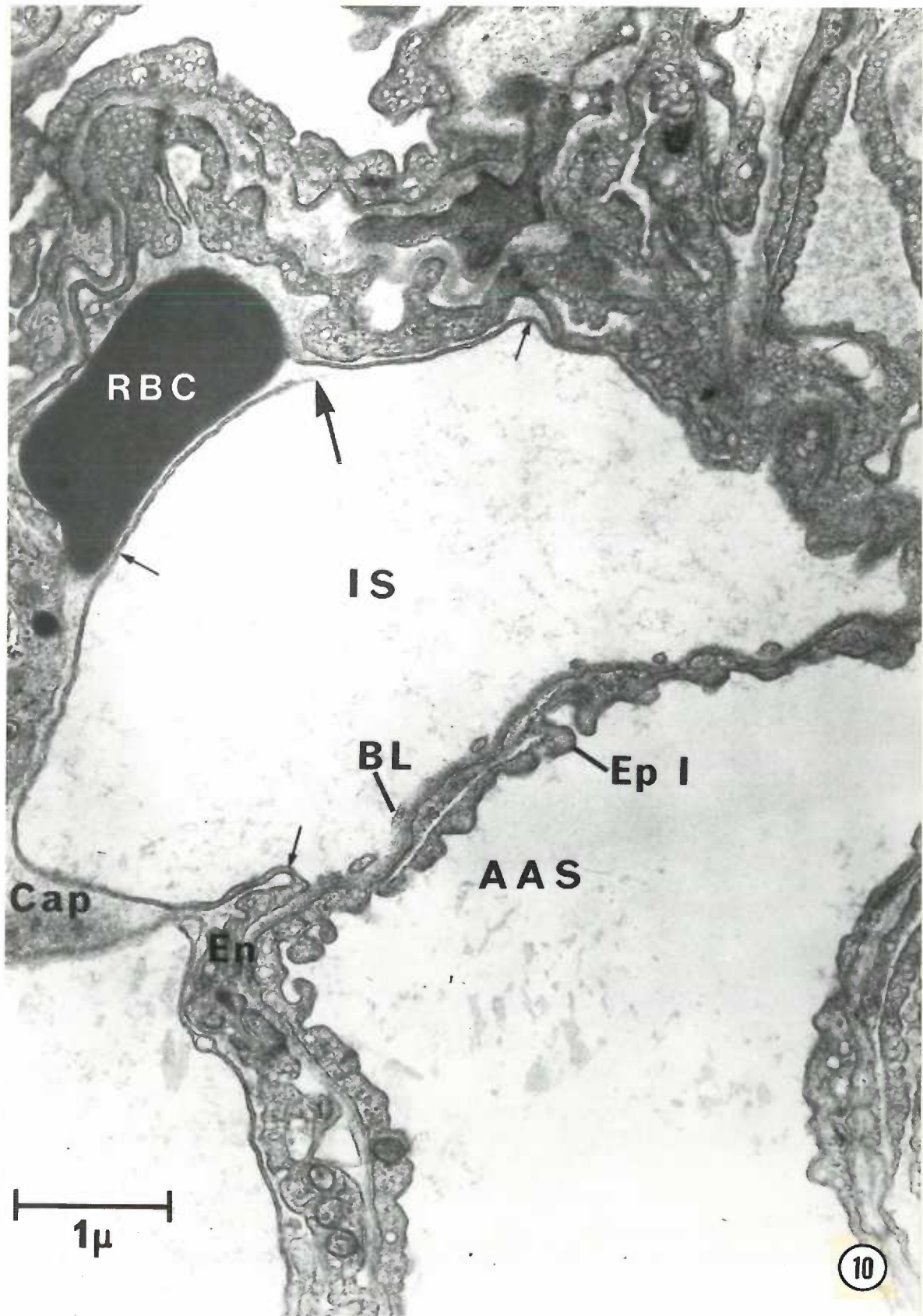


Fig. 11. Lungs from a rat injected with 774 μ moles/kg of aconitine.
The lungs are completely covered with dark punctate hemorrhages (grade 5).
The LW/BW was 1.43.



Fig. 12. Lung biopsy from a rat injected with 1550 pmoles/kg of aconitine. Three features that characterized the degeneration of type I epithelium can be observed: The type I cell is rarefied and slightly swollen (1), discontinuous and appears as spherical blebs (2) or absent, exposing the basal lamina (BL) (3). The LW/BW was 0.99. Mi, mitochondria; P, platelets; Cap, capillary; En, endothelium; AAS, alveolar air space; RBC, red blood cell.

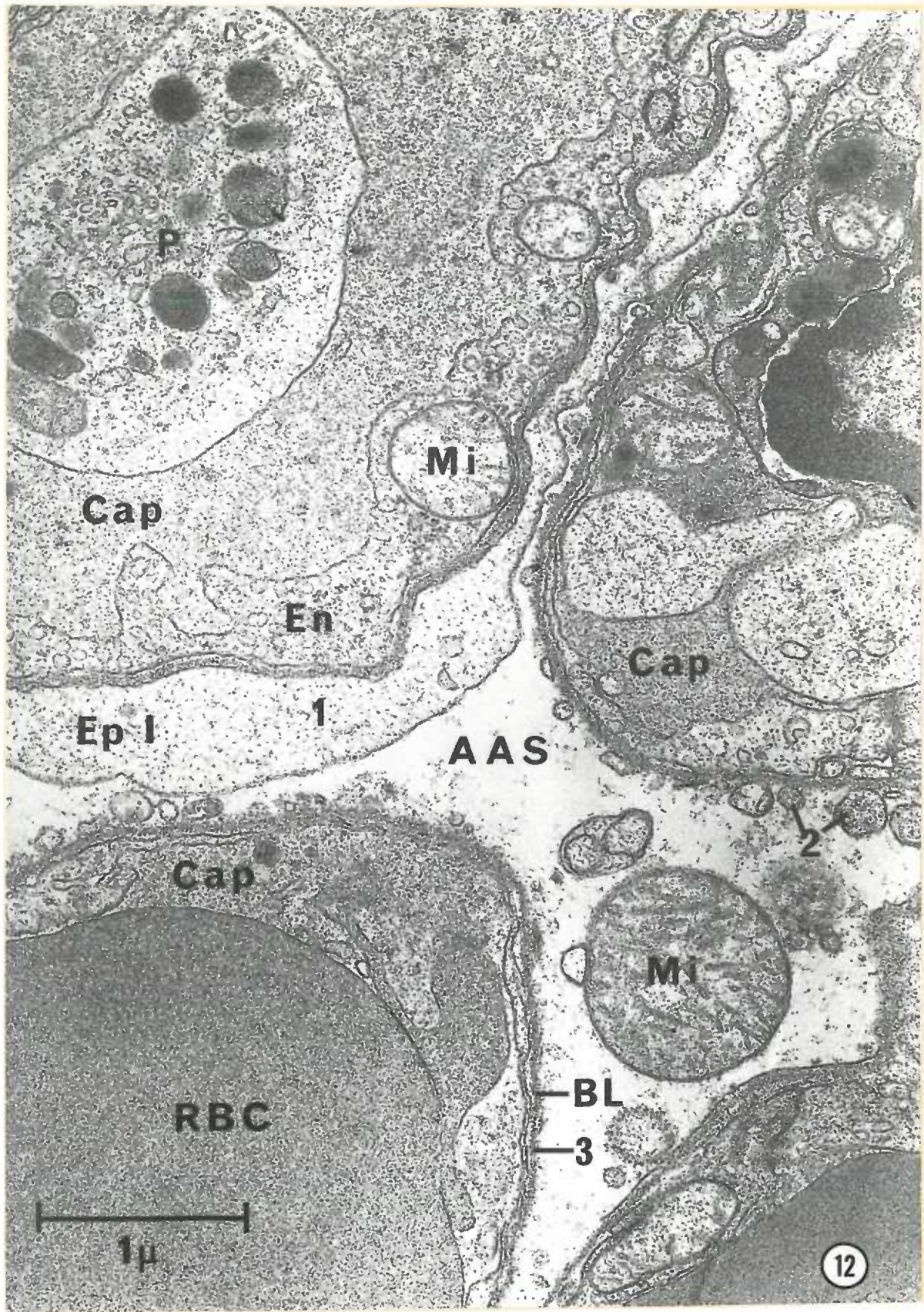


Fig. 13. Lung biopsy from a rat injected with 1550 pmoles/kg of aconitine. The type I epithelium (Ep I) and capillary endothelium (En and small arrows) are discontinuous and appear as spherical blebs (large arrows). A dense accumulation of exudates fills the alveolar air space (AAS). The LW/BW was 0.94. Cap, capillary; RBC, red blood cell.

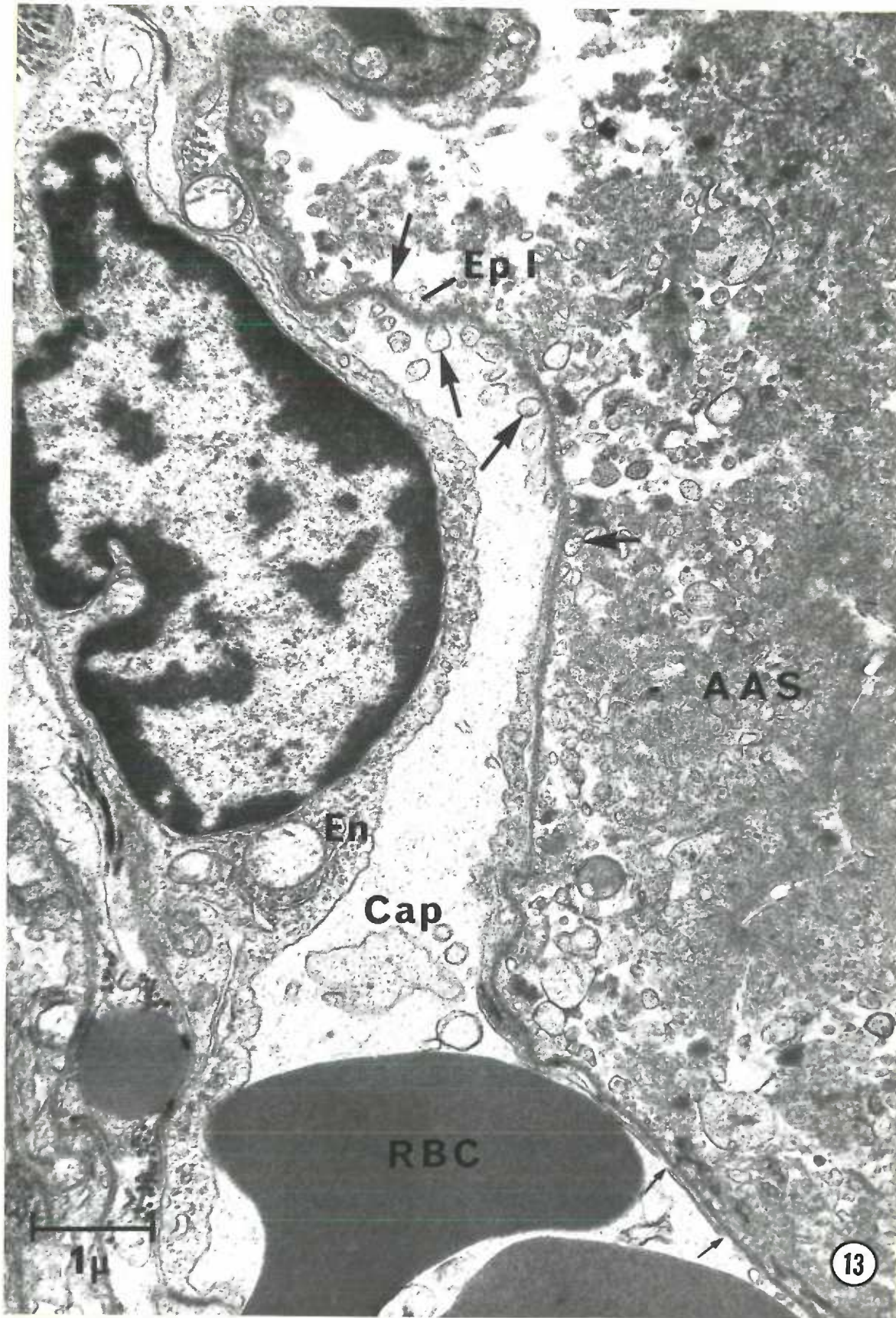
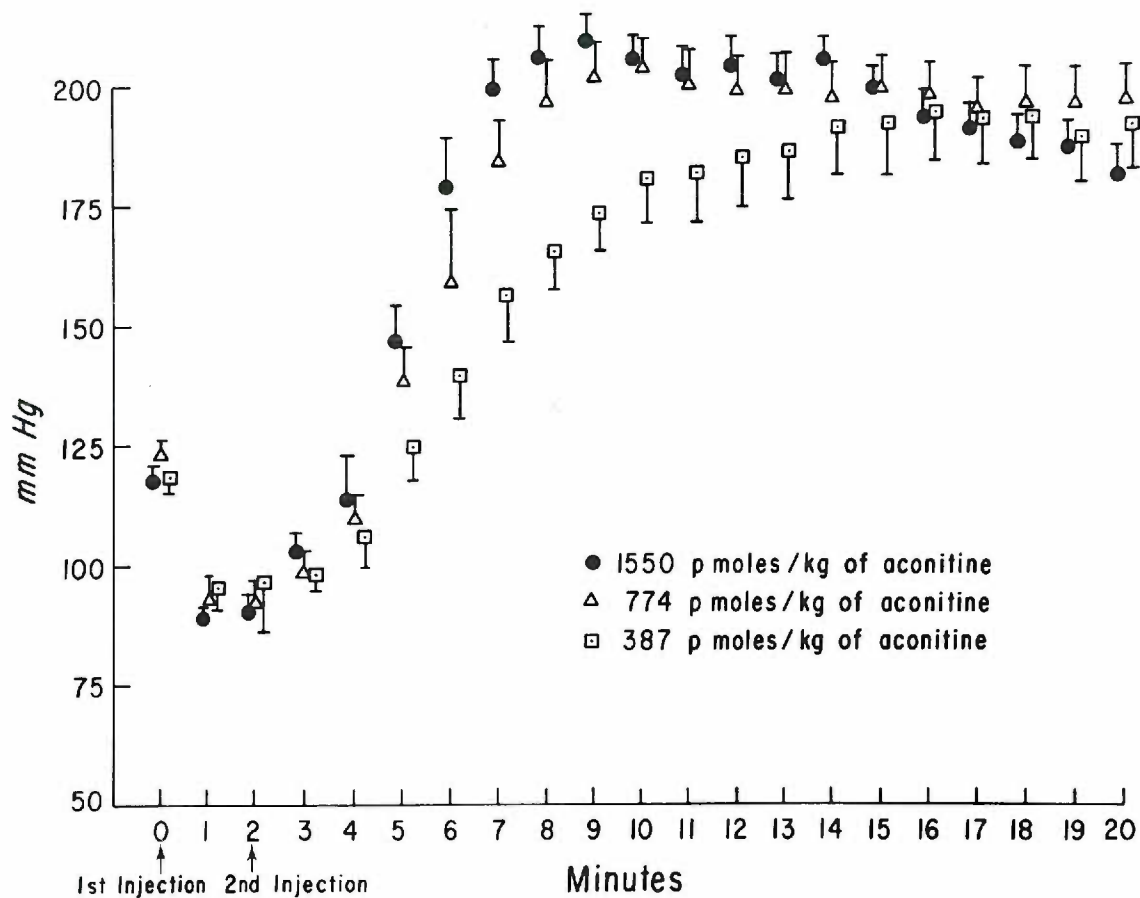


Fig. 12. Lung biopsy from a rat injected with 1550 pmoles/kg of aconitine. Three features that characterized the degeneration of type I epithelium can be observed: The type I cell is rarefied and slightly swollen (1), discontinuous and appears as spherical blebs (2) or absent, exposing the basal lamina (BL) (3). The LW/BW was 0.99. Mi, mitochondria; P, platelets; Cap, capillary; En, endothelium; AAS, alveolar air space; RBC, red blood cell.



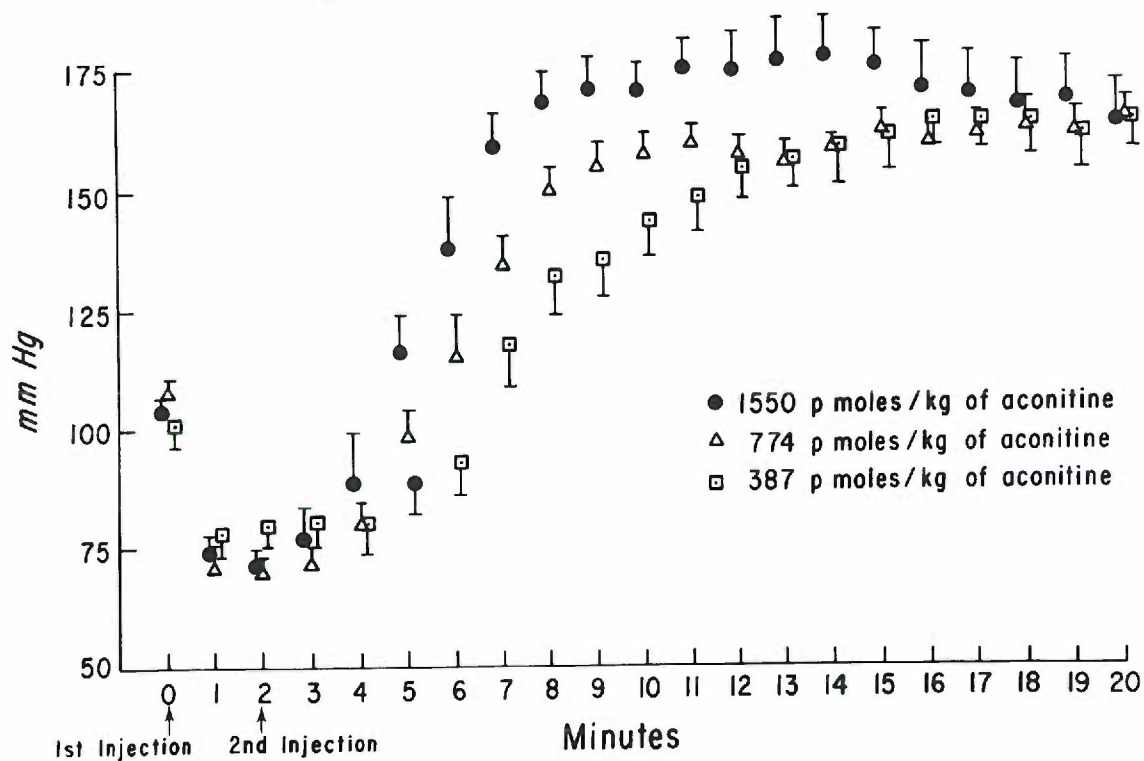
Fig. 15. The effects of different doses of aconitine, injected into the preoptic region, on systolic (a) and diastolic (b) blood pressures. Values are mean \pm SEM (7-10 rats/group). The results of the statistical analysis are presented in Tables 5 and 6.

Systolic Blood Pressure - Response to Preoptic Injections of Increasing Doses of Aconitine



15a

Diastolic Blood Pressure - Response to Preoptic Injections of Increasing Doses of Aconitine



15b

Table 5. The effect of aconitine injected into the preoptic area on systolic blood pressure

| Dose of Aconitine (pmoles/kg) | n | Time after injection (min) | | | | | | | | | | | |
|-------------------------------------|----|----------------------------|--------------------------|------------------------|------------------------|------------------------|-------------------------|-----|-----|-----|-----|-----|-----|
| | | 5 | 6 | 7 | 8 | 9 | 10 | 11 | 12 | 13 | | | |
| 1550 | 10 | *147 ^a +7 | 178 ^a +11 | 199 ^a +7 | 206 ^a +6 | 209 ^a +6 | 206 ^a +5 | 202 | 204 | 201 | 204 | 204 | 201 |
| 774 | 11 | 138 ^{ab} +8 | 159 ^{ab} +10 | 184 ^a +9 | 197 ^a +8 | 202 ^a +7 | 204 ^a +7 | 200 | 199 | 200 | 199 | 199 | 200 |
| 387 | 7 | 124 ^b +7 | 139 ^b +9 | 156 ^b +9 | 166 ^b +8 | 174 ^b +8 | 181 ^b +10 | 182 | 185 | 186 | 182 | 185 | 186 |

*Systolic blood pressure mmHg (mean \pm SEM)

Superscripts with a letter in common designate means within columns that do not differ ($P > 0.05$); conversely, the lack of a common letter in the superscript indicates means that differ ($P < 0.05$).

Table 6. The effect of aconitine injected into the preoptic area on diastolic blood pressure

| Dose of Aconitine (pmoles/kg) | n | Time after injection (min) | | | | | | | | | | |
|-------------------------------------|----|----------------------------|------|------|-------|------|-------|-------|-------|------|------|--|
| | | 5 | 6 | 7 | 8 | 9 | 10 | 11 | 12 | 13 | | |
| 1550 | 10 | *116a | 138a | 160a | 168a | 172a | 171a | 176a | 176a | 176a | 177a | |
| | | +7 | +10 | +7 | +6 | +6 | +6 | +6 | +6 | +8 | +9 | |
| 774 | 11 | 98ab | 116c | 134b | 150ab | 156a | 158ab | 160ab | 157ab | 156b | | |
| | | +6 | +9 | +6 | +5 | +4 | +4 | +4 | +4 | +3 | +4 | |
| 387 | 7 | 89b | 93b | 118b | 132b | 136b | 144b | 149b | 155b | 157b | | |
| | | +6 | +6 | +10 | +9 | +8 | +8 | +8 | +7 | +7 | +7 | |

*Diastolic blood pressure mmHg (mean \pm SEM)

Superscripts with a letter in common designate means within columns that do not differ ($P > 0.05$); conversely, the lack of a common letter in the superscript indicates means that differ ($P < 0.05$).

PAPER 2

Alterations in the Capillary-Alveolar Barrier Associated
with Increased Permeability in Aconitine-Induced
Neurogenic Pulmonary Edema

ABSTRACT

Ferritin was used as a vascular marker to trace the route taken by edema fluid as it crossed the capillary-alveolar barrier in aconitine-induced neurogenic pulmonary edema (NPE). Adult female rats received bilateral injections of aconitine in the preoptic area of the brain and were killed either at the time of peak systemic arterial blood pressure (8 min after injection of aconitine) or the initiation of frothing from the nose (15 min). An increase in permeability of the capillary-alveolar barrier to ferritin was observed at 8 min, and pulmonary edema (as measured by an increase in the ratio of lung weight to body weight) developed between 8 and 15 min after injection of aconitine. Ferritin was observed in intercellular clefts, occasionally within endothelial junctions and frequently in the interstitial and alveolar air spaces. The capillary endothelium generally appeared intact except for the occasional observation of open endothelial junctions or a damaged cell. Although tight junctions of alveolar epithelium appeared intact and impermeable to ferritin, the type I alveolar epithelial cells were starting to degenerate at 8 min and were severely damaged by 15 min. It is suggested that in NPE plasma enters the interstitial space through loosened endothelial junctions and damaged areas in the endothelium and then crosses the alveolar epithelial barrier through structural alterations in type I epithelial cells.

INTRODUCTION

Accumulation of fluid in the lungs leading to respiratory distress occurs after various injuries to the brain or spinal cord (4,7,24). This syndrome, known as neurogenic pulmonary edema (NPE), varies in severity depending on the amount of fluid that escapes from the circulatory system and collects in the interstitial or alveolar air spaces of the lung. The route taken by the edema fluid as it crosses the capillary-alveolar barrier is unclear. Hücker et al. (14) used horseradish peroxidase as a vascular marker to trace the pathway of edema fluid after increasing intracranial pressure by the infusion of homologous blood in the cisterna magna. The tracer was found within the junctions of the capillary endothelium but not in those of the alveolar epithelium. Despite the observations that capillary endothelial and type I epithelial cells appeared damaged and that frank ruptures of the capillary-alveolar barrier had occurred, it was suggested that the pathway of edema fluid from the vascular to the alveolar air space was primarily through loosened tight junctions of both capillary endothelium and alveolar epithelium. More recently, the pulmonary ultrastructure in NPE induced by the injection of aconitine into the preoptic area of the brain has been characterized (21). In contrast to the findings of Hücker et al. (14), damaged type I epithelium was consistently found in association with intact capillary endothelium, and frank ruptures of the capillary-alveolar barrier were not observed. Although fibrin and exudates were present in the alveolar air spaces, the pathway by which plasma crossed the capillary-alveolar barrier could not be determined.

In the present study, cadmium-free ferritin was used as a vascular tracer to determine the route taken by plasma as it crossed the capillary-

alveolar barrier in rats during aconitine-induced NPE.

MATERIALS AND METHODS

The tail arteries of 30 adult female Charles River (CD) rats weighing 272 to 363 g were cannulated under ether anesthesia with PE-50 tubing to monitor the systemic arterial blood pressure (SAP). SAP was measured by a Statham P23Db strain gauge and recorded on a Grass Model 79D polygraph. The patency of the cannula was maintained by continuous infusion (0.5 ml/h) of 1% heparinized saline through a Sorenson valve. A second cannula was placed in the right external jugular vein to provide a route for injection of ferritin. Following cannulation, the rats were placed in a stereotaxic instrument, the dorsal surface of the skull was exposed, and a portion of the calvarium anterior to bregma was removed. Cadmium-free ferritin (200 mg, Polysciences) was injected into the external jugular vein over a 6 min period, while the animal was under light ether anesthesia, followed immediately by an injection of aconitine (1550 pmol/kg, Sigma) in the preoptic area as previously described (21). The animals were then placed in a cage that restricted movement, and the SAP was monitored. Ten animals were killed at peak SAP (8 min after the injection of aconitine), and 11 at the initiation of frothing from the nose or when the pulse pressure narrowed (15 min). Nine rats that received only the saline vehicle in the preoptic area served as sham-operated controls and were killed 8 or 15 min after injection of aconitine.

All animals were killed by severing the abdominal aorta. The thoracic cavity was opened, and the lungs were excised and weighed to the nearest 0.1 g. A lung weight to body weight ratio (LW/BW) was calculated (lung weight/body weight x 100) for each rat and used as an index of pulmonary edema. The extent of grossly visible hemorrhages on the surfaces of

the lungs was recorded. The upper and lower lobes of both the right and left lungs were biopsied, and the tissues were cut into 1 mm cubes, fixed by immersion in glutaraldehyde and osmium tetroxide and processed for electron microscopy as previously described (21), with the exception that the tissues were stained en bloc with 5% uranyl acetate for 15 min. Thin sections were further stained with 5% uranyl acetate for 5 min and lead citrate for 10 min. Examination of the pulmonary ultrastructure for assessing the distribution of ferritin was done as a single-blind study. Tight junctions of capillary endothelium and alveolar epithelium were considered to be loosened if the dark membranes of adjacent cells were separated throughout the entire length of the junctional complex and if ferritin was present within the junction or in the adjacent interstitial space.

Brains were removed at autopsy and fixed in formalin. The placements of injections in the preoptic area were verified histologically on alternate frozen sections (50 μ m) stained with thionin. Animals with injection sites located outside the preoptic-anterior hypothalamic area were rejected from the study.

Statistical Analysis

The LW/BWs of control and experimental groups were compared using a student's t test. Differences were considered significant at $P < 0.05$.

RESULTS

Representative tracings of SAP from rats injected with aconitine and killed either at the time of peak SAP or the initiation of frothing from the nose are shown in Figs. 1 and 2. The SAP in animals injected with aconitine reached a peak level of $222 \pm 4 / 176 \pm 4$ mmHg (mean \pm SEM) in 7.6 ± 0.4 min (Fig. 1), and the animals were frothing from the nose at

14.5±1.4 min. The SAPs of sham-operated rats killed at either 8.2±0.5 or 15.8±1.8 min were not different from those before anesthesia was induced.

As shown in Table 1, LW/BWs of rats injected with aconitine and killed at 15 min were greater ($P < 0.001$) than those of controls or the aconitine-injected animals killed at 8 min. This finding demonstrates that pulmonary edema occurred between 8 and 15 min after injection of aconitine.

The lungs of rats killed 8 min after administration of aconitine appeared normal or exhibited punctate hemorrhages restricted to one lobe of a lung (Fig. 3), whereas those in animals killed at 15 min had light-colored punctate hemorrhages that partially covered all lobes of a lung (Fig. 4). The lungs of sham-operated rats had no detectable hemorrhages.

The pulmonary ultrastructure appeared normal in 6 of the 10 rats killed 8 min after injecting aconitine, and ferritin was confined to the capillary lumen in these animals (Fig. 5); examples of normal appearing tight junctions of capillary endothelium and alveolar epithelium are shown in Figs. 6,7 and 8. Ferritin was present in the interstitial (Figs. 7,9,10,11,12 and 13) and alveolar air spaces (Fig. 12) in the remaining 4 rats killed at 8 min and in all rats killed 15 min after injection of aconitine. Ferritin was also observed in intercellular clefts between endothelial cells (Fig. 10) and occasionally in junctions that appeared open (Fig. 13) in these animals. Although there was no evidence of increased pinocytotic activity, ferritin was observed a few times free within endothelial and type I epithelial cells (Figs. 9 and 11). Exudates and fibrin were occasionally observed in the alveolar air spaces at 8 and 15 min, and fibrin was found in alveoli in 1 rat that reached peak SAP as early as 3 min after injection of aconitine (Fig. 12). In sham-

operated controls, the pulmonary ultrastructure was normal, and ferritin was confined to the blood vessels.

Although the capillary endothelium generally appeared intact, lesions were occasionally observed at both 8 and 15 min. When altered, the endothelium was either separated from its underlying basal lamina and protruded into the capillary lumen (Fig. 7) or was actually discontinuous, exposing the basal lamina to the vascular space (Figs. 9 and 14). Endothelial junctions were also occasionally observed to be open at both time periods (Figs. 11, 12 and 13).

In contrast to the relatively normal appearance of capillary endothelium, the type I epithelium was starting to degenerate at 8 min and was severely damaged by 15 min. The cytoplasm of type I cells appeared rarefied (less electron-dense) (Figs. 7 and 8), and the cells were swollen or discontinuous, with the underlying basal lamina exposed to the air space (Figs. 8 and 15). Occasionally, type I cells were absent or appeared as spherical blebs adjacent to the denuded basal lamina. Although ferritin was present in the alveolar air spaces in aconitine-injected rats, the tight junctions of alveolar epithelium appeared intact and free of ferritin, and frank ruptures of the capillary-alveolar barrier were not observed.

DISCUSSION

The ultrastructural changes and the distribution of ferritin observed in the present study suggest that pulmonary edema produced by injection of aconitine in the preoptic area is due to the passage of plasma into the interstitial space through loosened endothelial junctions and damaged areas in the endothelium. It was observed further that exudates were present in the alveolar air spaces in the absence of frank ruptures of the capillary-alveolar barrier and in association with tight junctions

between alveolar epithelial cells that appeared impermeable to ferritin. However, many type I cells were observed in various stages of degeneration. Thus, these findings suggest that it is damage to the type I cells, and not an increase in permeability of alveolar epithelial junctions, that allows plasma to leave the interstitial space and enter the alveoli. These observations and interpretations agree in part with those reported by Hücker et al. (14). In that study, loosened endothelial junctions were also demonstrated, with horseradish peroxidase as the vascular marker; however the suggestion that loosened tight junctions of alveolar epithelium are the main route by which plasma crosses the alveolar epithelial barrier was not confirmed by the present observations.

An increase in permeability of the capillary-alveolar barrier to ferritin was observed at 8 min after injection of aconitine in some rats, and pulmonary edema (as measured by an increase in LW/BW) developed between 8 and 15 min. Ferritin was frequently found in the interstitial space but was only occasionally observed within endothelial junctions. Furthermore, the capillary endothelium for the most part appeared intact except for the occasional observation of open endothelial junctions and damaged areas in the endothelium. These findings agree with those of Barrios et al. (2) and others (9,10,13) that the opening of a few endothelial junctions or minimal damage to endothelial cells throughout the pulmonary microvasculature may account for the change in permeability observed in hemorrhagic shock (2) and in experimentally induced neurogenic pulmonary edema (5,6,20).

The mechanisms by which cell junctions of endothelium become permeable or endothelial cells become structurally damaged in NPE are not known. It has been proposed that endothelial junctions are loosened in NPE by

substances such as histamine, sudden metabolic changes or direct neural effects (5,6,20). In support of the latter possibility, there is evidence from studies of adipose tissue and the lung that the sympathetic nervous system affects capillary permeability (1,17,19). Pretreatment with an alpha adrenergic blocking agent (phenoxybenzamine or phentolamine) has been shown to prevent the increase in vascular permeability in adipose tissue or the lungs after the stimulation of the sympathetic nerve supply to adipose tissue or small increases in intracranial pressure, respectively. Although it was suggested by Hurley (16) that high concentrations of plasma catecholamines produce pulmonary edema by increasing capillary hydrostatic pressure, it has been shown by Bowers et al. (5), Brigham (6) and Malik et al. (20) that the increase in pulmonary vascular permeability following a small elevation in intracranial pressure occurs in the presence of small increases in pulmonary artery and left atrial pressures. Therefore, catecholamines may affect endothelial cells in some other way, possibly by causing actomyosin to contract and open cell junctions (20). Structural damage to endothelial cells may occur in NPE due to frictional forces or direct impact (inertial force) of blood flowing at a high linear velocity through a vasoconstricted pulmonary vascular bed (23,24). In support of this hypothesis, it has been shown that a high velocity of blood flow directed against the systemic vasculature causes degeneration of the endothelium (11). Other possible causes of endothelial damage such as histamine, bradykinin, vasoactive peptides, degradation products of fibrin and lysosomes released from degenerating microemboli have also been proposed (12,23). Since pulmonary hemodynamics were not monitored in this study, it could not be determined whether the increase in vascular permeability precedes or follows changes in pulmonary

vascular pressures and blood flow rates that may cause the endothelial damage reported here.

In contrast to the relatively normal appearance of the capillary endothelium, the type I epithelium was found in various stages of degeneration 15 min after the injection of a lethal dose of aconitine. This observation confirms a previous finding in this laboratory (21) that damaged type I cells were consistently found in the presence of intact capillary endothelium 1 h after a sublethal dose of aconitine. The reason for the differential sensitivity of the type I epithelium and the capillary endothelium in NPE is not known. That a direct toxic effect of aconitine was responsible was ruled out because the injection of lethal doses of aconitine into the systemic circulation did not damage either type of cell (21). It has also been suggested that the presence of exudates and fibrin in the alveolar air spaces may damage type I cells by means of a colloid osmotic effect (15) or by causing collapse of the air spaces and the subsequent shunting of blood to more functional areas of the lungs (8,21). Thus, the reduction of oxygen and metabolic substrates from both the alveolar and capillary sides may affect the metabolic processes of the type I cells and lead to their degeneration. The observation by Meyrick (22) that leakage of fluid occurred through type I cells 2 h before damage to the cells could be detected, in ANTU-induced pulmonary edema, is compatible with the above explanations. Kistler (18), however, has shown that the type I cells were unaffected when exposed to alveolar exudates and fibrin for 6 h. The present observation that type I cells were damaged at the onset of NPE in the absence of alveolar exudates detectable with the electron microscope suggests that the cells are damaged before exudates enter the alveoli. Thus, it seems unlikely that direct

effects of plasma are responsible for the damage to the type I epithelium observed in the present study. That the capillary endothelium was less vulnerable to the rapid development of NPE may be due to a lower requirement for metabolites or its proximity to a source of nutrients. Further studies are necessary to answer these questions.

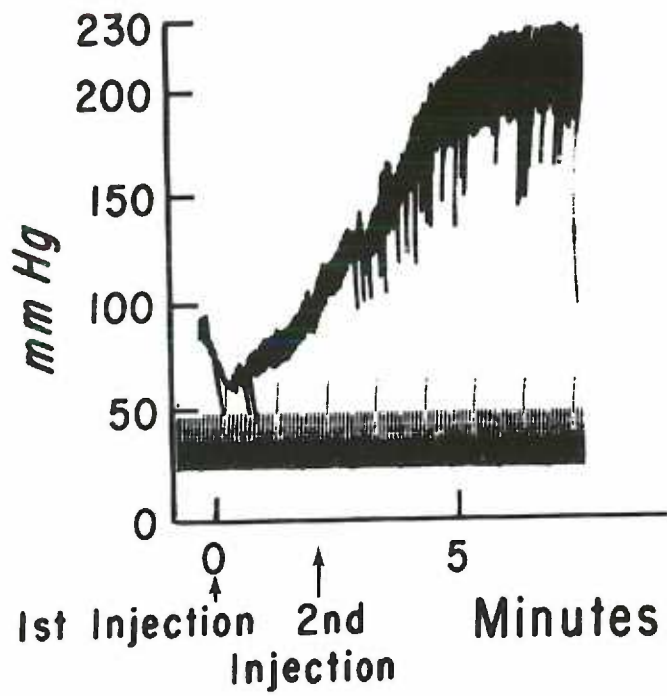
REFERENCES

1. Ballard, K. W. Functional characteristics of the microcirculation in white adipose tissue. *Microvasc. Res.*, 16: 1-18, 1978.
2. Barrios, R., Inoue, S. and Hogg, J. C. Intercellular junctions in "shock lung": A freeze-fracture study. *Lab. Invest.*, 36: 628-635, 1977.
3. Becker, C. G. and Murphy G. E. Demonstration of contractile protein in endothelium, intima, arteriosclerotic plaques, and Aschoff bodies of rheumatic heart disease. *Am. J. Pathol.*, 55: 1-37, 1969.
4. Bonbrest, H. C. Pulmonary edema following an epileptic seizure. *Am. Rev. Respir. Dis.*, 91: 97-100, 1965.
5. Bowers, R. E., McKeen, C. R., Park, B. E. and Brigham, K. L. Increased pulmonary vascular permeability follows intracranial hypertension in sheep. *Am. Rev. Respir. Dis.*, 119: 637-641, 1979.
6. Brigham, K. L. Factors affecting lung vascular permeability. *Am. Rev. Respir. Dis.*, 115: 165-172, 1977.
7. Brisman, R., Kovach, R. M., Johnson, D. O., Roberts, C. R. and Ward, G. S. Pulmonary edema in acute transection of the cervical spinal cord. *Surg. Gynecol. and Obstet.*, 139: 363-366, 1974.
8. Chiu, C. J. Epithelial lesions in low flow states: A unifying concept. *Med. Hypotheses*, 3: 159-161, 1977.
9. Cunningham, A. L. and Hurley, J. V. Alpha-naphthyl-thiourea-induced pulmonary oedema in the rat: A topographical and electron-microscope study. *J. Pathol.*, 106: 25-35, 1972.
10. Finegold, M. J. Interstitial pulmonary edema. *Lab. Invest.*, 16: 912-924, 1967.
11. Fry, D. L. Acute vascular endothelial changes associated with increased blood velocity gradients. *Circ. Res.*, 22: 165-197, 1968.
12. Hogg, J. C., Staub, N. C., Bergosky, E. H. and Vreim, C. E. Workshop on the pulmonary endothelial cell. *Am. Rev. Respir. Dis.*, 119: 165-170, 1979.
13. Hovig, T., Nicolaysen, A. and Micolaysen, G. Ultrastructural studies of the alveolar-capillary barrier in isolated plasma-perfused rabbit lungs. Effects of EDTA and of increased capillary pressure. *Acta Physiol. Scand.*, 82: 417-431, 1971.
14. Hücker, H., Frenzel, H., Kremer, B. and Richter, I. E. Time sequence and site of fluid accumulation in experimental neurogenic pulmonary edema. *Res. Exp. Med.*, 168: 219-227, 1976.

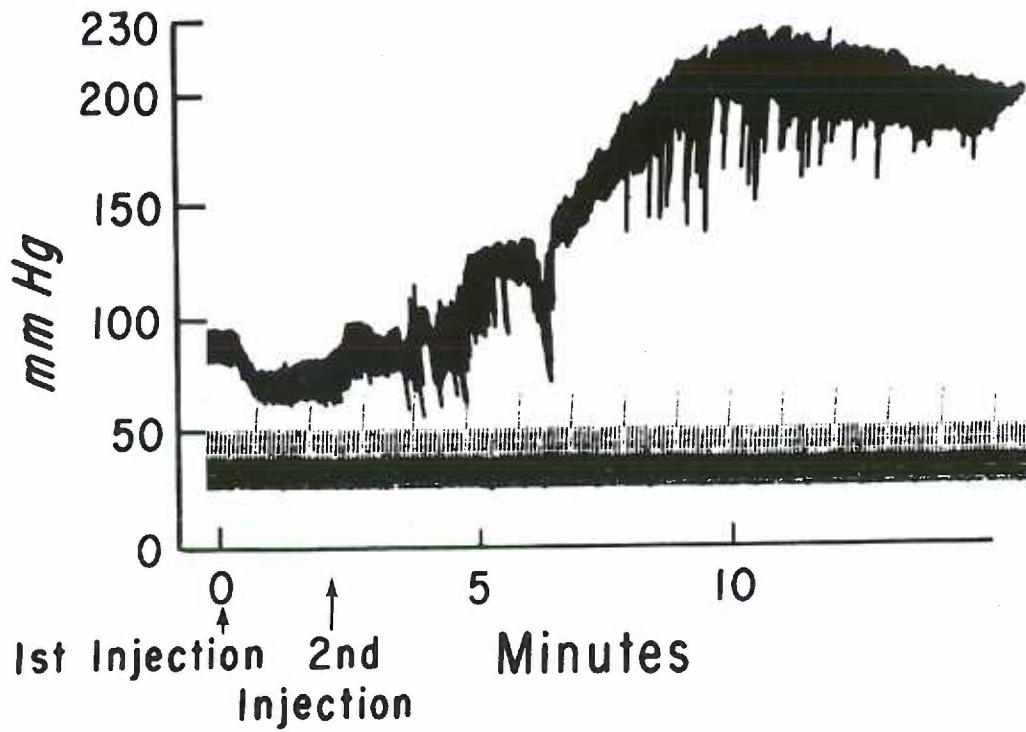
15. Hücker, H., Schäfer, U. and Meinen, K. Early morphological alterations of the rat lung with increased intracranial pressure. I. A light and electron microscopic study. *Virchows Arch. A. Path. Anat. Histol.*, 362: 331-342, 1974.
16. Hurley, J. V. Current views on the mechanisms of pulmonary edema. *J. Pathol.*, 125: 59-79, 1978.
17. Intaglietta, M. and Rosell, S. Capillary permeability and sympathetic activity in canine subcutaneous adipose tissue. *Nature*, 249: 481-482, 1974.
18. Kistler, G. S., Caldwell, P. R. B. and Weibel, E. R. Development of fine structural damage to alveolar and capillary lining cells in oxygen-poisoned rat lungs. *J. Cell Biol.*, 32: 605-628, 1967.
19. Malik, A. B. Personal communication.
20. Malik, A. B., Lee, B. C., van der Zee, H. and Johnson, A. Mechanism of neurogenic pulmonary edema. *Am. Rev. Respir. Dis.*, 117: 367, 1978.
21. Minnear, F. L. and Connell, R. S. A comparison of changes in pulmonary ultrastructure in mild and severe forms of aconitine-induced neurogenic pulmonary edema. Manuscript in preparation.
22. Meyrick, B., Miller, J. and Reid, L. Pulmonary edema induced by ANTU, or by high or low oxygen concentrations in rat - an electron microscopic study. *Br. J. Exp. Pathol.*, 53: 347-358, 1972.
23. Staub, N. C. Pulmonary edema due to increased microvascular permeability to fluid and protein. *Circ. Res.*, 43: 143-151, 1978.
24. Theordore, J. and Robin, E. D. Speculations on neurogenic pulmonary edema (NPE). *Am. Rev. Respir. Dis.*, 113: 405-411, 1976.

Fig. 1. Representative tracing of SAP from a rat injected with aconitine (1550 pmoles/kg) and killed at the time of peak SAP (8 min after injection).

Fig. 2. Representative tracing of SAP from a rat injected with aconitine (1550 pmoles/kg) and killed at the initiation of frothing from the nose (15 min) or when the pulse pressure narrowed (15 min).



①



②

Table 1. The effect of aconitine injected into the preoptic region on the ratio of lung weight to body weight (LW/BW) in rats

| Time after injection | LW/BW* | | | |
|----------------------|-----------------|-----|-------------------|------|
| | Saline | (n) | Aconitine | (n) |
| 8 min | 0.58 \pm 0.02 | (5) | 0.62 \pm 0.02 | (10) |
| 15 min | 0.55 \pm 0.03 | (4) | 1.15 \pm 0.06** | (11) |

*Values indicate means \pm SEM.

**Different from other values ($P < 0.001$).

Fig. 3. Lungs from a rat injected with aconitine (1550 pmoles/kg) and killed at the time of peak SAP (8 min). A punctate hemorrhage can be seen in the upper lobe of the right lung. The LW/BW was 0.65.

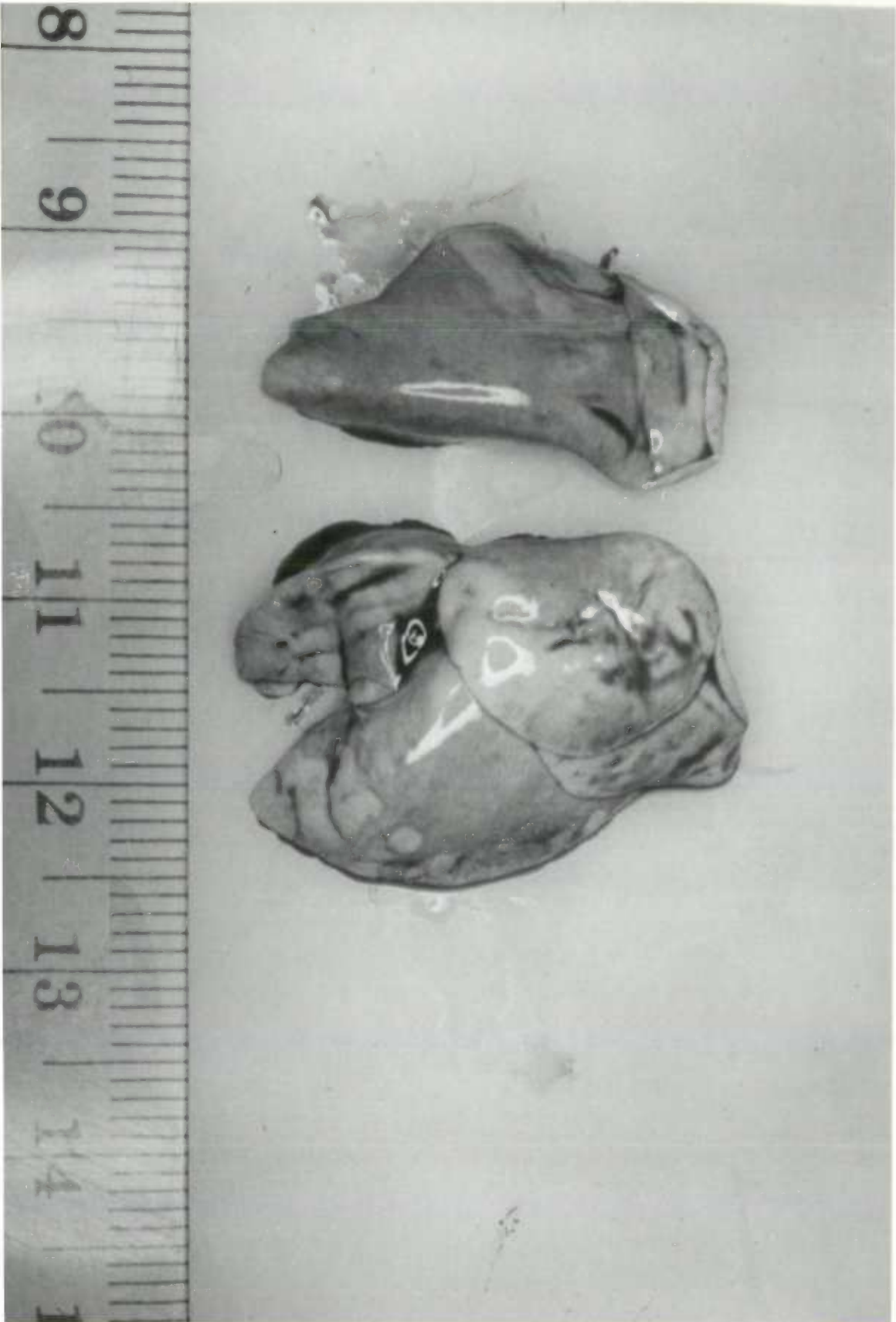


Fig. 4. Lungs from a rat injected with aconitine (1550 μ moles/kg) and killed at the time of frothing (15 min). All the lobes of both lungs are partially covered with light-colored, punctate hemorrhages. The LW/BW was 1.03.

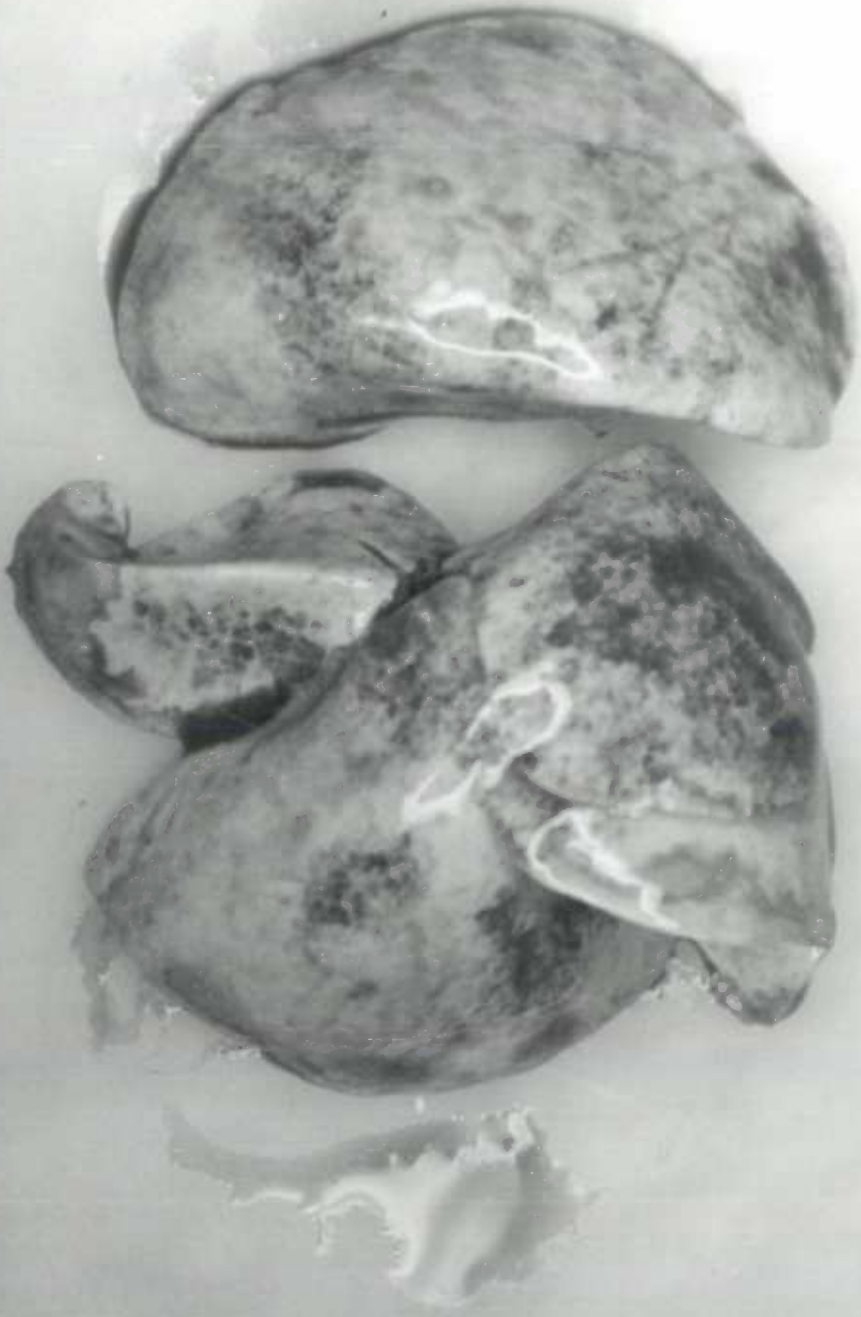
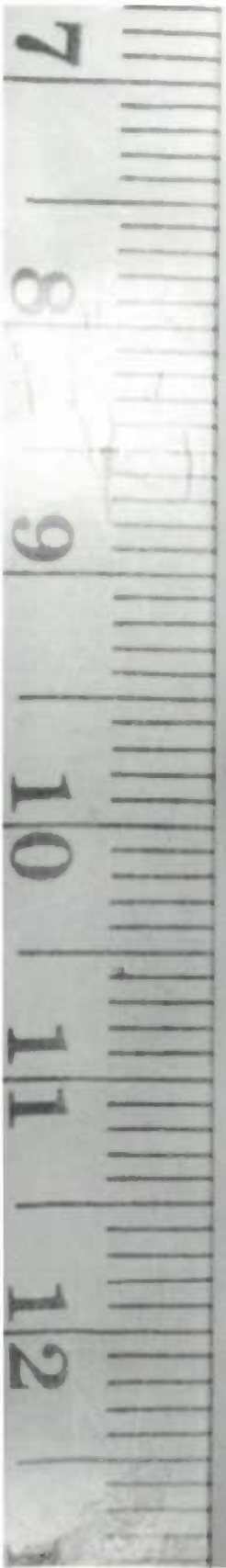


Fig. 5. Lung biopsy from a rat injected with aconitine (1550 pmoles/kg) and killed at the time of peak SAP (8 min). Ferritin (small arrows) occupies the capillary lumen (Cap) but is not present in the interstitial (IS) or alveolar air spaces (AAS). The darkened membranes (large arrows) of two adjacent endothelial cells (En) outline a junctional complex that appears separated but does not contain ferritin. The LW/BW was 0.54. Ep I, type I alveolar epithelium.

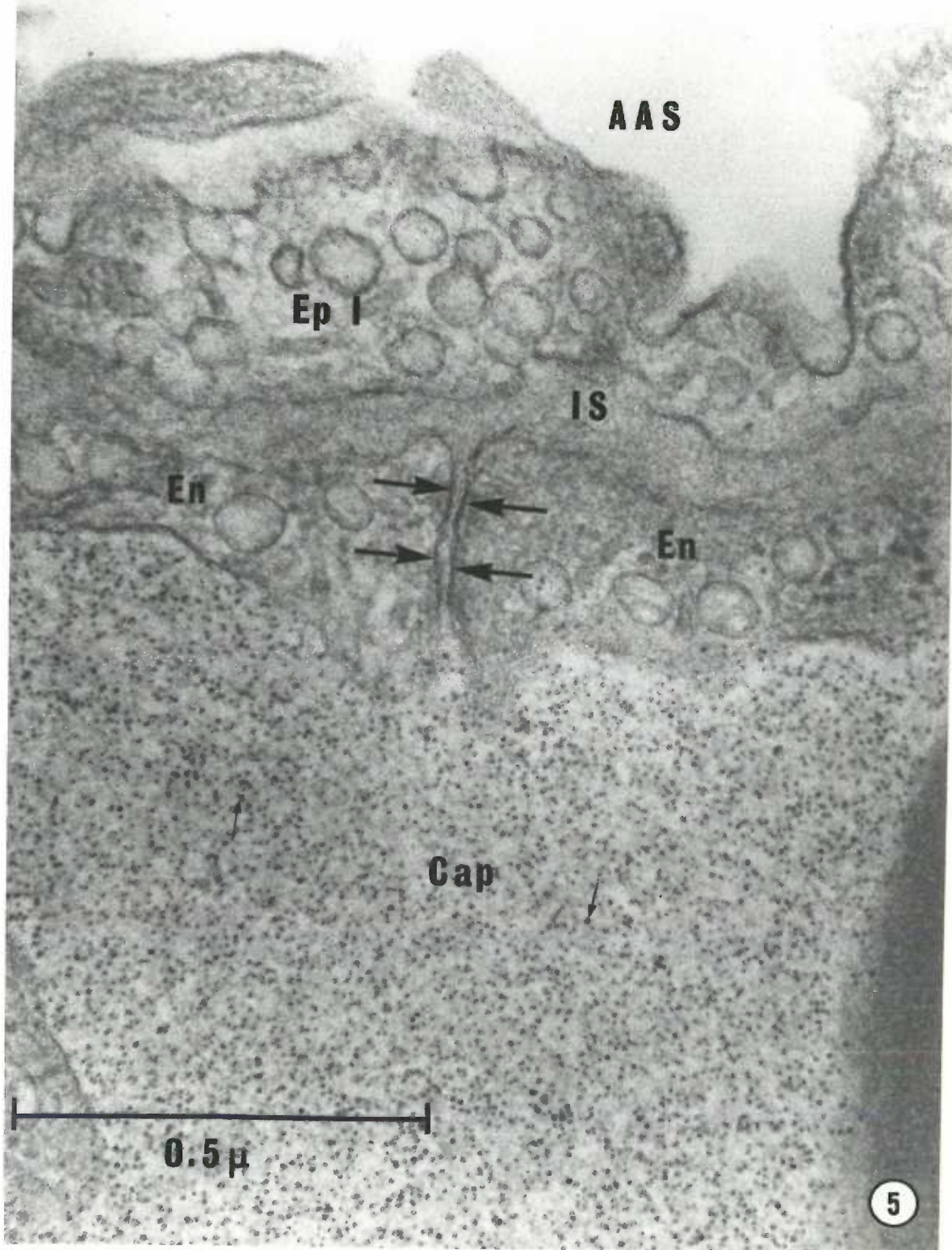


Fig. 6. Lung biopsy from a rat injected with aconitine (1550 μ moles/kg) and killed at the time of frothing (15 min). Note that two endothelial cells (En) are contiguous at the junctional complex (large arrows). The LW/BW was 1.29. AAS, alveolar air space; Ep I, type I alveolar epithelium; Cap, capillary; small arrows, ferritin.

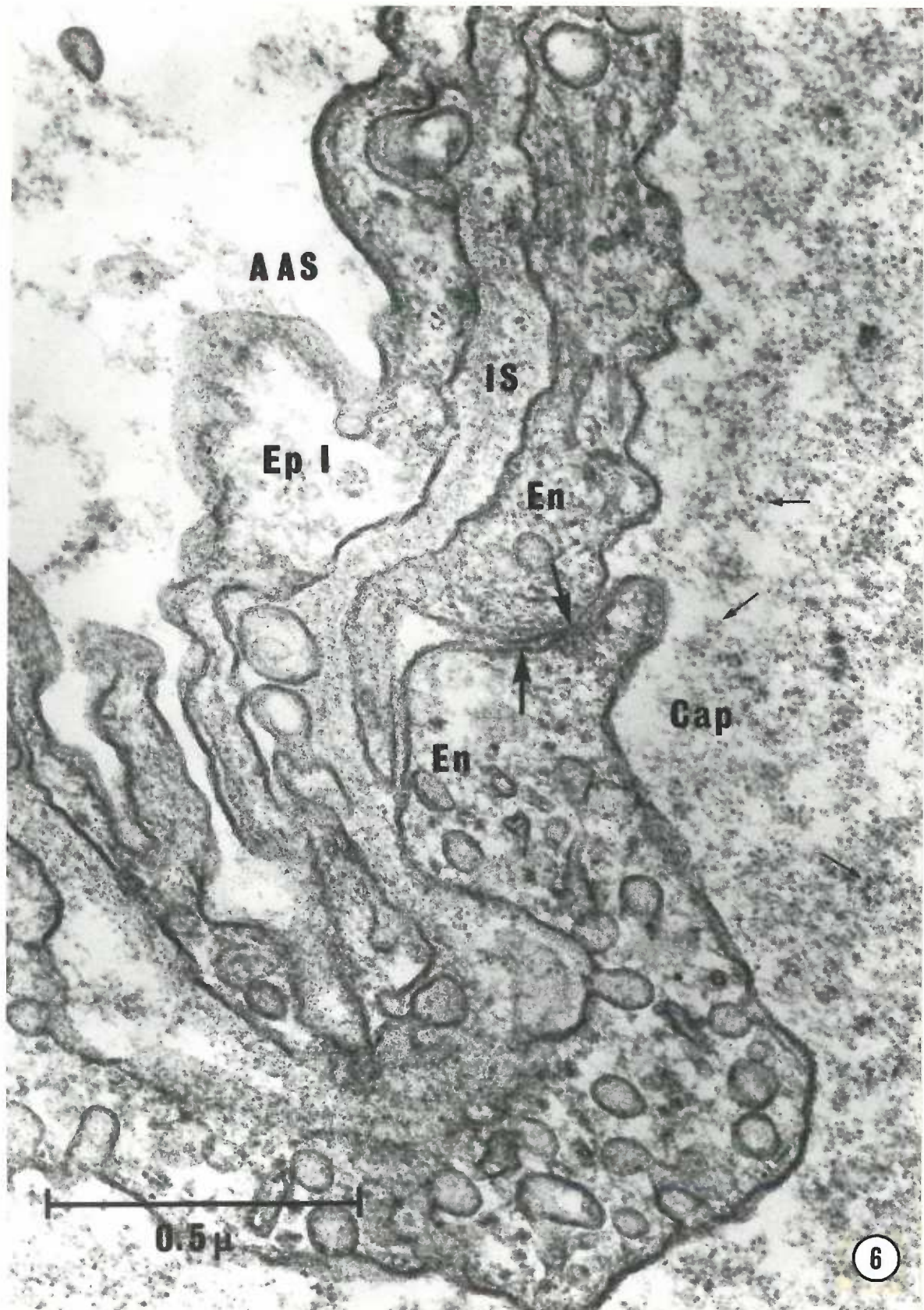


Fig. 7. Lung biopsy from a rat injected with aconitine (1550 pmoles/kg) and killed at the time of frothing (15 min). The capillary endothelium (En) is separated from the basal lamina (BL) and protrudes (small arrows) into the capillary lumen (Cap). Ferritin (small arrowhead) occupies the interstitial space (IS). A rarefied type I epithelial cell (Ep I*) is adjacent to the protruded endothelial cell. A normal type I epithelial cell (Ep I) and an intact tight junction (large arrows) between two type I epithelial cells can be seen in the lower left-hand side. The LW/BW was 1.20. AAS, alveolar air space.

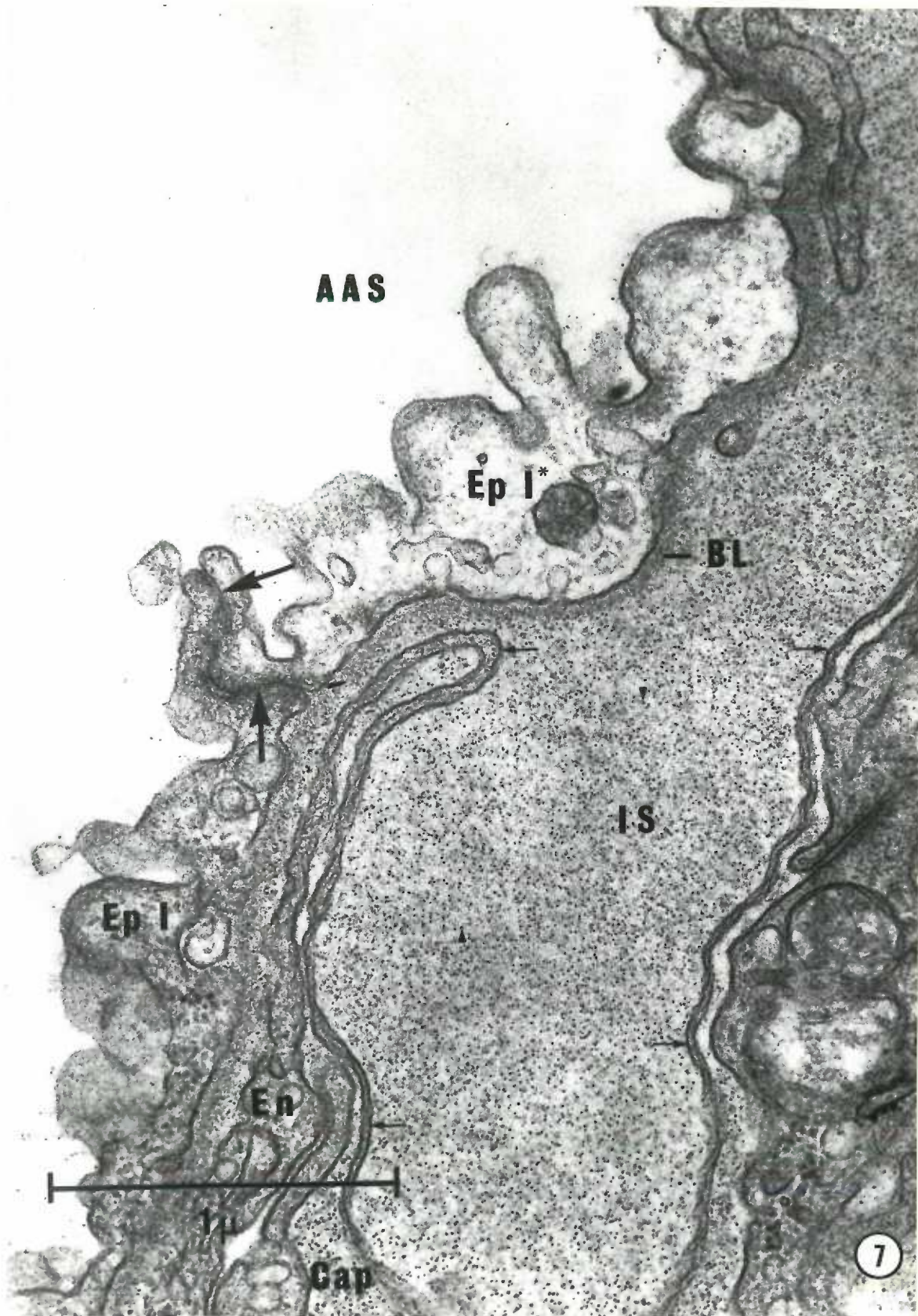


Fig. 8. Lung biopsy from a rat injected with aconitine (1550 pmoles/kg) and killed at the time of frothing (15 min). A rarefied and swollen type I epithelial cell (Ep I) is adjacent to two intact endothelial cells (En). Note the normal appearing tight junction (large arrows) between two epithelial cells in the lower right-hand corner. The LW/BW was 1.29. AAS, alveolar air space.

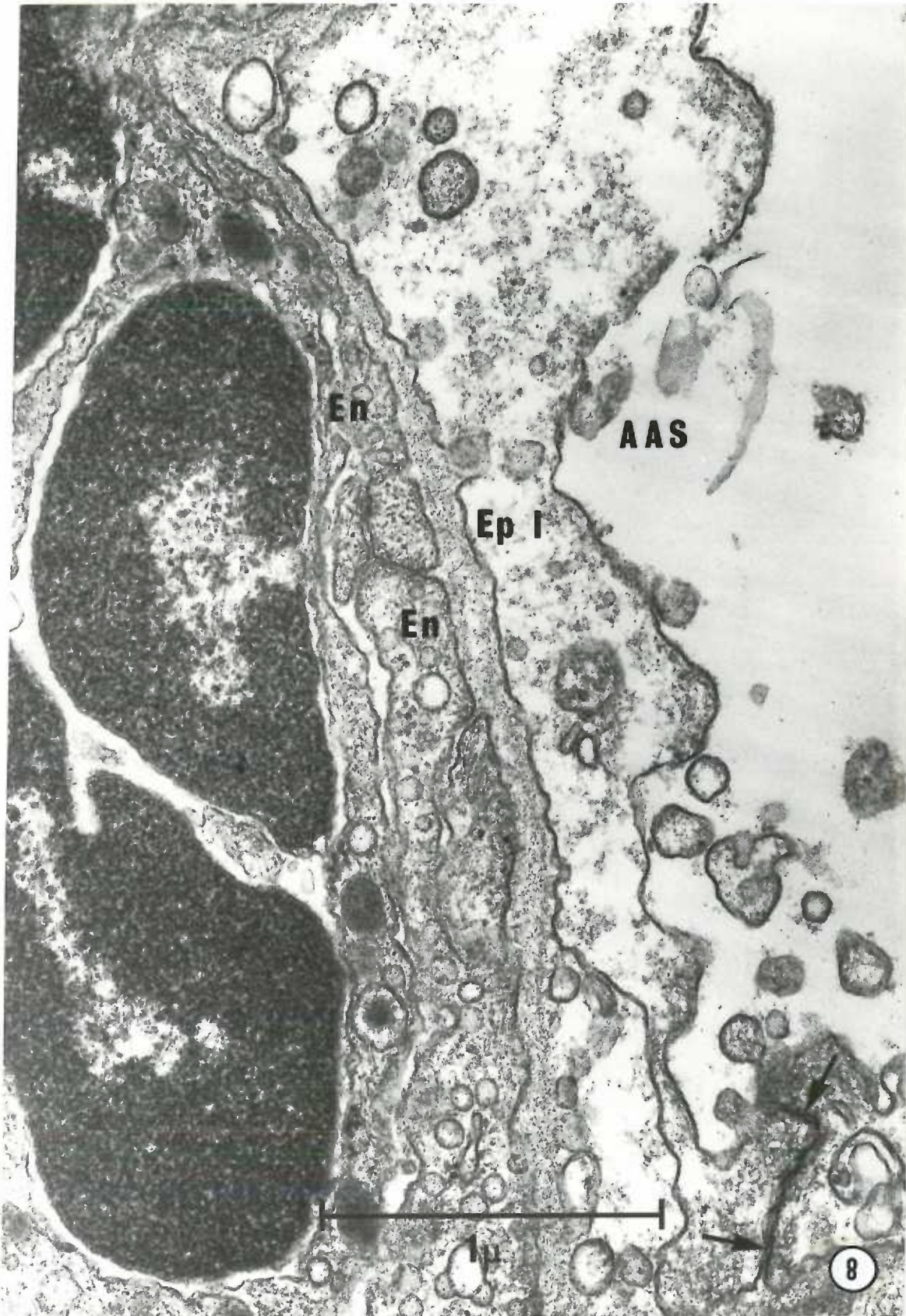


Fig. 9. Lung biopsy from a rat injected with aconitine (1550 $\mu\text{moles/kg}$) and killed at the time of frothing (15 min). The capillary endothelium (En) is separated into a number of blebs (large arrows). Ferritin (small arrows) is present in the interstitial space (IS) and in endothelial and type I epithelial (Ep I) cells. The LW/BW was 1.25. AAS, alveolar air space; RBC, red blood cell.

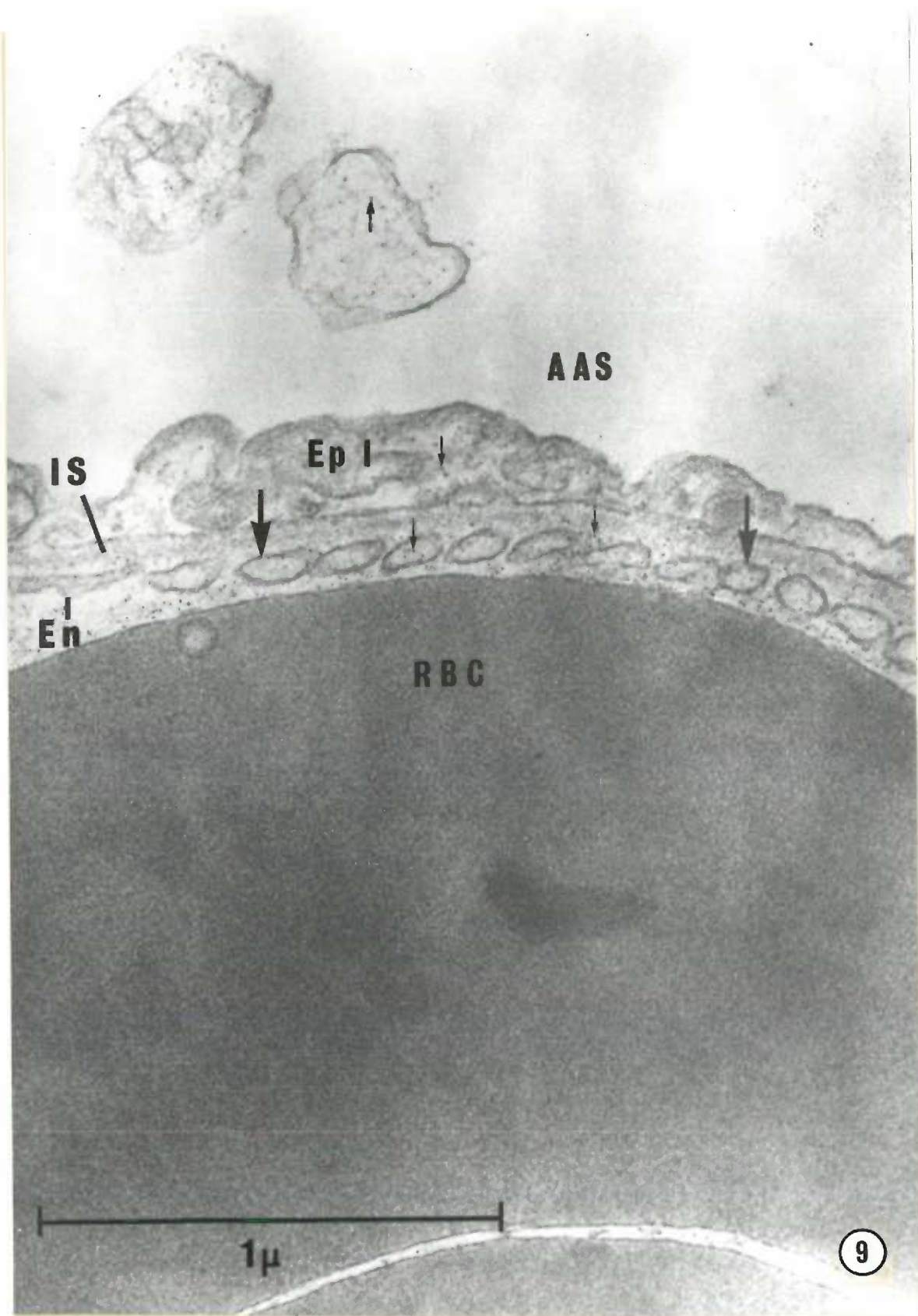


Fig. 10. Lung biopsy from a rat injected with aconitine (1550 pmoles/kg) and killed at the time of frothing (15 min). Whether the junctional complex (large arrows) shown here is open or closed cannot be determined. However, the presence of ferritin (small arrows) in the intercellular cleft (IC) between two endothelial cells (En) and in the interstitial space (IS) suggests that the junction was open. The LW/BW was 1.20. Ep I, type I alveolar epithelium; Cap, capillary; RBC, red blood cell.

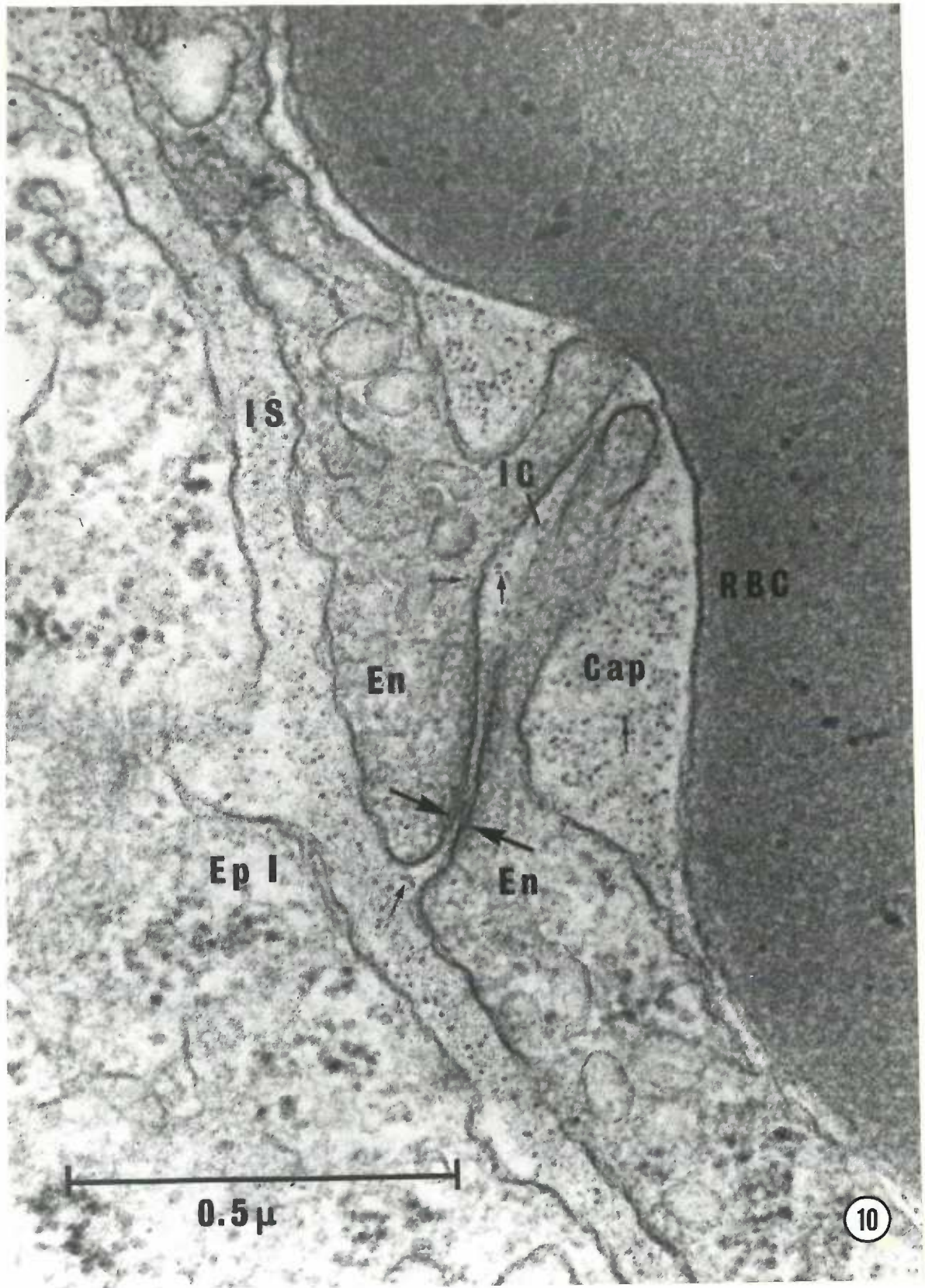
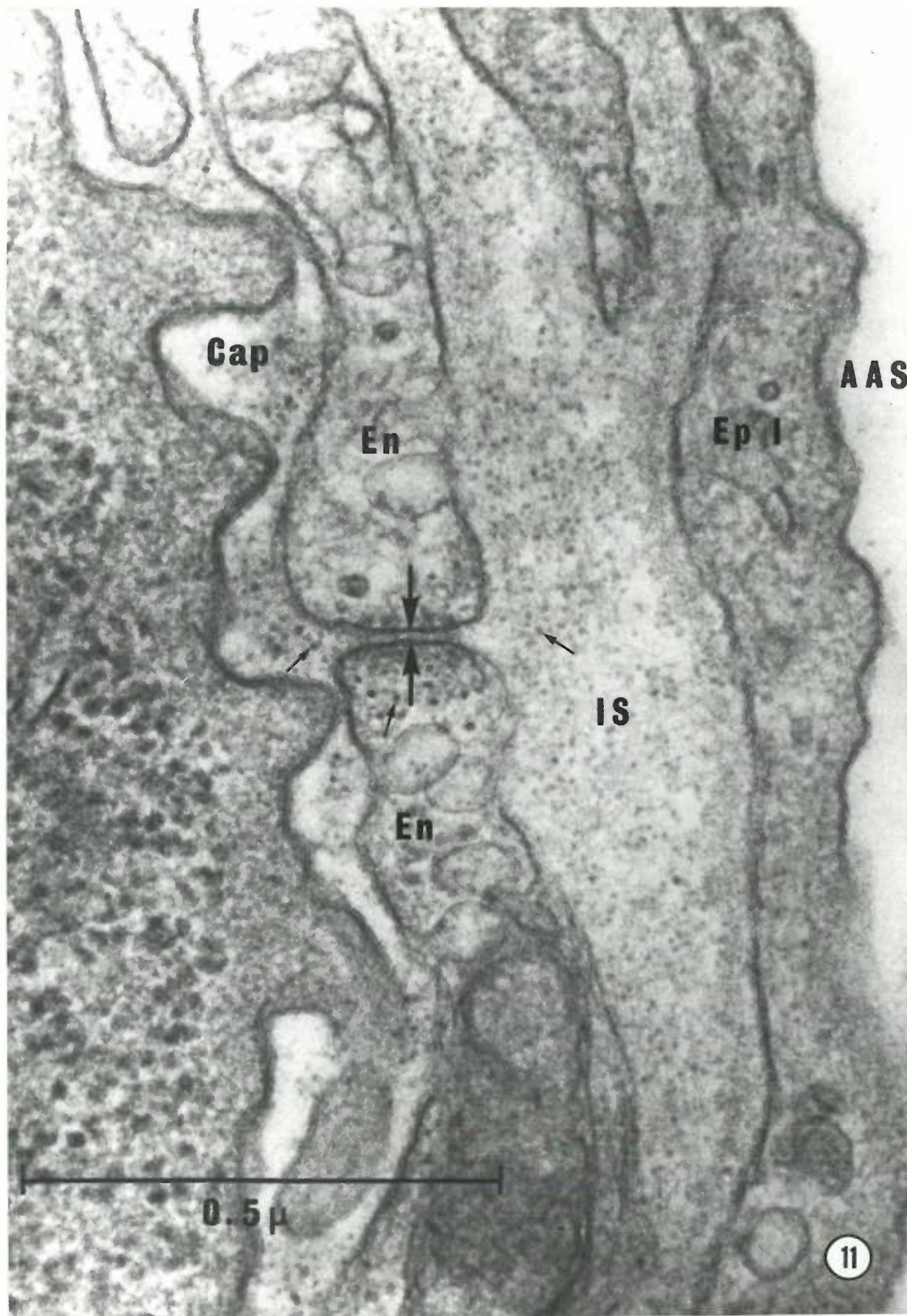


Fig. 11. Lung biopsy from a rat injected with aconitine (1550 pmoles/kg) and killed at the time of peak SAP (8 min). The dark membranes (large arrows) of two endothelial cells (En) outline a junction that appears open. Ferritin (small arrows) is present in the interstitial space (IS) and in an endothelial cell. The LW/BW was 0.71. AAS, alveolar air space; Ep I, type I alveolar epithelium; Cap, capillary.



oniti
itin
titia
alveo
o end
open

Fig. 12. Lung biopsy from a rat injected with aconitine (1550 pmoles/kg) and killed at the time of peak SAP (8 min). Ferritin (small arrows) occupies the capillary lumen (Cap) and the interstitial (IS) and alveolar air spaces (AAS). Fibrin (F) can be seen in the alveolar air space. Note that the dark membranes (large arrows) of two endothelial cells (En) outline an endothelial junction that appears open. The LW/BW was 0.71. Ep I, type I alveolar epithelium.

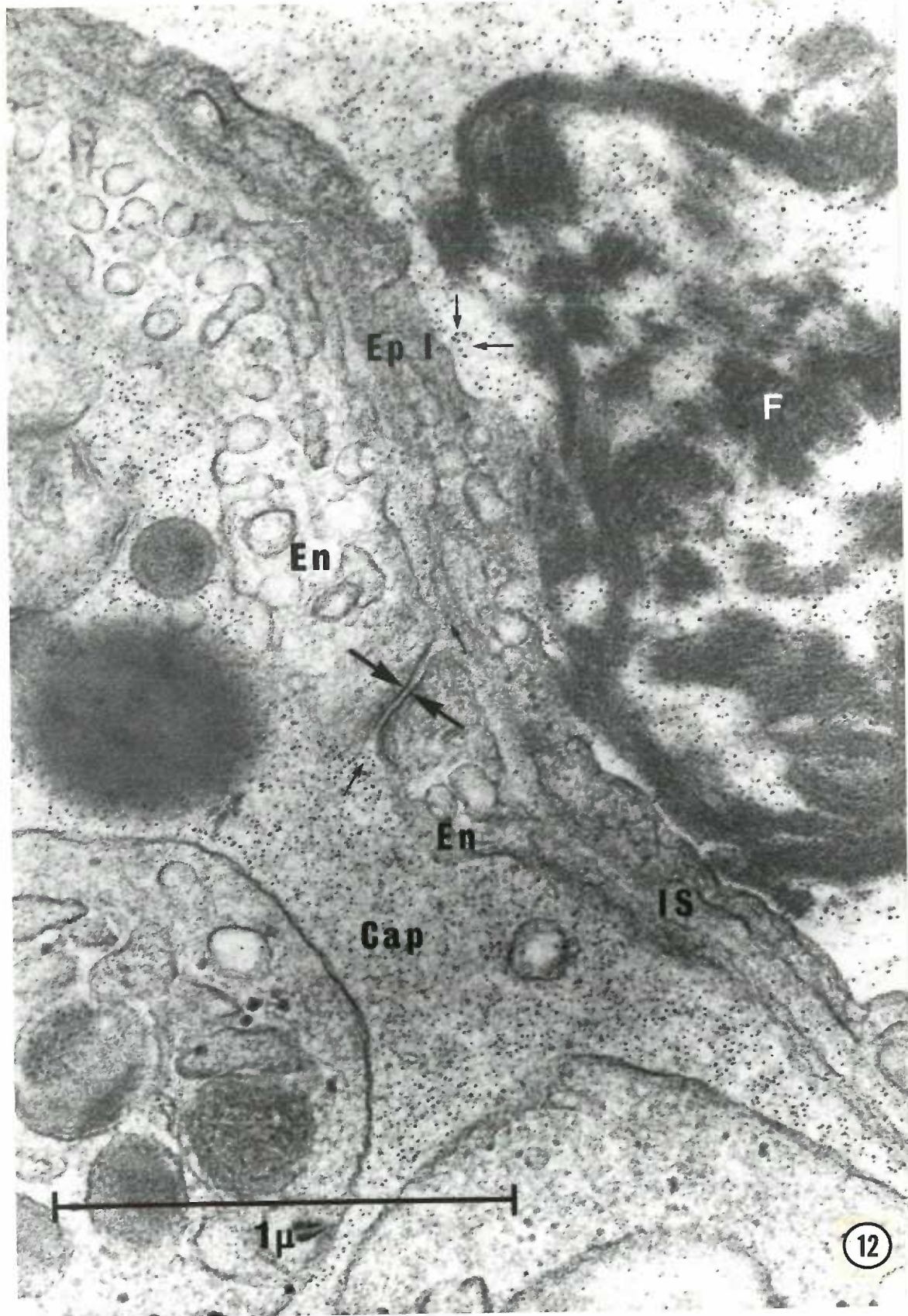
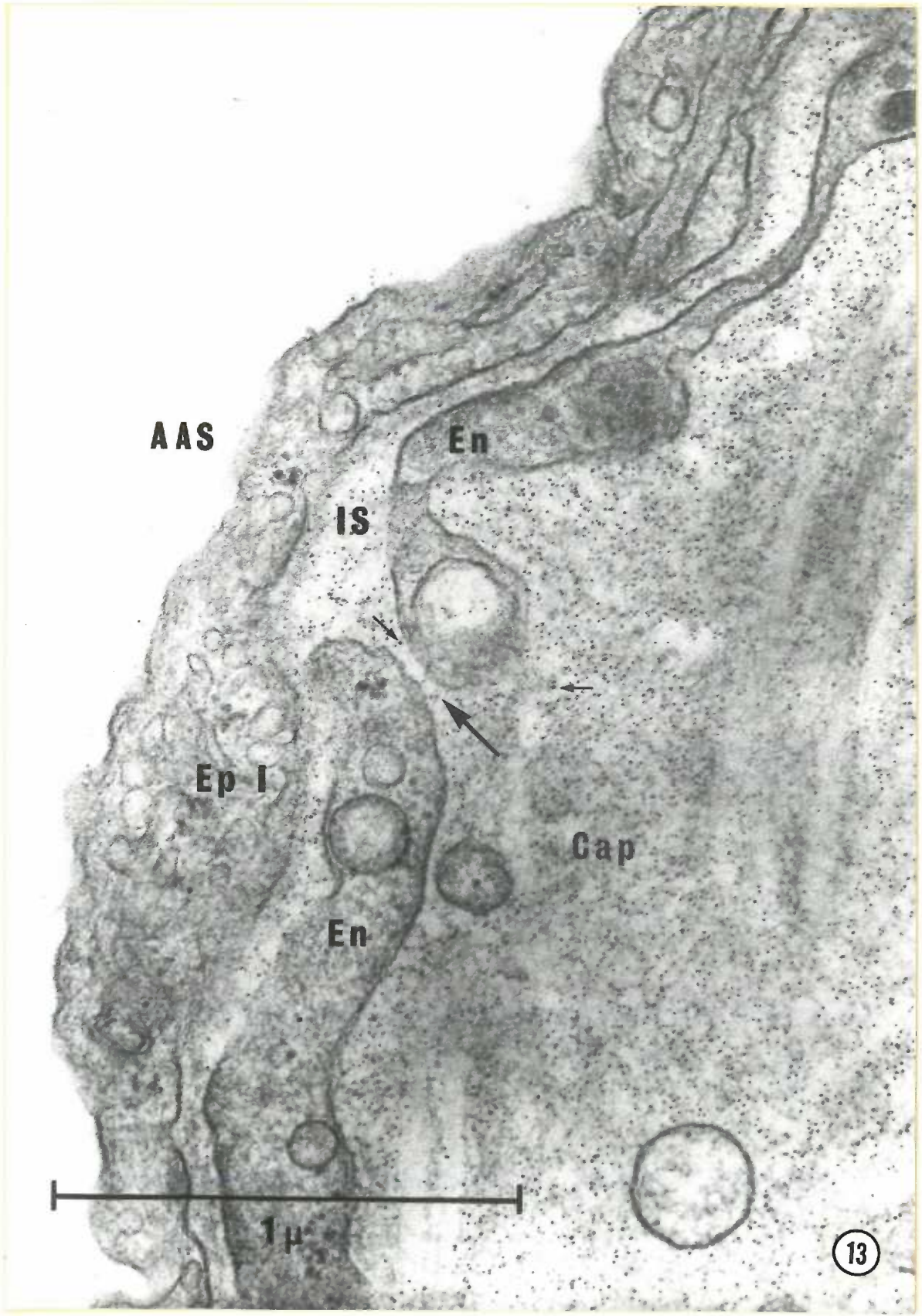


Fig. 13. Lung biopsy from a rat injected with aconitine (1550 pmoles/kg) and killed at the time of peak SAP (8 min). Two endothelial cells (En) are separated (large arrows) at what appears to be a junctional complex. Ferritin (small arrows) is present in the junction and in the interstitial space (IS). The LW/BW was 0.71. AAS, alveolar air space; Ep I, type I alveolar epithelium; Cap, capillary.



AAS

En

IS

Ep I

Gap

En

1 μ

13

Fig. 14. Lung biopsy from a rat injected with aconitine (1550 pmoles/kg) and killed at the time of peak SAP (8 min). The endothelium (En and large arrows) is discontinuous. Note that an adjacent type I epithelial cell (Ep I) appears intact. The LW/BW was 0.71. WBC, white blood cell; RBC, red blood cell; Cap, capillary; AAS, alveolar air space.

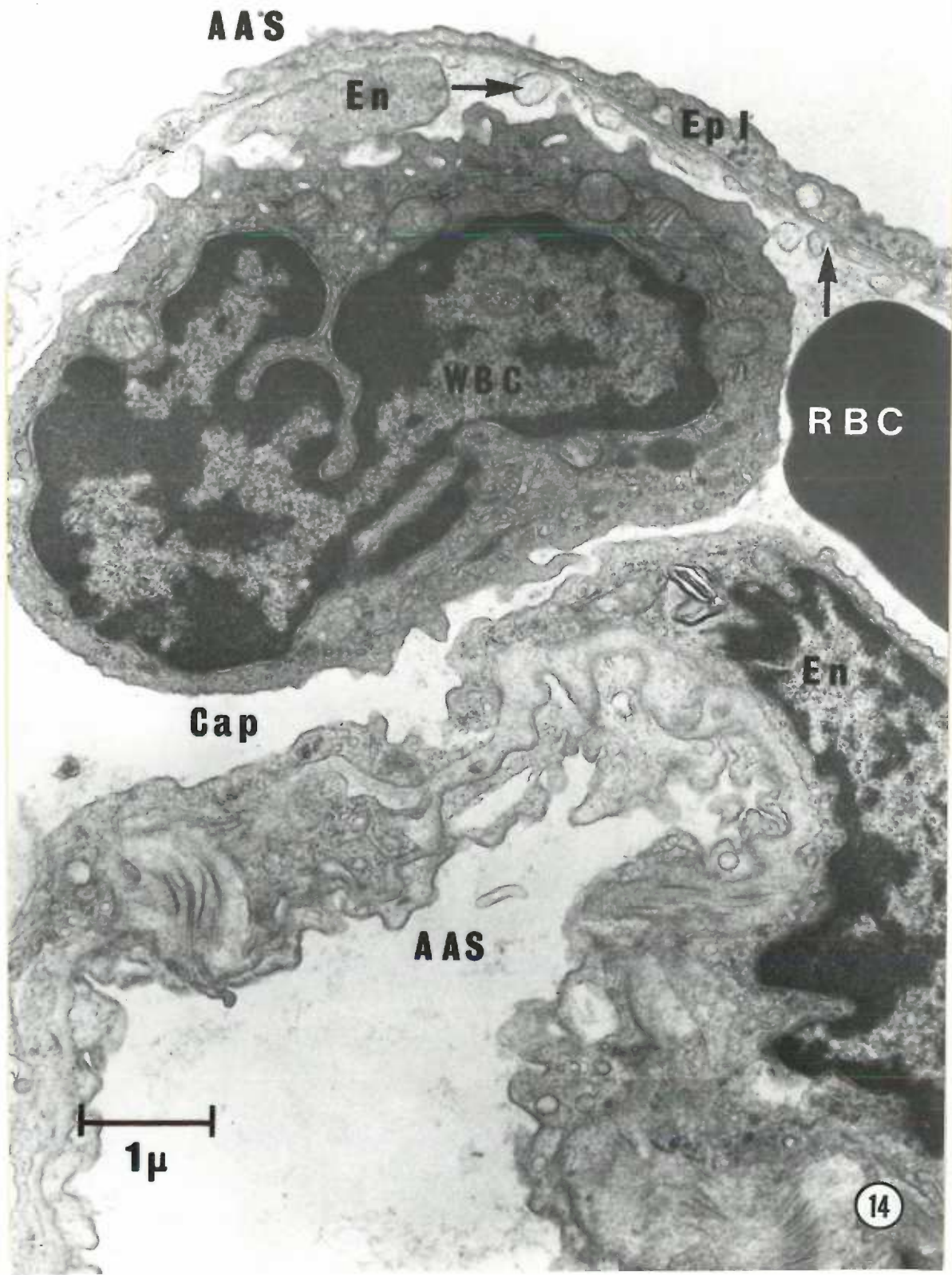
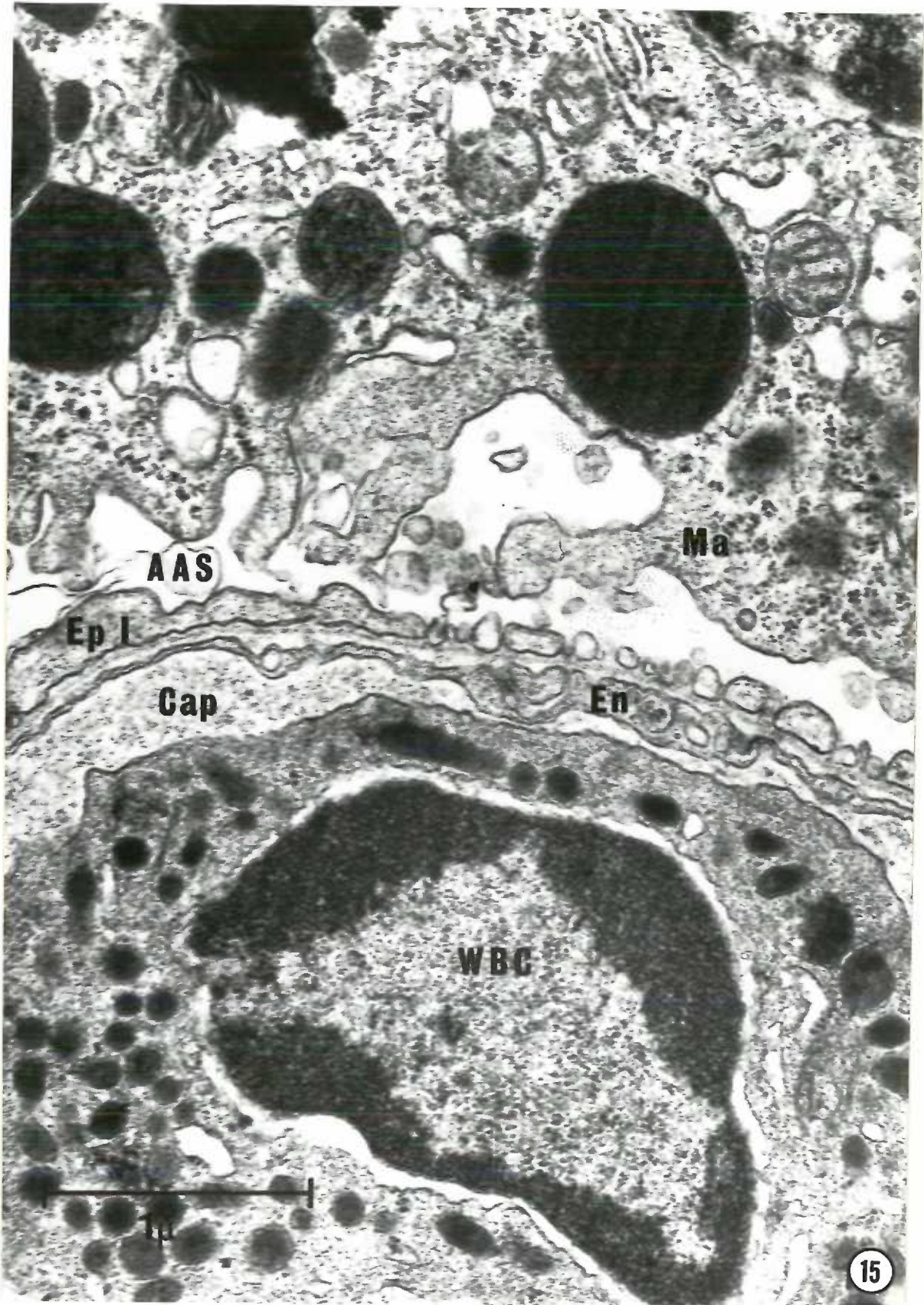


Fig. 15. Lung biopsy from a rat injected with aconitine (1550 pmoles/kg) and killed at the time of frothing (15 min). The type I epithelium (Ep I) is discontinuous and adjacent to an intact endothelial cell (En). The LW/BW was 1.29. Ma, macrophage; AAS, alveolar air space; Cap, capillary; WBC, white blood cell.



PAPER 3

Prevention of Aconitine-Induced Neurogenic Pulmonary
Edema by Phlebotomy or Pretreatment with
Methylprednisolone Sodium Succinate

ABSTRACT

The efficacy of phlebotomy or iv injection of methylprednisolone sodium succinate (MPSS) in preventing neurogenic pulmonary edema (NPE) was examined in rats following the injection of aconitine into the preoptic area of the brain. Adult female rats were phlebotomized 20% of the calculated blood volume either before injection of 774 pmoles/kg or after injection of 1550 pmoles/kg of aconitine. Another group of rats was treated with MPSS (40 mg/kg) before receiving aconitine (774 pmoles/kg). Animals injected with aconitine (774 or 1550 pmoles/kg) and given no further treatment served as controls.

Severe pulmonary edema, as measured by an increase in the ratio of lung weight to body weight, developed in rats injected with aconitine (774 or 1550 pmoles/kg) only. The pulmonary ultrastructure in these rats was severely damaged. In contrast, rats phlebotomized before or after injection of aconitine or pretreated with MPSS did not develop pulmonary edema, and the pulmonary ultrastructure of these animals appeared normal except for the occasional observation of a focally swollen or rarefied type I alveolar epithelial cell and exudates in the alveolar air spaces. Although the mechanism by which these treatments prevented damage to the lungs could not be determined from this study, it is suggested that phlebotomy was effective because it lowered the pulmonary blood volume and that MPSS provided a beneficial effect by suppressing the sympathetic response involved in NPE.

INTRODUCTION

Various injuries to the brain or spinal cord lead to the development of pulmonary edema (8,24,26,29). The syndrome, known as neurogenic pulmonary edema (NPE), is characterized by transient increases in systemic and pulmonary blood pressures (7,14,22,26,27) and pulmonary blood volume (3,7,9,20,21) and persistent increases in pulmonary vascular permeability (2,4,15,29) and lung water content (14,26). Treatment for NPE has focused on ameliorating pulmonary function with positive pressure ventilation and reducing the pulmonary edema and pulmonary blood volume with diuretics, controlled phlebotomy and morphine (8,24,25). Therapy aimed at reversing the increase in permeability of the capillary endothelium as well as reducing the hemodynamic changes has not been used (25). Since corticosteroids such as methylprednisolone sodium succinate (MPSS) have been shown to reduce capillary permeability and the hemodynamic changes in patients and animals on cardiopulmonary bypass and those with endotoxic and hemorrhagic shock (6,10,16,19), they might also be useful in the treatment of NPE. Therefore, the present study was undertaken to examine the effects of MPSS as well as phlebotomy on the development of NPE, produced in rats by injecting aconitine into the preoptic area of the brain. The efficacy of these two treatments was tested by measuring changes in systemic arterial blood pressure (SAP), determining ratios of lung weight to body weight and examining the changes in gross appearance and ultrastructure of the lungs.

MATERIALS AND METHODS

Forty-two adult female Charles River (CD) rats weighing 220 to 341 g were used. Under ether anesthesia, the external jugular vein was cannulated with PE-50 tubing to provide a route for either the removal of

blood or the administration of MPSS. A second cannula was inserted into the tail artery to monitor SAP in 13 of the rats. SAP was measured by a Statham P23Db strain gauge and recorded on a Grass Model 79D polygraph. The patency of the cannula was maintained by continuous infusion (0.5 ml/h) of 1% heparinized saline through a Sorenson valve. Aconitine (Sigma) was injected into the preoptic area under light ether anesthesia. With the aid of a stereotaxic instrument, a 22 gauge stainless steel guide tube was positioned 1.3 mm anterior to bregma, 0.7 mm lateral from midline and 2.85 mm below the cortical surface. A 50 μ l Hamilton syringe connected by 10 mm of polyethylene tubing to a 28 gauge stainless steel cannula was lowered through and extended 5 mm past the guide tube into the preoptic area. Aconitine (774 or 1550 pmoles/kg), prepared fresh in saline, was injected in a volume of 100 μ l/kg within 15 sec. The same procedure was repeated contralaterally within 2 min.

Following the injection of aconitine, the animals were placed in a cage that restricted movement, anesthetized with ether 1 h later and killed by severing the abdominal aorta. The thoracic cavity was opened, and the lungs were excised and weighed to the nearest 0.1 g. A lung weight to body weight ratio (LW/BW) was calculated (lung weight/body weight \times 100) for each rat and used as an index of pulmonary edema. The extent of grossly visible hemorrhages on the lungs was recorded. The upper and lower lobes of the right and left lungs were biopsied, and the tissues were cut into 1 mm cubes, fixed by immersion in glutaraldehyde and osmium tetroxide and processed for electron microscopy as previously described (17).

Brains were removed at autopsy and fixed in formalin. The placements of injections in the preoptic area were verified histologically on alternate

frozen sections (50 μm) stained with thionin.

Three experiments were performed to evaluate the effects of phlebotomy and MPSS on the development of aconitine-induced NPE.

1. Effects of Phlebotomy Performed before Injection of Aconitine

Eight rats were phlebotomized by removing 20% of their calculated blood volume through a cannula placed in the external jugular vein. Aconitine (774 pmoles/kg) was injected into the preoptic area 22 min later. Ten rats that received aconitine (774 pmoles/kg) but were not phlebotomized served as controls. In addition, to assess the effects of hypovolemia per se, 20% of the blood volume was removed in 4 rats, but aconitine was not injected. The animals were killed 1 h after injection of aconitine, and the lungs were removed and evaluated as described above.

2. Effects of Phlebotomy Performed after Injection of Aconitine

Since pulmonary edema has been shown to develop between 8 and 15 min after injection of 1550 pmoles/kg of aconitine (18), 5 rats were injected with that dose and phlebotomized when SAP reached a peak level (about 8 min). Five rats received aconitine (1550 pmoles/kg) only and served as controls. The animals were monitored for SAP and killed 1 h after injection of aconitine. The lungs were removed and evaluated as described above except lung tissue from the control animals was not processed for electron microscopy.

3. Effects of Methylprednisolone Sodium Succinate

MPSS (40 mg/kg, 0.25 ml, Solu-Medrol^R) was injected into the external jugular vein in 10 rats, and 30 min later aconitine (774 pmoles/kg) was injected into the preoptic area. SAP was monitored in 4 of these rats. The same 10 rats described in the first experiment (i.e., those

that received 774 pmoles/kg of aconitine without treatment with MPSS) served as controls. SAP was monitored in 4 of these rats. The animals were killed 1 h after injection of aconitine, and the lungs were removed and evaluated as described above.

Statistical Analysis

LW/BWs were analyzed between groups with a one-way analysis of variance and a Newman-Keuls' multiple-range test. Systolic and diastolic blood pressures were averaged at each minute for the first 20 min after injection of aconitine and analyzed using a two-way analysis of variance for repeated measures (28). Differences were considered significant at $P < 0.05$.

RESULTS

Severe pulmonary edema developed in the rats injected with aconitine (774 or 1550 pmoles/kg) only. In these animals, LW/BWs were high (Table 1); the SAP increased rapidly and reached a maximum value of $203 \pm 6 / 158 \pm 4$ mmHg (774 pmoles/kg) (Fig. 1) or $209 \pm 6 / 172 \pm 6$ mmHg (1550 pmoles/kg); the lungs were completely covered with hemorrhages (Fig. 2); and the pulmonary ultrastructure, in animals that received 774 pmoles/kg, showed severe and widespread changes (Fig. 3). Both capillary endothelial and type I alveolar epithelial cells in these animals were often absent or appeared as spherical blebs adjacent to the denuded basal lamina. Fibrin and dense accumulations of exudates were frequently found in the alveolar air spaces, and fibrin was also observed interwoven with degranulated platelets in the capillary lumen. The ultrastructure of the lungs was not examined in animals administered 1550 pmoles/kg.

Effects of Phlebotomy Performed before Injection of Aconitine

Phlebotomy performed before the injection of aconitine (774 pmoles/kg)

was effective in preventing the development of pulmonary edema. LW/BWs of this group were lower ($P < 0.01$) than those of controls injected with the same dose of aconitine and given no further treatment (Table 1). The gross appearance (Fig. 4) and the ultrastructure of the lungs appeared normal except for the occasional observation of rarefied and swollen type I epithelial cells or exudates in the alveolar air spaces. A small amount of fibrin was found in a few alveoli in approximately 50% of the rats. The 5 rats subjected to the removal of 20% of the blood volume and used to assess the effects of hypovolemia per se had low LW/BWs (Table 1), and the gross appearance and ultrastructure of the lungs were normal.

Effects of Phlebotomy Performed after Injection of Aconitine

Phlebotomy performed at 8 min after injection of 1550 pmoles/kg of aconitine prevented the pulmonary edema in 4 of 5 animals that usually develops 15 min after injection of this dose. LW/BWs in these animals were lower ($P < 0.01$) than those of controls that received aconitine (1550 pmoles/kg) only (Table 1). Changes in gross appearance and ultrastructure of the lungs (Figs. 5 and 6) were comparable to those observed in animals phlebotomized before receiving 774 pmoles/kg of aconitine. However, 1 rat in this group developed pulmonary changes characteristic of a severe form of NPE; the LW/BW was 0.84; the lungs were completely covered with hemorrhages; and at the cellular level, exudates and fibrin were present in the alveoli, and the type I epithelium was discontinuous, exposing the underlying basal lamina (Fig. 7). This rat frothed from the nose 41 min after injection of aconitine and died before 1 h.

The SAP was also monitored in these animals. It increased rapidly after injection of aconitine (1550 pmoles/kg) reaching a maximum value

of $210_{\pm 8}/157_{\pm 5}$ mmHg at 8 min, falling to $141_{\pm 7}/119_{\pm 6}$ mmHg at the start of phlebotomy and rising again to $192_{\pm 3}/159_{\pm 5}$ mmHg at approximately 15 min after injection of aconitine. A representative tracing of the SAP response to phlebotomy is shown in Fig. 8. In the control animals that received aconitine (1550 pmoles/kg) only, the SAP reached a maximum value of $209_{\pm 6}/172_{\pm 6}$ mmHg at 9 min, then fell slowly to $199_{\pm 5}/176_{\pm 7}$ mmHg at 15 min after injection of aconitine. Thus, phlebotomy only temporarily reduced the SAP response to aconitine.

Effects of Methylprednisolone Sodium Succinate

The results obtained in 9 of the 10 rats treated with MPSS were comparable to those observed in the phlebotomized animals. LW/BWs were lower ($P < 0.01$) than those of animals injected with aconitine (774 pmoles/kg) only (Table 1). The lungs of 50% of these rats appeared normal and those of the remainder had punctate hemorrhages restricted to 1 or 2 lobes of a lung (Fig. 9). The pulmonary ultrastructure of the MPSS-treated rats was comparable to that observed in the phlebotomized rats (Fig. 10). However, 1 rat treated with MPSS had severe changes in pulmonary ultrastructure characteristic of NPE. In this animal, fibrin and exudates were present in the alveolar air spaces, and the type I epithelium was discontinuous resulting in exposure of the basal lamina (Fig. 7). Following treatment with MPSS, the SAP increased rapidly after administration of aconitine but attained a peak value ($161_{\pm 9}/120_{\pm 6}$ mmHg) that was lower ($P < 0.01$) than that observed in controls (Fig. 1).

DISCUSSION

The results of the present study demonstrate that phlebotomy performed before or after injection of aconitine or pretreatment with MPSS prevented

aconitine-induced NPE. The mechanism by which these treatments prevented damage to the lungs could not be determined from this study.

An increase in pulmonary blood volume, probably resulting from an increase in peripheral vasoconstriction and a subsequent shift in blood from the systemic to the lower resistance pulmonary circulation (12,20), is a characteristic feature of a severe form of NPE and may be important in determining the amount of edema that accumulates in the lungs. How the increase in pulmonary blood volume affects the pulmonary circulation is not known, but Sarnoff (22) and Lloyd (11) showed that it is essential for the development of pulmonary vascular hypertension in severe forms of NPE. Staub (25) has suggested that structural damage to endothelial cells occurs in NPE due to frictional or inertial forces of blood flowing at a high linear velocity through a vasoconstricted pulmonary vascular bed. An increase in pulmonary vascular pressure and pulmonary blood volume may contribute to the injurious effects of high linear blood flow.

Sarnoff et al. (21), using a gravimetric technique for estimating changes in pulmonary blood volume, have shown that the intracisternal injection of fibrin in dogs leads to an immediate increase in lung weight and pulmonary and systemic blood pressures. These changes were reversed by the removal of 13-19% of the calculated blood volume (20) or iv injection of a peripheral vasodilator, Ro 2-2222 (21). Thus, it was suggested that the increase in pulmonary blood volume, which was estimated to double following injection of fibrin, produces both the increase in lung weight and pulmonary vascular pressures. Peripheral vasodilation as well as phlebotomy were thought to reverse the changes in lung weight and pulmonary vascular pressures by lowering the pulmonary blood volume. In support

of this hypothesis, Simmons et al. (24) reviewed the case studies of 56 patients that had developed pulmonary edema following head trauma. Two of the 56 patients did not develop pulmonary edema, one of which lost a large amount of blood before a fatal head wound. It was suggested that the development of NPE requires a "relatively full and intact circulatory system". The findings in the present study that SAP was temporarily reduced, and the LW/BWs were unchanged from normal values at 1 h in animals phlebotomized 8 min after injection of 1550 pmoles/kg of aconitine agree with the findings of Sarnoff et al. (20,21) and Simmons and associates (24). In addition, the LW/BWs (0.60 ± 0.07 , mean \pm SEM) and changes in pulmonary ultrastructure in the phlebotomized animals at 1 h were similar to those previously reported (18) in animals injected with aconitine (1550 pmoles/kg) only and killed at 8 min. In that study, the LW/BWs were low (0.62 ± 0.02) at 8 min, and the pulmonary ultrastructure appeared normal except for the occasional observation of damaged capillary endothelium and type I epithelium and alveolar exudates. However, in animals killed at 15 min, the LW/BWs were high (1.15 ± 0.06), and the pulmonary ultrastructure showed severe damage. The finding in this study that phlebotomy performed at 8 min prevented the pulmonary edema and ultrastructural changes that are expected 15 min after injection of 1550 pmoles/kg of aconitine, suggests that the development of pulmonary edema was prevented by lowering the pulmonary blood volume at this critical period.

Adjunctive therapy with pharmacologic doses of MPSS has been shown to reduce systemic and pulmonary vascular resistance (6,16), stabilize capillary membranes (19) and prevent changes in pulmonary morphology (10) in patients and animals with endotoxic or hemorrhagic shock (10,16,19)

or on cardiopulmonary bypass (6). These effects of MPSS have been attributed to its ability to reduce peripheral vascular resistance either by modifying alpha adrenergic vasoconstriction or causing direct vasodilation (5,19,23). NPE is characterized by transient increases in systemic and pulmonary blood pressures (7,14,22,26,27) and pulmonary blood volume (3,7,9,20,21) and a persistent increase in pulmonary vascular permeability (2,4,15,29) that appear to be mediated by alpha adrenergic mechanisms because they can be prevented by pretreatment with appropriate blocking agents (phenoxybenzamine and phentolamine) (3,13,14,27). Motsay et al. (19) have emphasized the common ability of MPSS, phenoxybenzamine and epinephrine tolerance to reduce the sympathetic response to stress. The finding in the present study that the magnitude of the SAP response in MPSS-treated animals was lower than that of controls confirms the finding of Motsay (19). Therefore, it seems possible that MPSS may prevent aconitine-induced NPE by directly preventing the increase in pulmonary vascular permeability, pulmonary vasoconstriction or pulmonary blood volume; the latter by preventing peripheral vasoconstriction.

Although NPE occurs rapidly and the initial hemodynamic changes are short-lasting, one clinical case report documented recurrent episodes of changes in systemic and pulmonary blood pressures (29). Prophylactic therapy with MPSS might afford protection against further damage to the lung parenchyma caused by repeated changes in hemodynamics and the persistent change in permeability of the capillary-alveolar barrier. Consistent with the effects of MPSS observed in the present study, it has been reported that 5 patients with massive cerebral injuries that received dexamethasone, another synthetic corticosteroid, maintained satisfactory pulmonary function despite pulmonary contusions (1). Although pretreatment

with MPSS in the present study was shown to be effective in blocking the development of aconitine-induced NPE in rats, it remains to be determined whether the administration of this steroid after a cerebral insult would be useful in protecting the lungs in humans.

REFERENCES

1. Abrams, J. S., Deanne, R. S. and Davis, J. H. Pulmonary function in patients with multiple trauma and associated severe head injury. *J. Trauma*, 16: 543-549, 1976.
2. Bowers, R. E., McKeen, C. R., Park, B. E. and Brigham, K. L. Increased pulmonary vascular permeability follows intracranial hypertension in sheep. *Am. Rev. Respir. Dis.*, 119: 637-641, 1979.
3. Brashear, R. E. and Ross, J. C. Hemodynamic effects of elevated cerebrospinal fluid pressure: Alterations with adrenergic blockade. *J. Clin. Invest.*, 49: 1324-1333, 1970.
4. Brigham, K. L. Factors affecting lung vascular permeability. *Am. Rev. Respir. Dis.*, 115: 165-172, 1977.
5. Dietzman, R. H., Castaneda, A. R., Lillehei, C. W., Ersek, R. A., Motsay, G. J. and Lillehei, R. C. Corticoids as effective vasodilators in the treatment of low output syndrome. *Chest*, 57: 440-453, 1970.
6. Dietzman, R. H., Lunseth, J. B., Goott, B. and Berger, E. C. The use of methylprednisolone during cardiopulmonary bypass: A review of 427 cases. *J. Thorac. Cardiovasc. Surg.*, 69: 870-873, 1975.
7. Ducker, T. B. and Simmons, R. L. Increased intracranial pressure and pulmonary edema. II. The hemodynamic response of dogs and monkeys to increased intracranial pressure. *J. Neurosurg.*, 28: 118-123, 1968.
8. Frost, E. A. M. Respiratory problems associated with head trauma. *Neurosurg.*, 1: 300-306, 1977.
9. Korner, P. The effect of noradrenaline-induced systemic vasoconstriction on the formation of pulmonary edema. *Aust. J. Exp. Biol. Med. Sci.*, 31: 405-423, 1953.
10. Kusajima, K., Wax, S. D. and Webb, W. R. Effects of methylprednisolone on pulmonary microcirculation. *Surg., Gynecol., Obstet.*, 139: 1-5, 1974.
11. Lloyd, T. C., Jr. Effect of increased intracranial pressure on pulmonary vascular resistance. *J. Appl. Physiol.*, 35: 332-335, 1973.
12. Maire, F. W. and Patton, H. D. Role of the splanchnic nerve and the adrenal medulla in the genesis of 'preoptic pulmonary edema'. *Am. J. Physiol.*, 184: 351-355, 1956.
13. Malik, A. B. Personal communication.

14. Malik, A. B. Pulmonary vascular response to increase in intracranial pressure: role of sympathetic mechanisms. *J. Appl. Physiol.: Respirat. Environ. Exercise Physiol.*, 43: 335-343, 1977.
15. Malik, A. B., Lee, B. C., van der Zee, H. and Johnson, A. Mechanism of neurogenic pulmonary edema. *Am. Rev. Respir. Dis.*, 117: 367, 1978.
16. Massion, W. H., Rosenbluth, B. and Kux, M. Protective effect of methylprednisolone against lung complications in endotoxin shock. *So. Med. J.*, 65: 941-944, 1972.
17. Minnear, F. L. and Connell, R. S. A comparison of changes in pulmonary ultrastructure in mild and severe forms of aconitine-induced neurogenic pulmonary edema. Manuscript in preparation.
18. Minnear, F. L. and Connell, R. S. Alterations in the capillary-alveolar barrier associated with increased permeability in aconitine-induced neurogenic pulmonary edema. Manuscript in preparation.
19. Motsay, G. J., Alho, A., Jaeger, T., Schultz, L. S., Dietzman, R. H. and Lillehei, R. C. Effects of methylprednisolone, phenoxybenzamine, and epinephrine tolerance in canine endotoxin shock: Study of isogravimetric capillary pressures in forelimb and intestine. *Surg.*, 70: 271-279, 1971.
20. Sarnoff, S. J. and Berglund, E. Neurohemodynamics of pulmonary edema. IV. Effect of systemic vasoconstriction and subsequent vasodilation on flow and pressures in systemic and pulmonary vascular beds. *Am. J. Physiol.*, 170: 588-600, 1952.
21. Sarnoff, S. J., Berglund, E. and Sarnoff, C. Neurohemodynamics of pulmonary edema. III. Estimated changes in pulmonary blood volume accompanying systemic vasoconstriction and vasodilation. *J. Appl. Physiol.*, 5: 367-374, 1953.
22. Sarnoff, S. J. and Sarnoff, L. C. Neurohemodynamics of pulmonary edema. II. The role of sympathetic pathways in the elevation of pulmonary and systemic vascular pressures following the intracisternal injection of fibrin. *Circ.*, 6: 51-62, 1952.
23. Schumer, W. and Nyhus, L. M. The role of corticoids in the management of shock. *Surg. Clin. N. Amer.*, 49: 147-161, 1969.
24. Simmons, R. L., Martin, A. M., Jr., Heisterkamp, C. A., III and Ducker, T. B. Respiratory insufficiency in combat casualties: II. Pulmonary edema following head injury. *Ann. Surg.*, 170: 39-44, 1969.
25. Staub, N. C. Pulmonary edema due to increased microvascular permeability to fluid and protein. *Circ. Res.*, 43: 143-151, 1978.

26. Theordore, J. and Robin, E. D. Speculations on neurogenic pulmonary edema (NPE). *Am. Rev. Respir. Dis.*, 113: 405-411, 1976.
27. Wood, C. D., Seager, L. D. and Ferrell, G. Influence of autonomic blockade on aconitine induced pulmonary edema. *Proc. Soc. Exp. Biol. Med.*, 116: 809-811, 1964.
28. Winer, B. J. *Statistical Principles in Experimental Design*. McGraw-Hill, New York, 1962.
29. Wray, N. P. and Nicotra, M. B. Pathogenesis of neurogenic pulmonary edema. *Am. Rev. Respir. Dis.*, 118: 783-786, 1978.

Table 1. The effects of phlebotomy or methylprednisolone sodium succinate (MPSS) on the ratio of lung weight to body weight (LW/BW) in aconitine-induced neurogenic pulmonary edema

| <u>Treatment</u> | <u>n</u> | <u>Aconitine (pmoles/kg)</u> | <u>LW/BW (mean±SEM)</u> |
|-------------------|----------|------------------------------|-------------------------|
| None | 11 | 774 | 1.27±0.12* |
| None | 5 | 1550 | 1.35±0.12* |
| Phlebotomy before | 8 | 774 | 0.59±0.12 |
| Phlebotomy after | 5 | 1550 | 0.60±0.07 |
| Phlebotomy | 4 | None | 0.54±0.02 |
| MPSS | 10 | 774 | 0.60±0.05 |

*Different from other values (P < 0.01)

Animals were either phlebotomized before or after the injection of aconitine or administered MPSS before receiving aconitine.

Fig. 1. The effect of MPSS on systolic blood pressure after the injection of aconitine (774 pmoles/kg) in the preoptic area (4 rats/group).

Effect of MPSS on Systolic Blood Pressure After Preoptic Injections of Aconitine

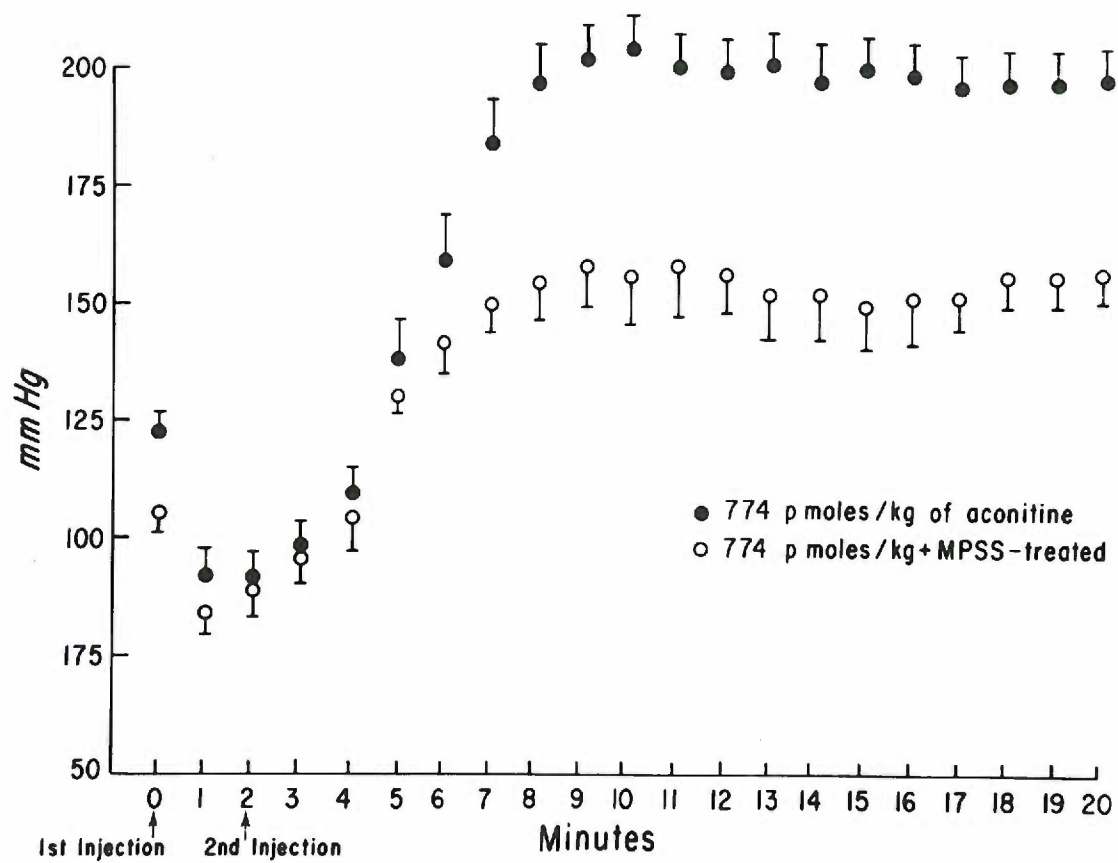


Fig. 2. Lungs from a rat injected with 774 μ moles/kg of aconitine.
Note that the lungs are completely covered with punctate hemorrhages.
The LW/BW was 1.43.

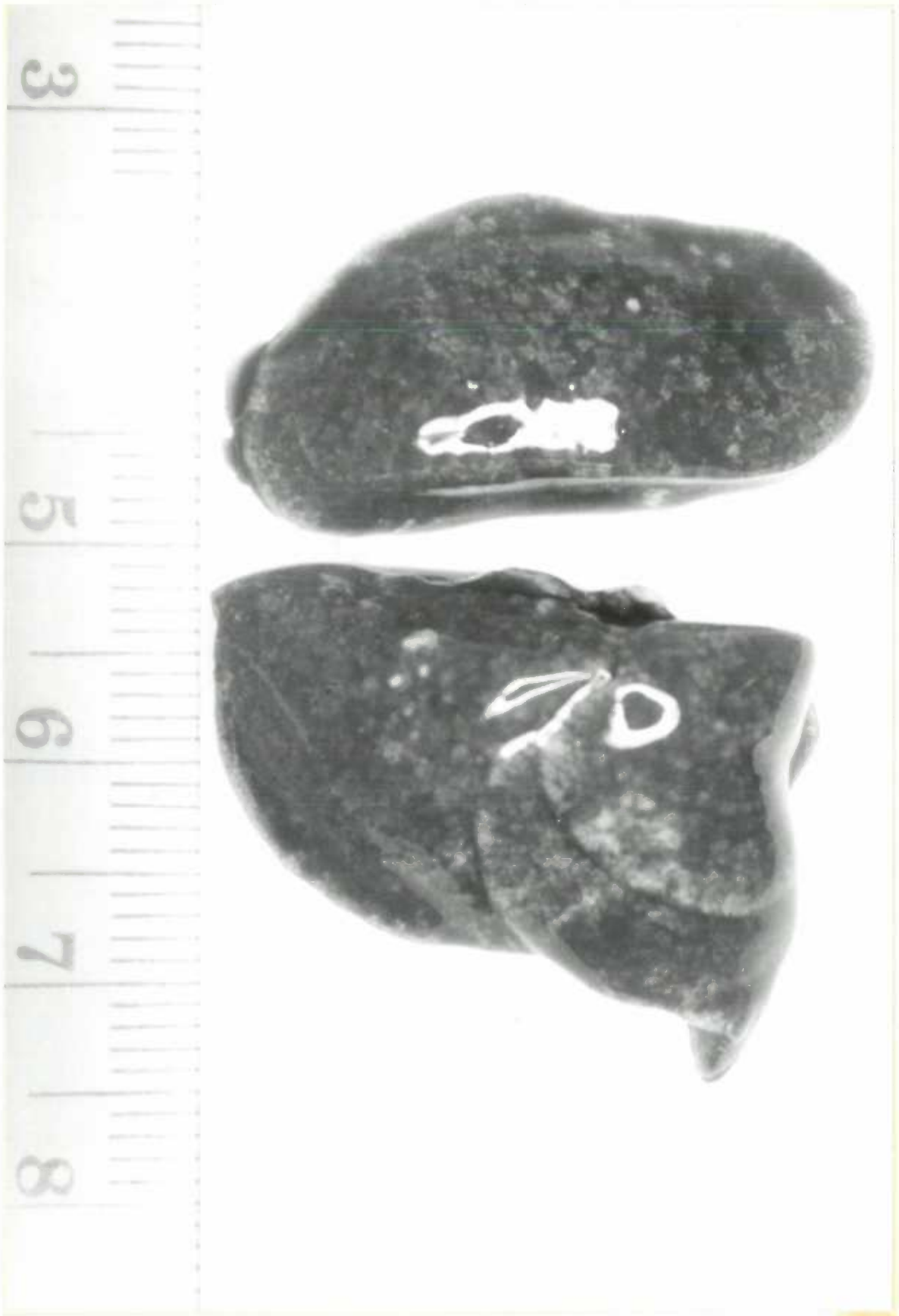


Fig. 3. Lung biopsy from a rat injected with 1550 pmoles/kg of aconitine. The type I epithelium (Ep I) and capillary endothelium (En and small arrows) are discontinuous and appear as spherical blebs (large arrows). A dense accumulation of exudates fills the alveolar air space (AAS). The LW/BW was 0.94. Cap, capillary; RBC, red blood cell.

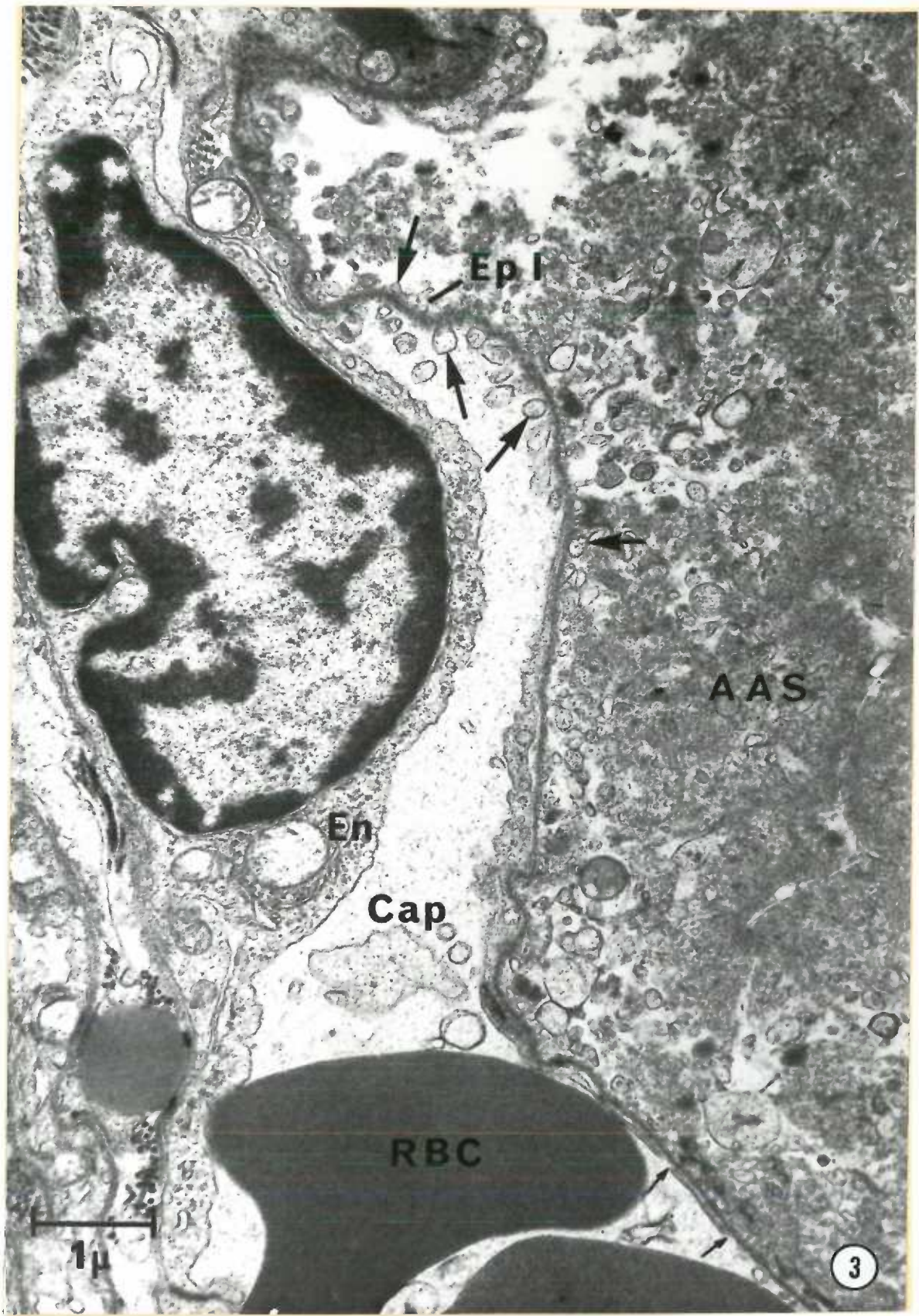


Fig. 4. Lungs from a rat injected with 1550 pmoles/kg of aconitine and phlebotomized when SAP reached a peak level. No gross abnormalities were observed. The LW/BW was 0.48.



Fig. 5. Lung biopsy from a rat injected with 1550 pmoles/kg of aconitine and phlebotomized when SAP reached a peak level. A rarefied type I epithelial cell (Ep I) is adjacent to an intact endothelial cell (En). The LW/BW was 0.52. AAS, alveolar air space; WBC, white blood cell.

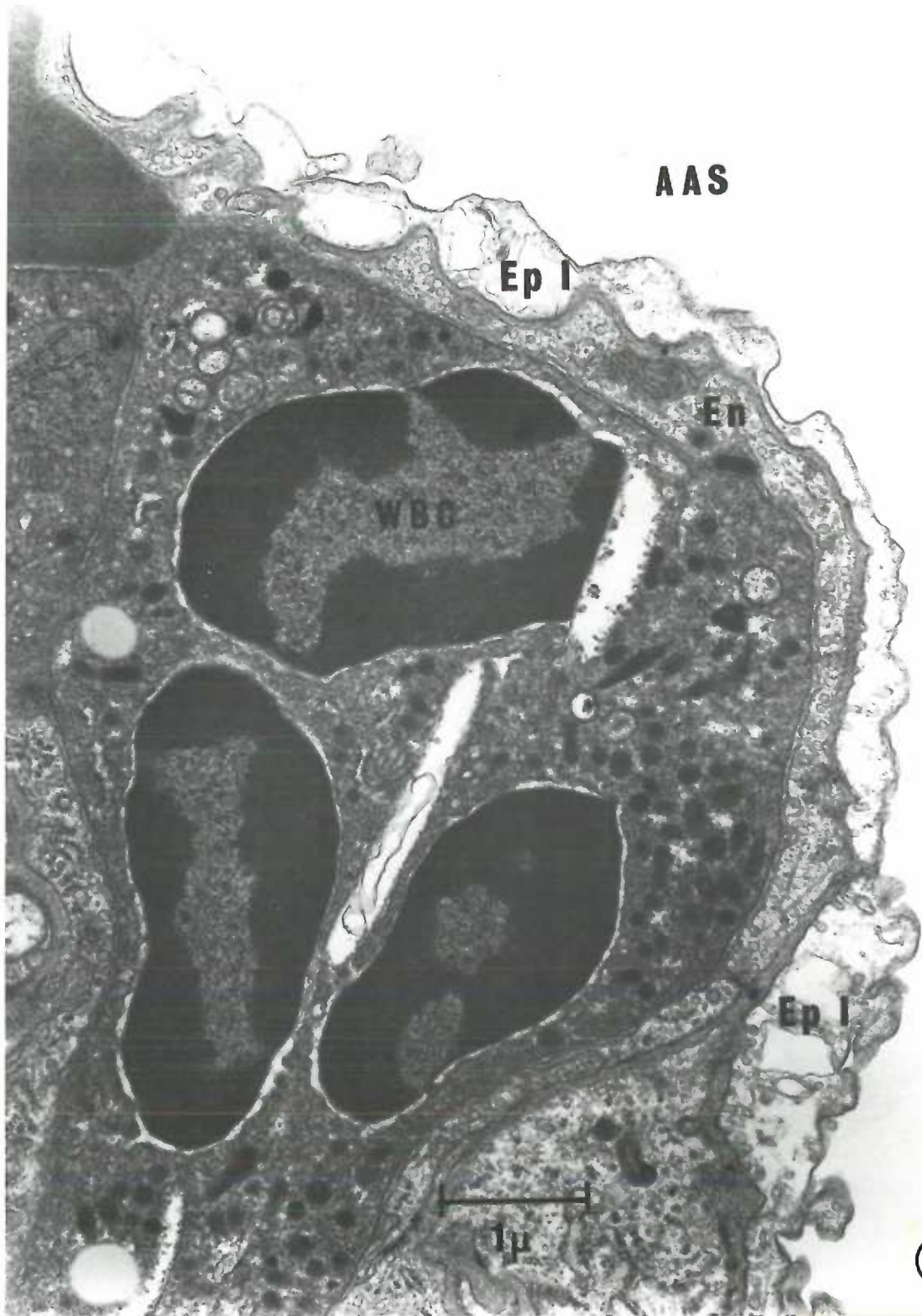


Fig. 6. Lung biopsy from a rat injected with 1550 pmoles/kg of aconitine and phlebotomized when SAP reached a peak level. Exudates occupy the alveolar air space (AAS) that is lined by normal appearing type I epithelium (Ep I), except in one area (large arrows), where the type I epithelium is discontinuous and appears as spherical blebs. The LW/BW was 0.52. En, endothelium; WBC, white blood cell.

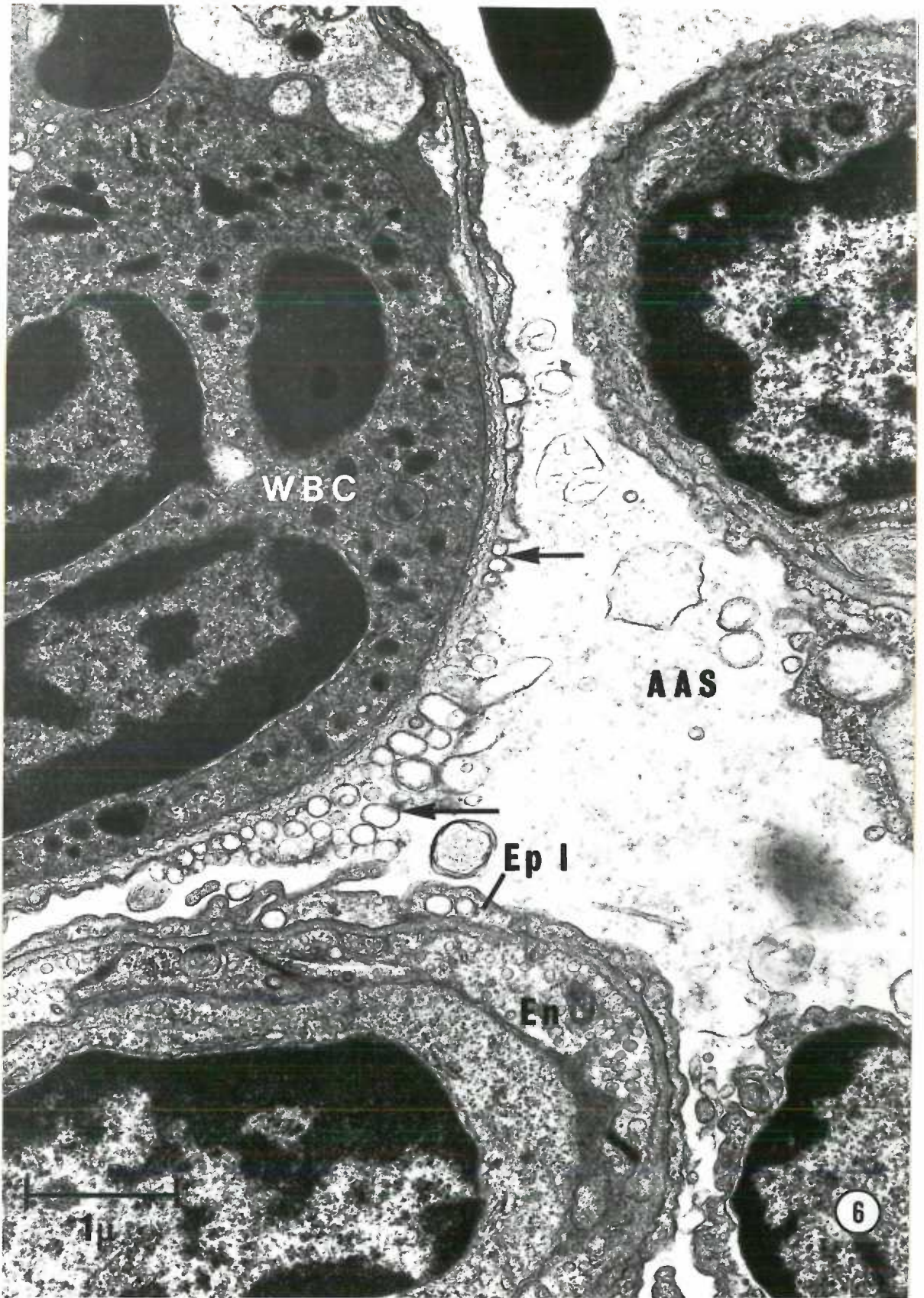


Fig. 7. Lung biopsy from a rat injected with 1550 pmoles/kg of aconitine and phlebotomized when SAP reached a peak level. A dense accumulation of exudates occupies the alveolar air space (AAS) that is lined by discontinuous type I epithelium (large arrows). The basal lamina (BL) is exposed where the type I epithelium is absent. Note that the endothelium (En) appears intact. The LW/BW was 0.88. RBC, red blood cell.

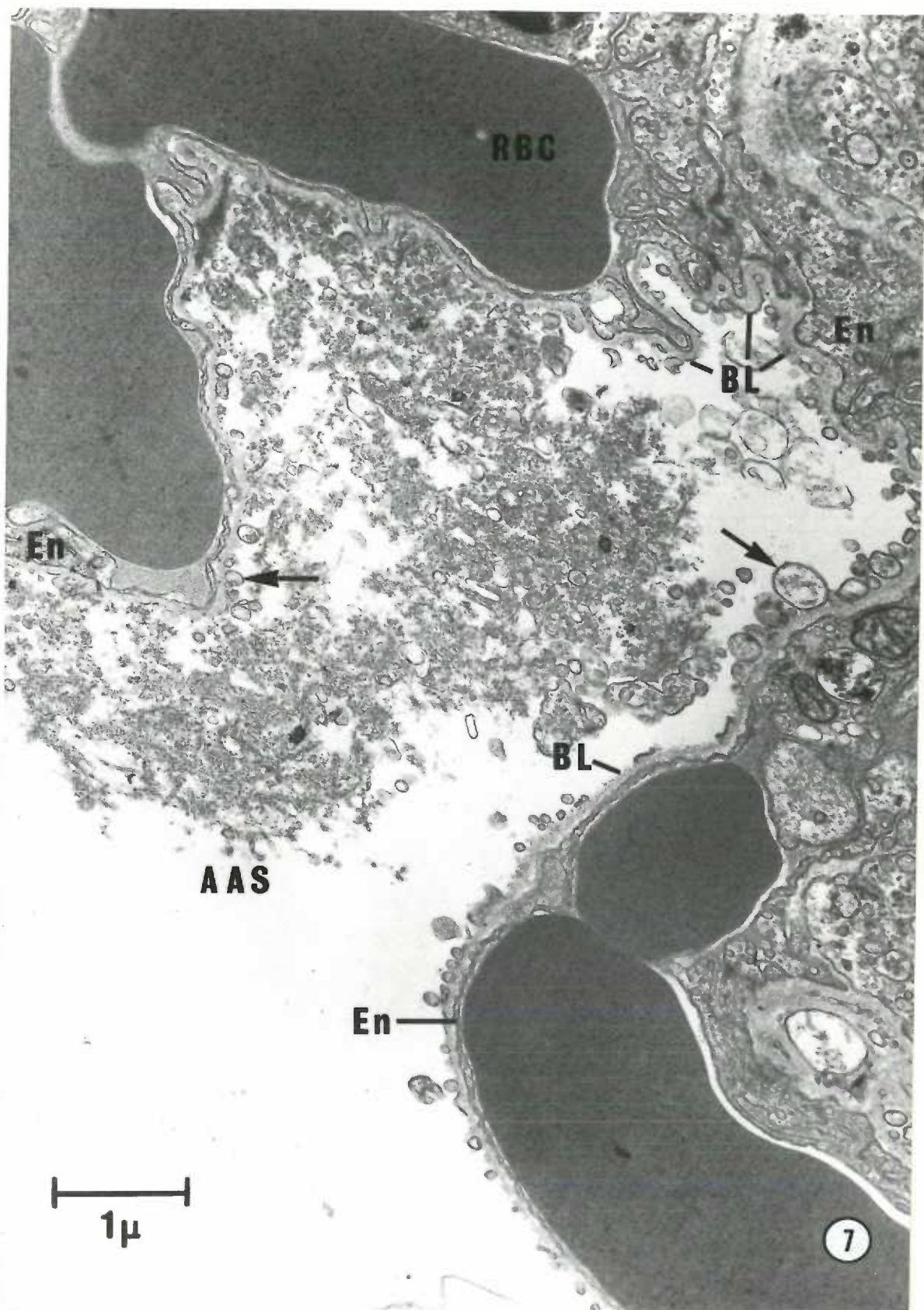


Fig. 8. The effect of phlebotomy on SAP following injection of 1550 pmoles/kg of aconitine. Rats were phlebotomized when SAP reached a maximum level (large arrow). Blood pressure fell immediately after phlebotomy but increased again to approximately 90% of maximum at 15 min.

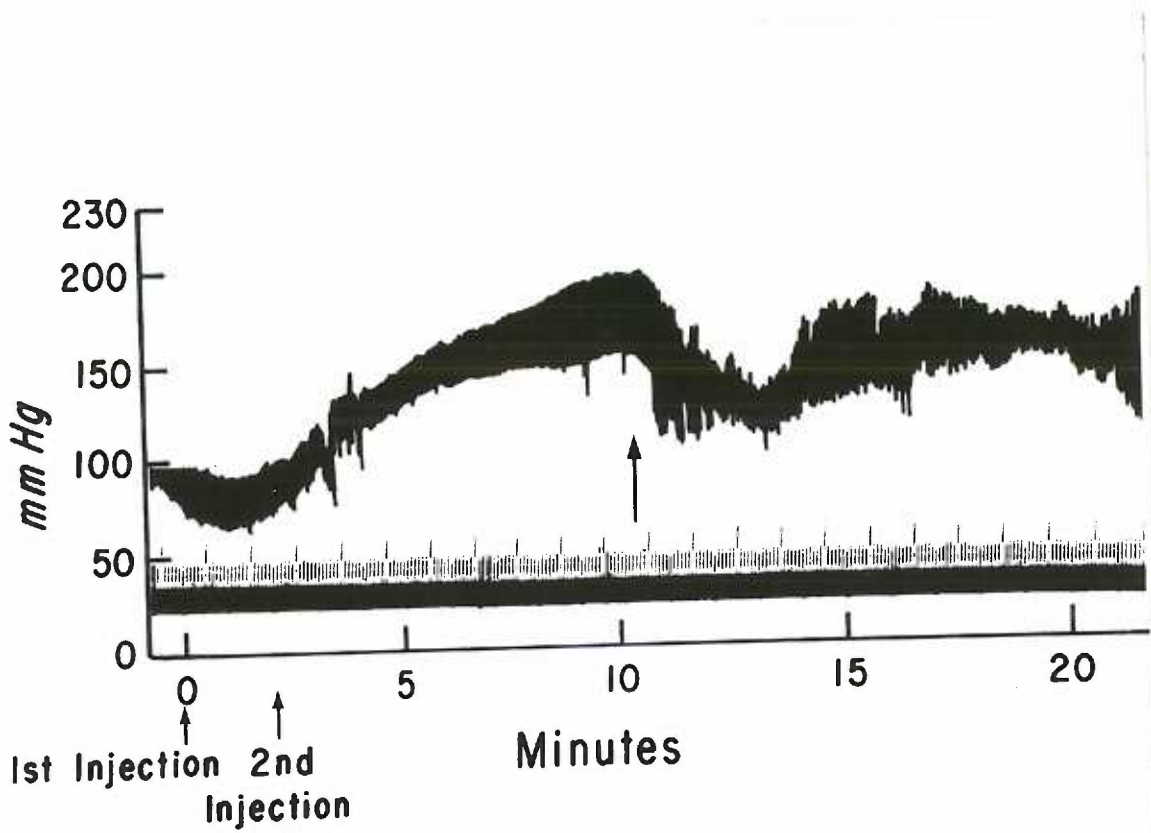
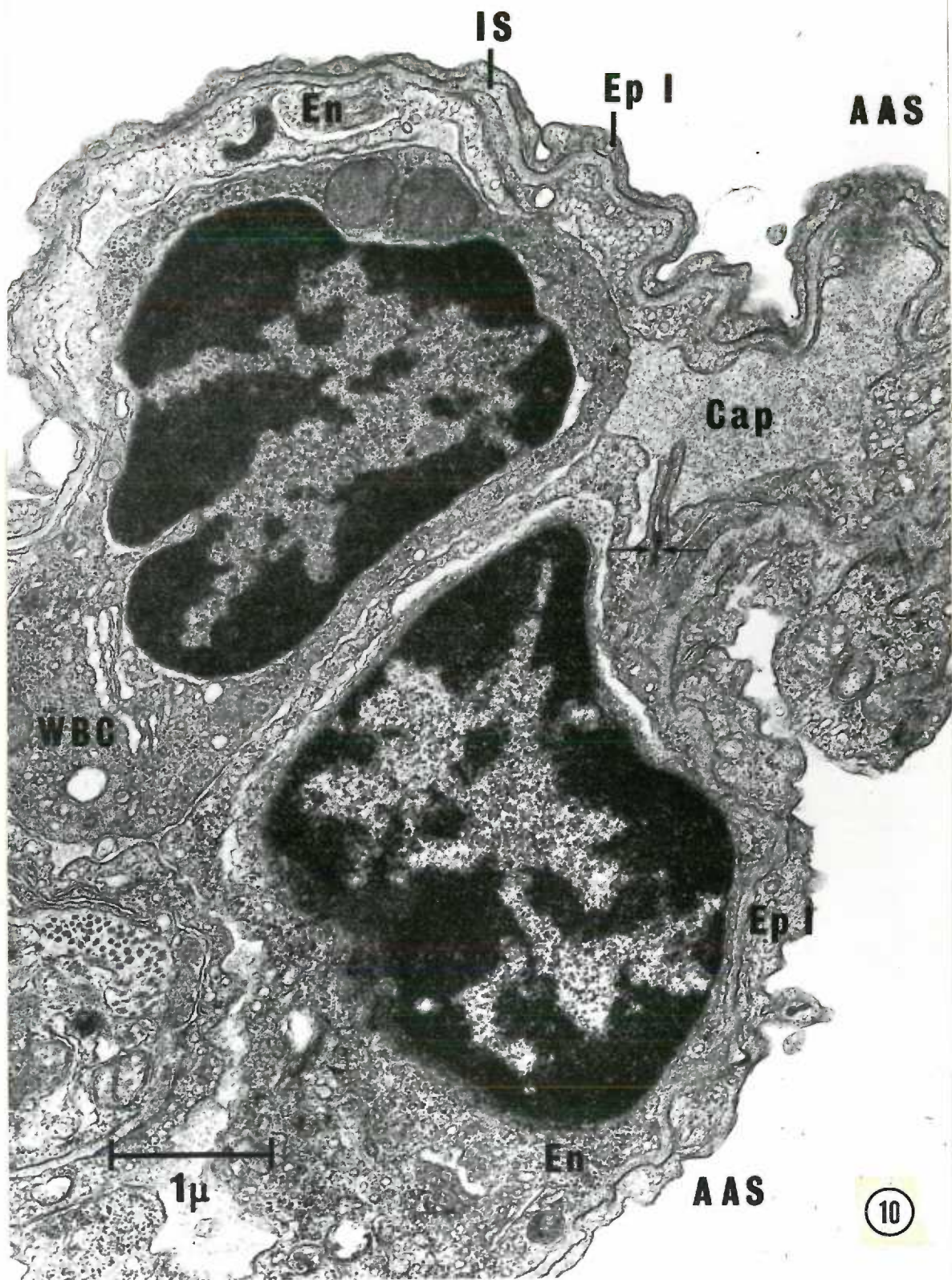


Fig. 9. Lungs from a rat treated with MPSS and injected with 774 pmoles/kg of aconitine. Punctate hemorrhages can be seen in two lobes of both right and left lungs. The LW/BW was 0.46.



Fig. 10. Lung biopsy from a rat treated with methylprednisolone sodium succinate and injected with 774 pmoles/kg of aconitine. The type I epithelial cell (Ep I) lining an alveolar air space (AAS) is separated from an endothelial (En)-lined capillary (Cap) by an interstitial space (IS). Note the intact capillary endothelial junction (small arrows). The LW/BW was 0.48. WBC, white blood cell.



SUMMARY

Neurogenic pulmonary edema (NPE) was produced in adult female rats by injecting aconitine into the preoptic area of the brain. The first objective of this study was to determine whether the severity of NPE could be varied by injecting different doses (197 to 3100 pmoles/kg) of aconitine. Animals were killed 1 h after injection, and the lungs were removed, weighed and processed for electron microscopy. Those animals injected with 1058 pmoles/kg or more developed severe pulmonary edema, as determined by lung weight/body weight ratios (LW/BWs) greater than 1.00, and were either dead or dyspneic at 1 h. In contrast, those animals administered 423 pmoles/kg or less had LW/BWs less than 1.00 and were conscious and ambulatory at 1 h and were not dyspneic. Half of the animals receiving the intermediate dose of 774 pmoles/kg had high LW/BWs and half had low LW/BWs. Therefore, this dose is considered the approximate median effective dose for aconitine-induced NPE in the rat. The extent of grossly visible hemorrhages and ultrastructural changes of the lungs generally increased in severity with an increase in dose but were more closely related with the amount of change in LW/BW. These findings demonstrate that NPE produced by injecting aconitine into the preoptic area can be varied between mild and severe forms depending on the dose used.

The second objective of the study was to characterize the ultrastructural changes associated with aconitine-induced NPE as the syndrome progressed and to determine the pathway of edema fluid across the capillary-alveolar barrier. At 8 min after injection of a lethal dose (1550 pmoles/kg) of aconitine, the capillary endothelium generally appeared intact except for the occasional observation of open junctions

and structural damage to the cells. The Type I epithelium, on the other hand, was starting to degenerate at 8 min. At 15 min after injection of aconitine, the capillary endothelium still remained intact, but the Type I epithelium was severely damaged. By 1 h, both the capillary endothelium and the Type I epithelium were severely damaged after a lethal injection, whereas damaged Type I epithelium was consistently found in association with intact capillary endothelium in animals given a sublethal dose. Thus, these observations demonstrate that the Type I epithelium is more susceptible to injury than the capillary endothelium in aconitine-induced NPE. The reason for the differential sensitivity of the two cell types in NPE could not be determined from this study.

Using ferritin as a vascular marker, it was shown that 8 min after injection of a lethal dose of aconitine the capillary endothelial barrier was permeable to ferritin. Since open endothelial junctions, which sometimes contained ferritin, and structurally damaged areas of the endothelium were occasionally observed, it is suggested that the main route by which plasma enters the interstitial space is through these alterations in the capillary endothelial barrier. It was observed further that exudates were present in the alveoli in the absence of frank ruptures of the capillary-alveolar barrier and in association with tight junctions of alveolar epithelium that appeared impermeable to ferritin. However, many Type I cells were observed in various stages of degeneration. These findings suggested that it is damage to the Type I cells and not an increase in permeability of alveolar epithelial junctions that allows plasma to leave the interstitial space and enter the alveoli.

The third objective of the study was to determine the efficacy of either phlebotomy or I.V. injection of methylprednisolone sodium succinate (MPSS) in preventing aconitine-induced NPE. Rats were phlebotomized (20% of the calculated blood volume was removed) either before or after the injection of aconitine (774 or 1550 pmoles/kg, respectively). Another group of rats was treated with MPSS (40 mg/kg) before receiving aconitine (774 pmoles/kg). It was found that all of these procedures prevented the development of aconitine-induced NPE. In these animals, LW/BWs and the pulmonary ultrastructure were normal, 1 h after injection of aconitine, except for the occasional observation of a rarefied and swollen Type I epithelial cell and exudates in the alveolar air spaces. Although the mechanism by which these treatments prevented damage to the lungs could not be determined from this study, it is suggested that phlebotomy was effective because it lowers the pulmonary blood volume and that MPSS provides a beneficial effect by suppressing the sympathetic response involved in NPE.